Phytochrome photoreceptors and the environmental regulation of plant water use and development.

Julian Adams

A thesis submitted in partial fulfilment of the requirements for the degree of
Doctor of Philosophy

The University of Sheffield
Faculty of Science
School of Biosciences

September 2024

In loving memory of my mum, Michelle Jane Adams.

Declaration

I, Julian Adams, declare that this thesis has been composed entirely by myself unless otherwise referenced in the text. I confirm that this thesis has not been submitted for any other degree. All quotations have been distinguished by quotation marks and the sources acknowledged.

Acknowledgements

First and foremost, I would like to thank my supervisor Dr Stuart Casson for his unwavering support over the past 4 years. His guidance, both for science and for personal issues along the way, and always with a smile has been a shining light and source of much enjoyment during my PhD. I couldn't have asked for a better primary supervisor and mentor.

Secondly, I would like to thank my co-supervisor Professor Julie Gray for her insightful contributions to my PhD as well as being a constant source of support over the 4 years. During my PhD a lot has happened in my personal life, and it hasn't been without its struggles but the supervision of both Dr Casson and Professor Gray has made everything that bit easier with the joyous environment created in the lab and so I am very grateful to them.

Next, I would like to thank my funding body, BBSRC and the White Rose DTP for providing me with the opportunity to carry out this PhD.

During the last 4 years, I have had the pleasure of working with many colleagues in the Casson lab, including, Dr Natalia Hurtado, Dr Kishwar Shethi and Dr Nicholas Zoulias, all of whom have been there to help at any time and of great support to me while also being valuable contributors to creating such a lovely environment to work in. I would also like to thank all other present and past members of C33 who have helped to make the last 4 years so special.

I would also like to thank my advisors, Dr Andrew Hitchcock and Dr Rob Fagan who have always been available when support and advice was needed. Also thank you to all of the technical staff in the Annex that help to maintain and run the plant growth chambers and to Dr Heather Walker and the staff who run the mass spec facility in the School of Biosciences.

Thank you to my dad, Terence Adams for always being there for me and being a great dad, and to my three sisters: Megan, Jessica and Charlotte, you all mean the world to me. I hope I have made you proud and thank you all for all your support and love throughout my life, I couldn't have asked for a better family. Thanks to my

grandparents too for their constant support and love including my late gran who passed in 2020.

All my friends in Sheffield and back home in Lincolnshire have been beacons of light for me and I am very much appreciative of them and that they are always there for me no matter what.

Lastly my mum. I miss her so much every day, but the motivation to make her proud has been a huge driving force behind me this whole time.

Abstract

Predicted increases in global temperatures due to climate change mean that plants must find ways to adapt. These increased temperatures may be coupled with a reduction in the availability of fresh water and so studies need to be undertaken to determine how plants can use their water more efficiently. Stomata, the microscopic pores on the surface of leaves that regulate gas exchange, are the main ways in which plants lose water and are therefore primary candidates to study in the context of water use efficiency (WUE). A key regulator of WUE, through the control of stomatal development and photosynthetic traits, is the red-light photoreceptor phytochrome B (phyB). Increased temperatures cause faster thermal reversion of phyB from its active Pfr form to the inactive Pr form. Therefore, this study aims to determine the impact of temperature on phytochrome activity and how this could impact upon plant development and WUE. I hypothesise that under increased temperatures, faster thermal reversion rates reduce the pool of active Pfr, impacting stomatal development, photosynthesis and morphology. The trade-off between these traits is decisive in determining the outcome on WUE. It was demonstrated that previously documented improvements in WUE of phytochrome mutants is not robust and that impacts on photosynthesis or canopy structures negate any gains in WUE resulting from a reduction in transpiration due to fewer stomata. The inclusion of end of day (EoD) far-red light (FR) demonstrated that night time temperature has an impact on the ability of plants to be more water use efficient. These warmer nights in turn impact upon epidermal patterning, with phyB being a buffer that regulates progression of cell divisions through the stomatal lineage and this could be acting through cell cycle cyclins and SMR4. This work also examined the interaction between phyB and fertiliser treatments in rice. Previous studies had shown that wild-type (WT) rice plants do not flower without the addition of fertiliser whereas *OsphyB-1* do. The removal of OsphyB caused improvements in WUE but at the expense of yield independent of fertiliser regimes, however, intermediate fertiliser treatments had similar impacts as full fertiliser treatments under most measurements and so there is the potential that lower levels of fertiliser could be used to grow rice in the future.

List of Abbreviations

ABA – Abscisic Acid

AMT – Ammonia transporters

A – Assimilation

BRs – Brassinosteroids

d.p.g – Days post germination

EPFs – Epidermal Patterning Factors

EoD – End of day

FR – Far-red

GC – Guard cell

GMC – Guard mother cell

gsw – stomatal conductance

HDT – High day temperature

HNT – High night temperature

IRGA – Infra-red Gas Analyser

iWUE – Instantaneous water use efficiency

JA – Jasmonic acid

LD – Long day

M – Meristemoid

MMC – Meristemoid Mother Cell

NB – Nipponbare

NPQ – Non-photochemical quenching

PCR – Polymerase chain reaction

PHYB – apoprotein of phyB

PHYB – phyB gene

phyB – the protein with its chromophore attached

phyB-9 – the mutant allele of PHYB

ROI – Regions of interest

SD – Stomatal density

SDs – Short days

SI – Stomatal index

SLGC – Stomatal lineage ground cell

WUE – water use efficiency

$\Delta^{13}C$ and CID – Carbon isotope discrimination; the isotopic ratio of ^{12}C and ^{13}C in the tissues of plants

Table of Contents

Chapter 1: Introduction

1.1 Increasing global temperatures due to climate change

Average global temperatures have been on the rise since the industrial revolution, with an average increase of 1.1°C since this period and an expectation that it will carry on increasing unless strict mitigations are put in place across the globe (IPCC, 2023) (Figure 1.1). These increased temperatures are a result of elevated atmospheric levels of carbon dioxide creating the greenhouse effect (NOAA, 2024). There are many consequences of increased temperatures through the greenhouse effect and one of the most devastating to humans is the impact on food security. Regions such as Africa, South America and Southeast Asia where economically important crops such as rice are predominantly grown are predicted to have the greatest losses in agricultural yields in the future, the main reason being from climate change induced drought events (Naikwade, 2017). A growing global population, one that is expected to reach 9.7 billion by 2050, further impacts these current and potential food losses (United Nations, 2024). The reduction in water availability is particularly important in the context of irrigated rice production, which is the main way rice is grown globally and in countries such as China, this method of rice growth contributing to 65% of all water used for crops (Li *et al.*, 2016). Rice is eaten by over half of the world's population and is the main source of calories around the globe (Cabral *et al.*, 2024). It has been predicted that rice yields could reduce by over 5% if the average global temperature increases by the 1.5°C mark, due to losses of water and the greater occurrence of droughts, but also due to impacts on plant developmental stages such as spikelet fertility (X. Wang *et al.*, 2020). Although many studies have focused on how daytime temperatures over the past couple of centuries have increased, the corresponding night-time temperatures have been increasing at a greater rate (Peng *et al.*, 2004). Increases in temperatures during plant growth and development is a key factor in the survival rate, grain quality and fertility. For example, higher temperatures, particularly at night, during the flowering transition in rice has the greatest impact with a severe loss in spikelet fertility and even no yield in some cases (Satake and Yoshida, 1978; Fu *et al.*, 2012). Rice yield losses under increased temperatures can be further exacerbated with the expensive cost of fertilisers required to grow higher quality, healthy crops. In the UK alone, ammonia nitrate fertiliser costs increased 152% between 2021 and 2022 (Eardley, 2022). To prevent large-scale crop losses due to increasing temperatures, more studies need to be carried out to understand the impact

of temperature on both plant development and how plants source and utilise water. The aim is to ensure that crop yields are sufficient to feed an ever-growing population. Increases in temperature impact upon the molecular processes occurring within organisms, particularly affecting upon the ability of proteins involved to fold correctly (Guo, Xu and Gruebele, 2012).

The main way in which plants lose water is through the stomata, the microscopic pores on the surface of the leaves, flanked by guard cells through which gas exchange occurs, and the main source of carbon for photosynthesis, with up to 90% of water loss occurring through these (Pei *et al.*, 1998). Plants must balance the amount of carbon gained from the atmosphere with the amount of water lost as a consequence of the opening of the stomata. The optimization of stomatal opening and closing to different stimuli is crucial for plant survival and influences plant water use efficiency (WUE) (Lawson and Matthews, 2020). WUE can be defined in several ways and is discussed in more detail in section 1.2.2. Therefore, it is important to study how stomatal numbers and/or their distribution could be manipulated to reduce water losses and hence make plants more water use efficient. In many plant species, stomatal aperture varies depending on the conditions (Hetherington and Woodward, 2003). Typically, they open in response to light during the day and close in response to darkness but other factors including carbon dioxide concentration, humidity and endogenous cues influence their aperture (Schulze *et al.*, 1972; Engineer *et al.*, 2014; Murata, Mori and Munemasa, 2015; Kostaki *et al.*, 2020).

Changes in temperature can have major impacts on plant growth and development. However, it should be added that even within a species, experimental manipulations of temperature vary significantly and a lack of consensus makes it difficult to define what constitutes elevated temperatures (Stavang *et al.*, 2009; Chiu *et al.*, 2016; Jung *et al.*, 2020). This diversity is seen further between the different ecotypes in Arabidopsis, although typically Col-0 is grown in the wide range of 15-30°C due to this accession coming from northern European latitudes and therefore experiencing varied temperatures throughout the year (Adams *et al.*, 2016). Temperature affects plant development in several ways. The best-studied impact of temperature on plant development is through the process of vernalisation, which is when plants flower after a prolonged period of cold exposure (Amasino, 2005; Kim *et al.*, 2009). Temperature does not just affect plant development at the large scale but also at the molecular

level, with cues feeding into the circadian clock and even down to the role of heat shock proteins that will bind to and protect other proteins upon exposure to higher temperatures (Seo and Mas, 2015; Hu *et al.*, 2022). More recently, temperatures have been found to control the translation of proteins such as PIF7 by altering RNA secondary structures in a reversible manner termed a RNA thermo switch (Chung *et al.*, 2020). There are changes at the DNA level too, with histone modifications such as the removal of H2A.Z, a key component of nucleosome bound heat shock proteins (Kumar and Wigge, 2010; Tasset *et al.*, 2018; John, Olas and Mueller-Roeber, 2021). In the case of flowering time, climate change appears to be significantly impacting this trait, with modelling studies showing that over the past 150 years, plants have flowered on average 9 days earlier (Berg, Brown and Weber, 2019). In Arabidopsis, the model organism for many plant developmental studies, higher temperatures lead to extended hypocotyls at the seedling stage (Gray *et al.*, 1998). As leaves begin to be produced, these have extended petioles and leaves become more angled compared to controls grown at ambient temperatures, due to a process called hyponastic growth, possibly to allow for airflow to reach more regions of the leaves and allow some cooling to occur (van Zanten *et al.*, 2009; Crawford *et al.*, 2012; Bridge, Franklin and Homer, 2013). This could be combined with greater transpiration rates to further reduce heat stress; however, the plant must balance these water losses carefully so as to not enter drought stress. The leaves produced are also smaller and have fewer but often larger stomata, most likely to prevent too much water being lost through the stomata because of the evaporative cooling (Crawford *et al.*, 2012; Bridge, Franklin and Homer, 2013).

The model organism used in many stomatal studies and in this study is that of Arabidopsis thaliana, a common plant that is found across the globe and in particular, the ecotype of Columbia-0 is a European based ecotype that is used for these studies. This is a good model because of its short life cycle, well known and fully sequenced genetic makeup and ease of growth and husbandry.

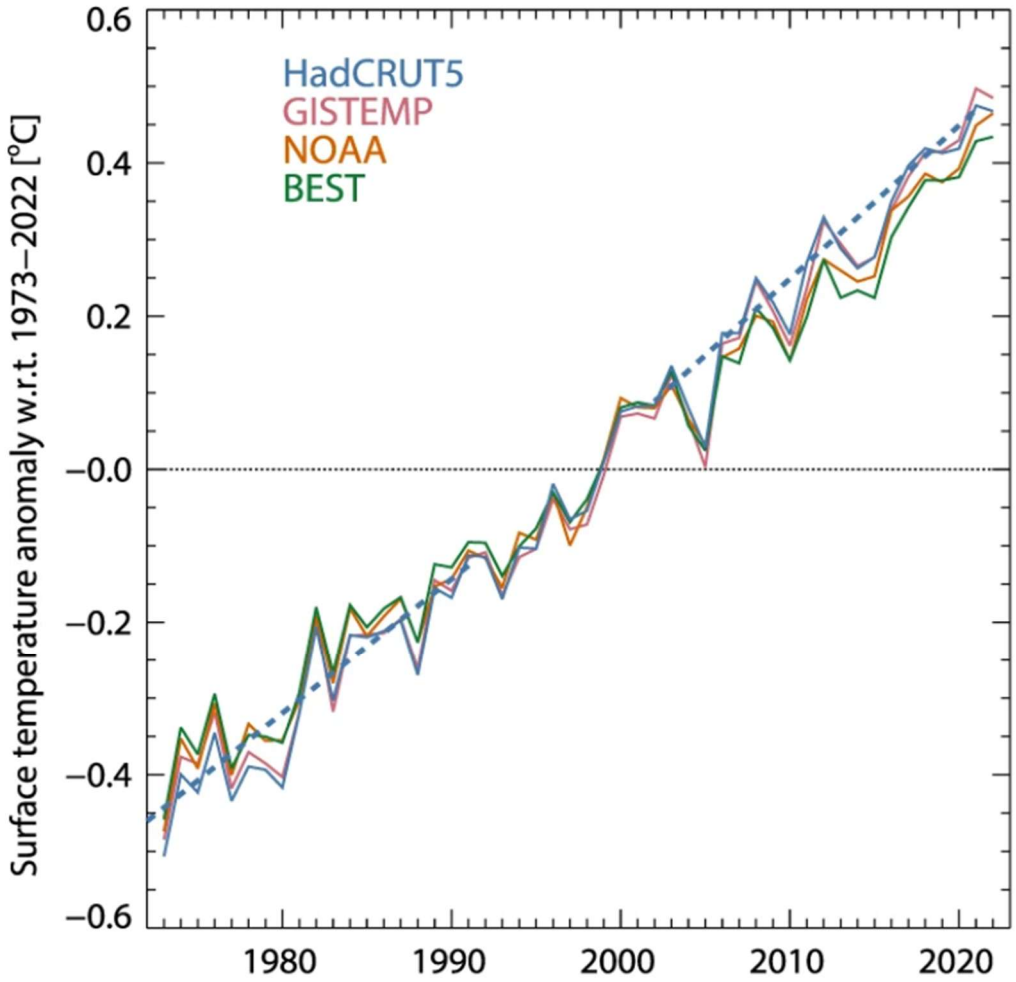

Figure 1.1 Surface temperature increases since 1970 to present day. Four different measurements of the change in temperature from around the globe (MET office, NASA, NOAA and BEST) showing how average surface temperature levels have increased over the past 50 years. Taken from (Samset *et al.*, 2023).

1.2 Plant water use efficiency

The ability of plants to use water efficiently is defined in multiple ways. The instantaneous WUE (iWUE) measures the efficiency of a particular leaf at a snapshot in time, calculating the net amount of assimilation, that being the amount of carbon gained from the atmosphere through the stomata per unit of water lost through the stomata via transpiration (Seibt *et al.*, 2008). This is typically measured using an infrared gas analyser (IRGA) in which a leaf is clamped into a chamber and parameters within the chamber are set to the conditions required for measurements before taking

a reading. Another way of measuring WUE is by determining the lifetime WUE. Lifetime WUE is a measure of the WUE for the whole plant over the course of its lifetime. This can be done by carbon isotope discrimination, in which leaves from a mature plant are taken and dried before ground into a powder and 1-2mg of this are subjected to isotope ratio mass spectroscopy (IRMS). The basic principle of IRMS is total combustion of the sample followed by gas chromatography to separate individual ions before they are passed into a mass spectrometer where the two forms of carbon ^{12}C and ^{13}C from CO_2 are ionised and separated by mass using a magnetic field. Due to the different masses between the two isotopic forms, they will be detected at different time points from which a ratio can be determined. The determination of the ratio of the two forms of carbon isotopes correlates with WUE through the Calvin cycle enzyme Rubisco. Rubisco catalyses the carboxylation of RuBP using carbon gained via assimilation in the form of CO_2 (Sharkey, 2023). Rubisco discriminates against ^{13}C over ^{12}C partially due to faster kinetics when ^{12}C is used (Tcherkez and Farquhar, 2005). The closer the value of carbon isotope discrimination is to zero, the more water use efficient a plant is. This is because the ratio of ^{12}C to ^{13}C being used by Rubisco gets lower due to reduced carbon assimilation and hence if there is reduced assimilation there should also be reduced transpiration because the two are directly proportional and therefore it is likely that less water will be lost via transpiration (Farquhar and Ehleringer, 1989).

1.2.1 Stomata and water use

Stomata are the main ways in which plants lose water, with up to 90% of water taken up by the roots being lost through evapotranspiration (Pei *et al.*, 1998). Plants can adjust the open state of pores through increasing turgor pressure. Ion flux into the guard cells reduces the osmotic potential in the cell leading to water movement into the cell via osmosis increasing the turgor and opening the stomata (Roelfsema and Hedrich, 2005). Decreases in turgor, however, have the opposing impact and lead to less open stomata which reduces the uptake of CO_2 but with the result meaning reduced water losses. The signals for opening and closing are fine-tuned to balance this carbon uptake for assimilation with water losses. In the shorter term (minutes to hours) changes in light (quantity and/or quality), temperature, CO_2 concentration in the

atmosphere and soil moisture levels can lead to changes in stomatal aperture. For example, increased temperatures inside the leaf lead to a process called evaporative cooling and the opening of stomata to allow water to be lost and cooling of the air around the leaf (Crawford *et al.*, 2012; Urban *et al.*, 2017; Kostaki *et al.*, 2020). In the longer term (hours to days), changes in these same environmental variables can lead to slower adaptable changes in stomatal patterning (Blatt, 2000; Outlaw, 2003; Dow, Bergmann and Berry, 2014). These developmental changes can lead to a change in leaf stomatal density and this is often correlated with a change in stomatal size (Franks, Drake and Beerling, 2009). These changes in density and size can influence the ability of a plant to be able to retain water better. Smaller stomata have less capacity to lose water than larger ones, although in cases where there are smaller stomata, typically there are more of them which impacts transpiration (Raven, 2014). Collectively, these short-term changes in stomatal aperture coupled with longer term developmental adaptations are a means of a plant optimising their carbon capture to water use ratio under the prevailing environmental conditions. Water use is measured in two main ways. Lifetime water use efficiency is a measure of the total carbon gained from assimilation over a plants life, whereas intrinsic water use efficiency (iWUE) is a snapshot measurement of water use at the leaf level for that moment in time (Farquhar and Ehleringer, 1989; Condon *et al.*, 2004).

1.3 Stomatal development

In Arabidopsis, stomata develop following a well-defined pathway (Pillitteri *et al.*, 2007) (Figure 1.2), though little is understood about the selection of a protodermal cell to enter the stomatal lineage. Once selected to enter the lineage, a protodermal cell undergoes differentiation to form a meristemoid mother cell (MMC) before this then divides asymmetrically to form a stomatal lineage ground cell (SLGC) and a meristemoid (M). The meristemoid can undergo several rounds of proliferation, with typically between one and three divisions, generating pavement cells or further meristemoids. Eventually, the meristemoid differentiates to form a guard mother cell (GMC), which will divide to form a pair of guard cells surrounding a central pore (Pillitteri *et al.*, 2007). Three basic helix-loop-helix transcription factors regulate the progression along the stomatal lineage pathway. SPEECHLESS (SPCH) regulates

entry into the lineage and is mainly found in the meristemoids, MUTE controls the differentiation from a meristemoid into a GMC and FAMA regulates the final division to create the guard cells (Ohashi-Ito and Bergmann, 2006; MacAlister, Ohashi-Ito and Bergmann, 2007; Pillitteri *et al.*, 2007). Further to this, there is a requirement of an interaction with ICE1/SCRM to stabilise the proteins and allow them to function (Kanaoka *et al.*, 2008). The levels of SPCH are influenced by several extracellular peptides that help to prevent neighbouring pavement cells becoming stomata. The epidermal patterning factors (EPF1 and EPF2) bind to receptors on the cell membrane which in turn activate a mitogen-kinase cascade to phosphorylate SPCH protein and prevent its activity (Bergmann, Lukowitz and Somerville, 2004; Wang *et al.*, 2007; Lampard, Macalister and Bergmann, 2008). In opposition to this, the epidermal patterning factor Stomagen or EPFL9 is a positive regulator of stomatal development by binding to the EPF1/2 receptors and preventing the activation of the kinase cascade (Sugano *et al.*, 2010).

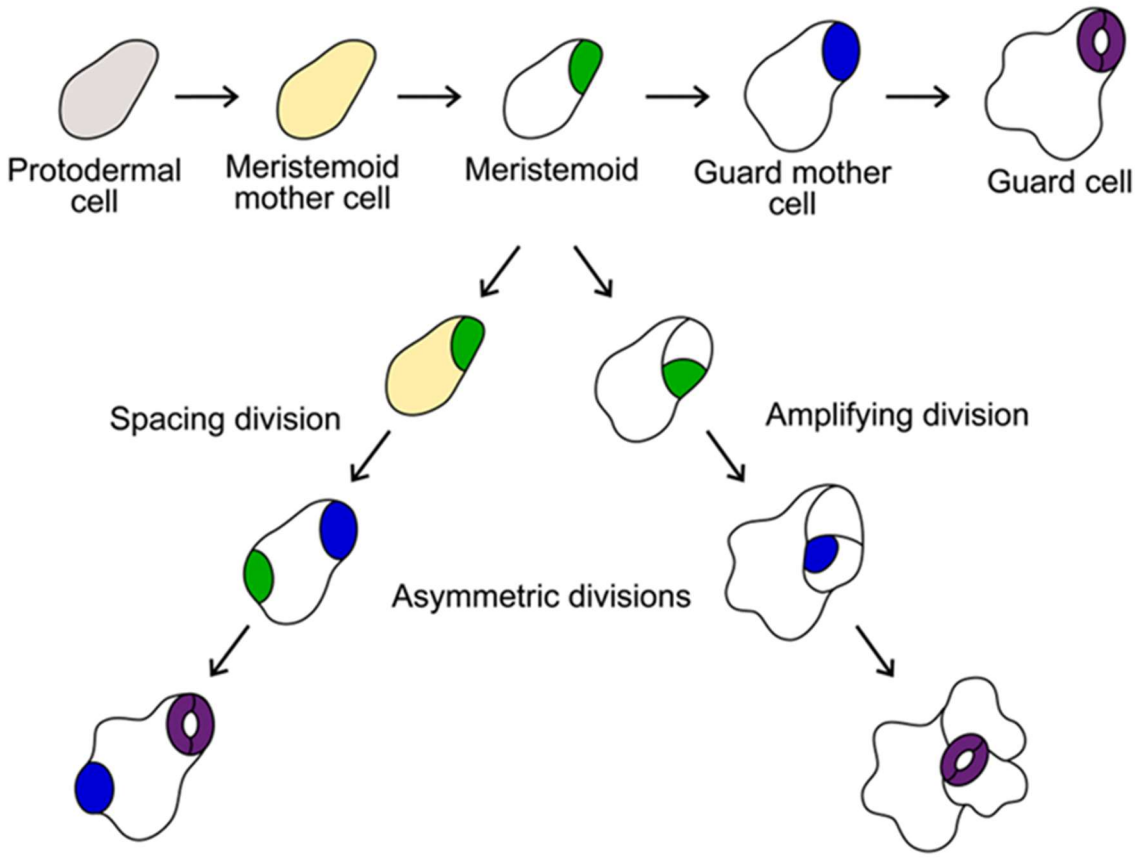

Figure 1.2 Stomatal lineage pathway. The divisions from protodermal cell to forming of the mature stomata and locations of SPCH (green), MUTE (blue) and FAMA (purple) proteins expression during the lineage. Taken from (Zoulias *et al.*, 2018).

1.4 Epidermal patterning

The mature leaf epidermis of Arabidopsis plants consists primarily of stomata and pavement cells arranged in a jigsaw-like structure along with the trichomes. In contrast to this rice stomata are arranged in highly ordered files that develop along the leaf blade (Luo *et al.*, 2012). It is well accepted that MUTE, which controls the division of the GMC to the guard cells, most likely does so by upregulating the expression of cell cycle regulators so that this division can occur (Han *et al.*, 2018). FAMA on the other hand is a negative regulator of cell cycle regulators, preventing the guard cells from dividing further at the end of the lineage (Lai *et al.*, 2005). To prevent two stomata forming next to each other, a rule known as the one cell spacing rule, cells need to communicate with each other (Nadeau and Sack, 2002). A main way in which the cells

communicate are through a small family of peptides, which bind to neighbouring cell receptors. The epidermal patterning factors (EPFs) are released from stomatal lineage cells to discourage neighbouring cells from entering the lineage and therefore promote stomatal lineage ground cell and pavement cell fate. EPF2 is secreted from MMCs and competes with the antagonistic Stomagen/EPFL9 to bind a receptor complex that consists of members of the ERECTA-family of leucine-rich repeat (LRR) receptor-like kinases, the TOO MANY MOUTHS (TMMs) LRR protein and members of the SOMATIC EMBRYOGENESIS RECEPTOR-LIKE KINASE (SERK) family (Lee *et al.*, 2012; Meng *et al.*, 2015). The outcome of this completion for binding determines whether a cell undergoes entry into the stomatal lineage with EPFL9 promoting entry and EPF2 inhibiting this step (Hara *et al.*, 2009; Hunt and Gray, 2009; Lee *et al.*, 2015). Mutation of TMM causes an epidermis with defects in the one cell spacing rule, as evidenced by the appearance of clusters of stomata (Hara *et al.*, 2009). The binding of EPF2 to the ERF/TMM/SERK complex is proposed to lead to activation of a MAP kinase pathway consisting of YODA, MKK4/5 and MPK 3/6. This MAPK cascade results in phosphorylating of SPCH, leading to its eventual degradation (Lampard, Macalister and Bergmann, 2008; Lau *et al.*, 2014). A fellow negative regulator of stomatal development, EPF1 also binds to the receptor complex as part of a complex with ERECTA-LIKE1 (ERL1) (Hara *et al.*, 2007; Lee *et al.*, 2012). Once bound, an EPF1 signal cascade prevents MUTE activity and therefore does not allow cells to transition into the guard cells (Qi *et al.*, 2017).

The cell cycle consists of four stages: Gap 1 (G1), DNA synthesis, Gap 2 (G2) and Mitosis (M) (Harashima, Dissmeyer and Schnittger, 2013). Cells that enter the G1 stage can leave the cycle (termed G0) and go on to differentiate into specialised cell types. DNA synthesis is the replication of DNA that is required when a new cell is forming before the division stage of mitosis (MacAlpine, 2021). The G1 specific cyclin CYCD3;2 has its expression upregulated by SPCH to drive the asymmetric division of the MMC to form the meristemoid and the SLGC (Lau *et al.*, 2014). Some of the key cell cycle regulators are the cyclins/CDKs and the CDK inhibitors with MUTE being shown to bind to the promoter of CYCD5;1, a cyclin that is present in the G1 phase of the cycle and allows the terminal symmetrical division to occur to form a stoma (Harashima, Dissmeyer and Schnittger, 2013; Han *et al.*, 2022; Zuch *et al.*, 2023). MUTE also prevents the asymmetric divisions brought on by SPCH from continuing

by upregulating SIAMESE-RELATED 4 (SMR4) which along with SMR8 inhibits the action of CYCD3;1 but allows the action of CYCD5;1 to regulate the terminal symmetric division (Han *et al.*, 2022). Mutation of the SMR4 gene leads to an accumulation of stomatal lineage precursor cells. A related SMR, SMR1 is also key in the cell cycle progression of self-renewing SLGCs and determines the exit of the SLGC from the cell cycle to irreversibly form pavement cells (Dubois *et al.*, 2023) (Figure 1.4).

The impact of elevated temperature on the leaf epidermis cell cycle has not been largely covered, however while leaf size may be impacted, in order for an impact on the stomatal index, there needs to be changes to the specific mechanisms that impact stomatal development (Sack *et al.*, 2003). One such mechanism predicted for this is the interaction between PHYTOCHROME INTERACTING FACTOR 4 (PIF4) and TEOSINTE BRANCHED1/CYCLOIDEA/PCF4 (TCP4), where TCP4 induces an increase in the transcript levels of PIF4 (Saini, Dwivedi and Ranjan, 2022). PIF4 binds to the promoter of the cell cycle inhibitor KIP-RELATED PROTEIN1 (KRP1) which in turn will inhibit the progression of the cell cycle from G1 by inhibiting both CYDKA;1 and CYCD3;1 (Wang *et al.*, 1998). Increased temperatures have already been shown to increase the expression level of PIF4 and in doing so causes the inhibition of SPCH and therefore reduces the number of stomata (Lau *et al.*, 2018). Therefore, PIF4 may have a two-pronged approach to regulating the divisions under high temperature.

Above ambient temperatures, an E3 ubiquitin ligase, HIGH EXPRESSION OF OSMOTICALLY RESPONSIVE GENES 1 (HOS1) has been shown to bind to and degrade ICE1, preventing it's binding to bHLH transcription factors such as SPCH and therefore not allowing as many cells to enter the stomatal lineage (Lazaro *et al.*, 2012). BRASSINOSTEROID-INSENSITIVE2 (BIN2) can phosphorylate ICE1, which targets it for degradation in a cold dependant manner (K. Ye *et al.*, 2019). Therefore, HOS1 through the action of degrading ICE1 may dictate stomatal patterning in a temperature dependent manner and should be considered in studies into epidermal patterning.

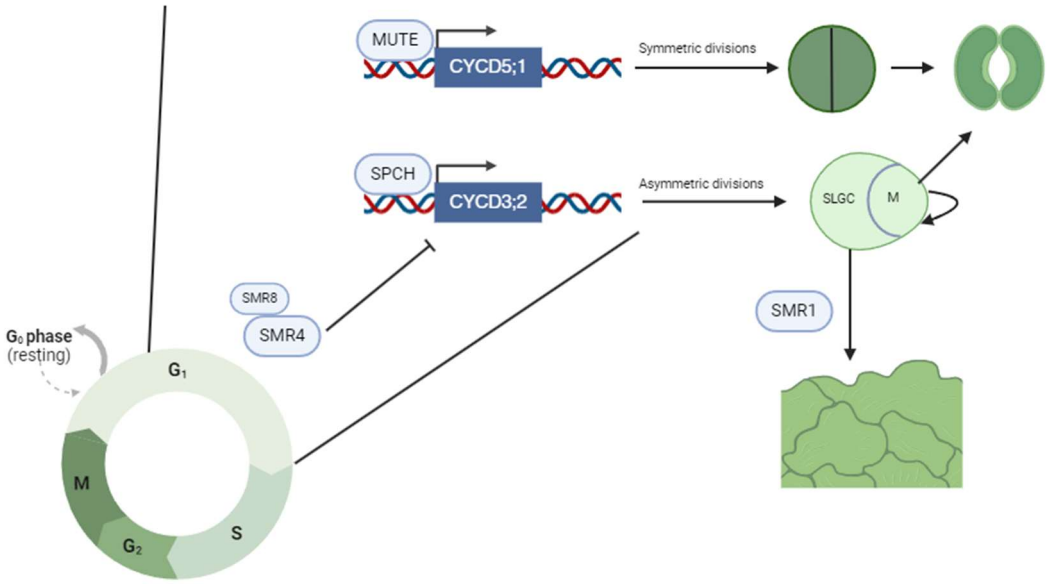

Figure 1.3. Cell cycle regulation in conjunction with SPCH and MUTE of epidermal patterning. Two key cyclins are involved in the determination of cellular fate with SPCH upregulating *CYCD3;1* to allow the asymmetric division to happen and MUTE binding to the promoter of *CYCD5;1* and promoting the final symmetric division to occur. SMR4 and SMR8 work in conjunction to prevent the asymmetric division through inhibition of CYCD3;1 while SMR1 promotes the SLGC to exit the lineage and form a pavement cell. Image created in Biorender.com.

Phyto-hormones have also been shown to be involved in the regulation of stomatal development. Abscisic acid (ABA), brassinosteroids (BRs) and jasmonate (JA) all have been shown to be influencers in stomatal development. ABA inhibits the number of stomata and the size of pavement cells, providing clues to a role in epidermal patterning (Tanaka *et al.*, 2013). ABA may regulate the expression of SPCH and MUTE because in an ABA deficient mutant, *aba2-2*, there were fewer meristemoids and guard mother cells going on to complete the lineage and form mature stomata (Tanaka *et al.*, 2013). ABA requires NAD^+ for biosynthesis and it has been shown that ABA could interact with NAD^+ to regulate stomatal formation. A reduction in the number of NAD^+ transporters reduces the stomatal index and number of cells in the stomatal lineage (Feitosa-Araujo *et al.*, 2020). BRs are positive regulators of stomatal

development, primarily through their regulation of the glycogen synthase kinases (GSKs), such as BIN2, which can target both SPCH and the scaffold protein POLAR, which regulates stomatal patterning (Gudesblat *et al.*, 2012; E.-J. Kim *et al.*, 2023). The inhibition of BIN2 leads to over proliferation of stomata and pavement cells (Gudesblat *et al.*, 2012; E.-J. Kim *et al.*, 2023). The mechanism of this action in the binding of BRs BRASSINOSTEROID INSENSITIVE 1 (BR1) which will recruit BRI-ASSOCIATED RECEPTOR KINASE (BAK1) to the cell membrane and in turn BAK1 inhibits BIN2 (Kinoshita *et al.*, 2005; He, Xu and Li, 2013). Jasmonate has a role in the regulation of the cell cycle. The hormone delays progression through the cycle, from the mitosis to replication stage (Noir *et al.*, 2013). When methylated, MeJA binds to the receptor COL1 and this enables the slowing or repressing of leaf expansion by preventing cells from expanding or dividing by preventing cells from exiting the G1 phase of the cycle (Noir *et al.*, 2013).

1.4.1 Environmental regulation of stomatal development

Plants are sessile organisms and thus, must adapt to their surroundings. Many abiotic factors influence stomatal development. These include light, temperature, carbon dioxide levels, humidity and stresses such as drought (Zhu, 2016). Light is the best understood environmental cue influencing stomatal number with higher light intensities increasing the stomatal density (Schoch, Zinsou and Sibi, 1980; Casson *et al.*, 2009). Evidence for this can be seen when Arabidopsis plants are stimulated to germinate but then grown only in darkness as there are fewer mature stomata developed and many of the earlier lineage cells do not progress (Lee, Jung and Park, 2017). Red, far-red and blue light all have overlapping pathways involved in light regulation of plant development (Wei *et al.*, 2020). This includes the elongation of the hypocotyls and petioles and hyponastic behaviour seen in a wild type (van Zanten *et al.*, 2009). Light signals are sensed, and information is passed on via the photoreceptors which include the phytochromes for red light signalling and the cryptochromes for blue light signalling (Section 1.5) (Galvão and Fankhauser, 2015). Light signalling directly inhibits the action of the negative regulator of stomatal development, PIF4, through the action of the phytochromes (Leivar and Quail, 2011). Two key regulators of stomatal development are influenced by both light and low temperature signals. These are the

basic helix-loop-helix transcription factor ICE1 which is required for stomatal development and the E3 ubiquitin ligase HOS1 which are both also involved in the cold temperature regulation, with HOS1 negatively regulating expression of cold response genes including ICE1 through degradation of ICE1 transcripts (Dong *et al.*, 2006). This prevents the binding of ICE1 to the other bHLHs that are required for stomatal development. ICE1 promotes the activation of cold responsive CBF genes to enable downstream activation of cold responsive genes (Ishitani *et al.*, 1998; Chinnusamy *et al.*, 2003). Warmer temperatures impact upon stomatal development through the key downstream regulator of the phytochromes PIF4, which accumulates under higher temperatures and will inhibit SPCH by binding to its promoter and therefore SPCH transcripts are unable to be formed preventing cells from entering into stomatal lineage (Lau *et al.*, 2018). Stomatal development has recently been shown to be regulated by the redox state of the electron transport chain during photosynthesis. When oxidised, the plastoquinone pool inhibits the action of SPCH and MUTE by preventing their expression through the activation of MPK6 (Zoulias *et al.*, 2021). Other non-photoreceptor driven stomatal regulation include CO_2 driven stomatal development. Mutations in two carbonic anhydrase genes (*ca1 ca4*) increased the number of stomata at higher CO_2 suggesting that the carbonic anhydrase genes prevent stomatal development under increased atmospheric CO_2 (Engineer *et al.*, 2014). The same study also showed that CRSP, a secreted protease, cleaves EPF2 and can inhibit stomatal development (Engineer *et al.*, 2014).

1.5 Photoreceptor regulation of plant development

Photoreceptors are proteins that were first characterised as being involved in light signalling and photomorphogenic growth (Paik and Huq, 2019). There are several classes of photoreceptors in plants that perceive different wavelengths of light and regulate numerous pathways. The cryptochromes, phytochromes and the phototropins all absorb light to regulate plant growth, development and physiology in overlapping pathways (Galvão and Fankhauser, 2015). There are three groups of blue/UV-A light perceiving photoreceptors: the cryptochromes (CRY1 and CRY2) as well as the ZEITLUPE (ZTL)/FLAVIN-BINDING, KELCH REPEAT, F-BOX1 (FKF1)/ LOV kelch protein 2 (LKP2) (Sawa *et al.*, 2007; Liu *et al.*, 2011). The blue/UV-A

receptors regulate various processes including flowering time and stomatal development (Huché-Thélier *et al.*, 2016). CRYs and PHOTs also function to regulate stomatal opening, though in this case this is primarily a PHOT driven process (Kinoshita *et al.*, 2005; Rizzini *et al.*, 2011; F. Wang *et al.*, 2020). Phytochromes are red-light/far-red light sensing photoreceptors. There are 5 phytochromes in Arabidopsis (phyA-E) and 3 within monocotyledons such as rice (phyA-C) (Bae and Choi, 2008; Li *et al.*, 2015). Phytochrome apoproteins are translated in the cytoplasm and here, bind to their chromophore, phytochromobilin (Rockwell, Su and Lagarias, 2006). Functional phytochromes exist as dimers and these can either be homodimers or heterodimers; for example phyC and phyE can only form heterodimers with phyB and phyD respectively (Sharrock and Clack, 2004; Clack *et al.*, 2009). Phytochromes are synthesised in an inactive, red light absorbing Pr form, which exists in the cytoplasm. Upon absorbance of R light, this leads to a conformational change that, in the case of PhyB-E leads to exposure of a presumptive nuclear localisation signal and translocation in the nucleus where they can become sequestered in photobodies (Chen *et al.*, 2005, 2022; Rockwell, Su and Lagarias, 2006; C. Kim *et al.*, 2023). These light-light phase separated droplets contain multiple factors that the phytochromes can interact with to regulate the expression of genes involved in light responsive developmental and growth pathways (C. Kim *et al.*, 2023). The conversion of the Pr form into the biologically active Pfr form is reversible; photoconversion can occur if the Pfr form absorbs far-red light (wavelength 705-740 nm) or can occur more slowly in darkness (Quail, 1997). Recently, the phytochromes have been shown to be impacted by temperature, with higher temperatures leading to a fast reversion back to the inactive Pr form from the Pfr form in a process called thermal reversion. Thermal reversion works by speeding up the kinetics of the Pfr:Pfr homodimer to the Pfr:Pr heterodimer (Legris *et al.*, 2016; Legris, Ince and Fankhauser, 2019). As discussed, darkness also reverts the active Pfr back to the inactive form in a process called dark reversion although the kinetics are slower than for thermal reversion. Therefore, throughout the night there is a slow depletion of phy Pfr, which is exacerbated when warmer nights occur, meaning plants grown under longer term higher night temperatures may have fewer stomata due to the faster thermal reversion occurring which, in the case of phyB, could lead to increased PIF4 activity, reducing SPCH and enable plants to be more water use efficient as a result (Lau *et al.*, 2018). Light and

temperature, therefore, have an impact on the equilibrium between the active and inactive states of phys and their downstream signalling (Figure 1.5).

Each of the five phytochromes in Arabidopsis have distinct roles, although some have been studied more extensively than the others have. phyA is light labile type I phytochrome that is able to sense far-red light and initiate responses to it and is shuttled into the nucleus through the proteins FHY1 and FHL (Genoud *et al.*, 2008; Yang *et al.*, 2009). The other phytochromes (B-E) are type II and of these, phyB is the most well characterised. phyB consists of a phytochromobilin chromophore at the N-terminus of the protein, while the C-terminus allows protein interactions and the binding of another monomer to form the dimer (Rockwell, Su and Lagarias, 2006). *phyB* mutants display a number of phenotypes; they flower earlier under both long and short days, in part due to the HOS1 driven morning degradation of CONSTANS (CO) (Putterill *et al.*, 1995; Lazaro *et al.*, 2012) and their leaves have fewer stomata and contain less chlorophyll than the corresponding wild-type plants (Casson and Hetherington, 2014; Inagaki *et al.*, 2015). They also have longer hypocotyls and hyponastic growth regardless of the temperature that they are grown at (Gray *et al.*, 1998; Koini *et al.*, 2009). phyC may work in tandem with phyB and has also been shown to potentially have a role in perceiving day length (Monte *et al.*, 2003). phyD and phyE are similar in structure to phyB, however less is known about their functions, although they have been shown to act redundantly with phyB to regulate developmental processes (Franklin *et al.*, 2003). In fact, phyD is very similar in structure to phyB, suggesting phyB underwent a recent gene duplication event (Clack, Mathews and Sharrock, 1994).

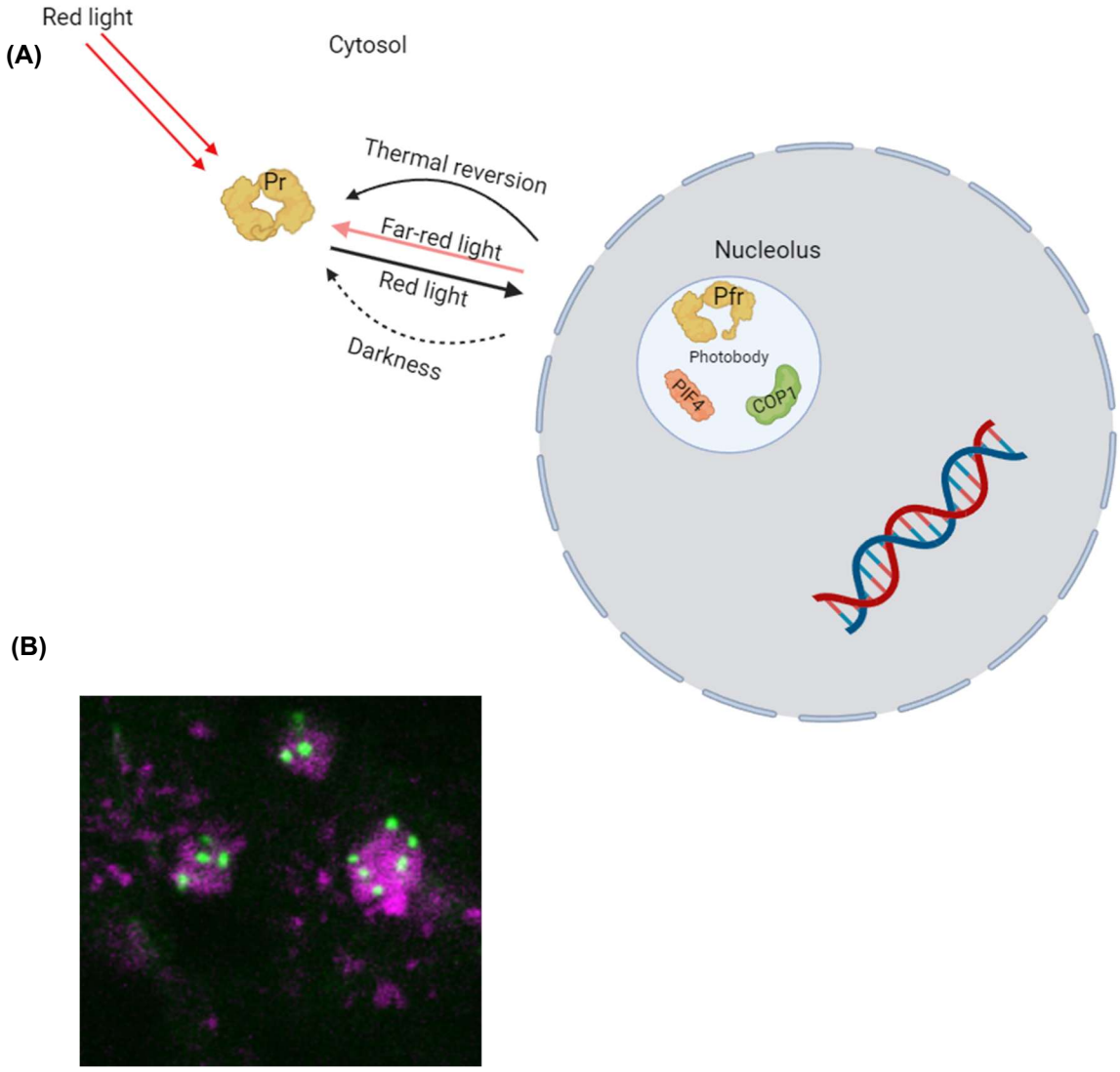

Figure 1.4 The activation and reversion of phyB and its sequestration into photobodies in the cytosol. (A) Red light absorption by the chromophore of phyB causes a conformational change to expose the nuclear localisation signal and allows the entry into the nucleus within the liquid-liquid phase separated photobodies where it can interact with other proteins and DNA via its interactions. Far-red light and darkness revert the active Pfr form back to the inactive Pr form and higher temperatures cause a fast thermal reversion inactivating the Pfr phyB. Image created in Biorender.com. **(B)** Confocal microscopic image of GFP tagged phyB sequestered in photobodies in the nucleus (stained pink) (Image from Stuart Casson, University of Sheffield).

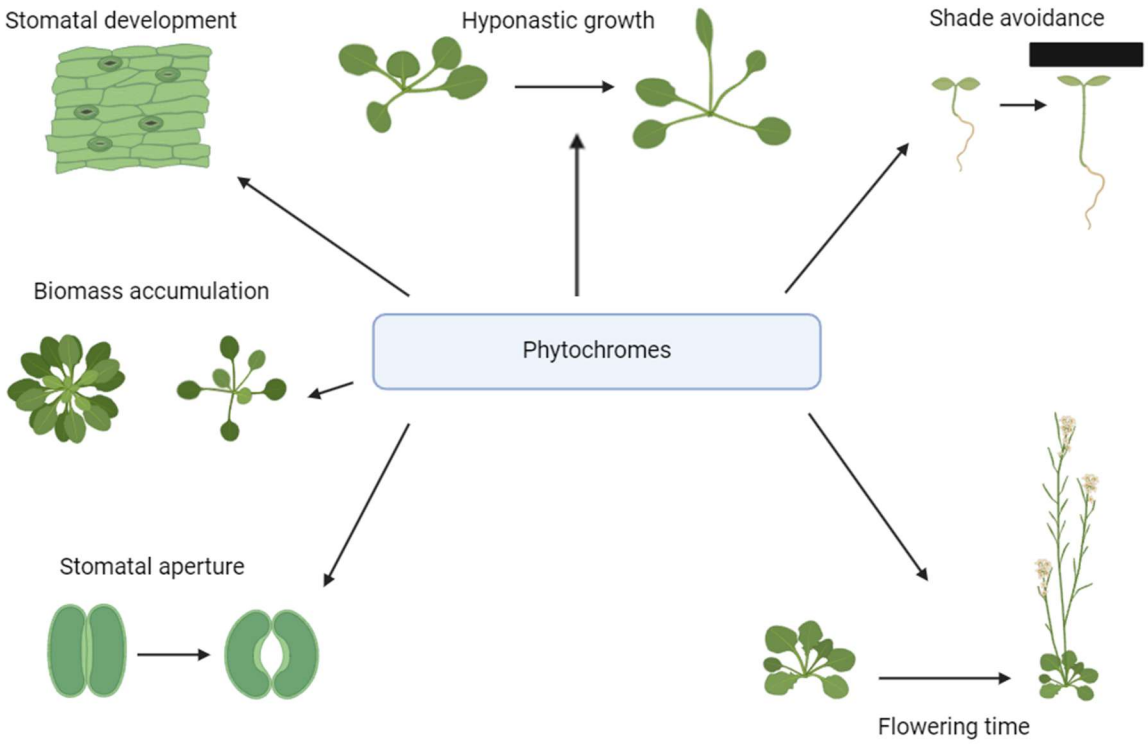

Figure 1.5. The role of phytochromes in regulating plant development and physiology. The phytochromes have several key roles in regula ting plant development and physiology such as flowering time, stomatal opening and development, biomass accumulation, hyponastic growth and shade avoidance responses. Created in Biorender.com.

1.5.1 Temperature regulation of phytochrome B

Due to the impact of higher temperatures on thermal reversion rates, it has been proposed that the phytochromes could function as a temperature sensor (Jung *et al.*, 2016; Legris *et al.*, 2016). This was demonstrated by looking at the change in absorbance levels for the phytochromobilin chromophore of phyB at 665nm and 725nm, which reflects the amount to Pfr, under either higher or lower temperatures, it was shown that the rate of transition from the Pfr:Pr heterodimer to the Pr:Pr homodimer increased significantly under higher temperatures, a change that was attributed to thermal reversion (Legris et al., 2016). The same results are shown when viewing the amount of Pfr present in photobodies under in vivo spectroscopy while changing temperatures (Legris et al., 2016). This shows that temperature does influence the sensitive balance between the amount of active and inactive

phytochromes. However, whether the phytochromes are “true” temperature sensors is still open for debate, though plants grown at higher temperatures phenocopy the elongated hypocotyl and petioles of phytochrome mutants (Koini *et al.*, 2009). It may be that temperatures are affecting the levels of active phytochromes without a subsequent change in signalling through phytochromes. As the pool of Pr:Pfr is influenced by environmental conditions it is no surprise that during the night, the equilibrium will shift so the dominant form becomes Pr. However, the Pfr form can persist in the population for hours due to the slow dark reversion process (Klose, Nagy and Schäfer, 2020). Higher night-time temperatures will lead to a faster shift of equilibrium from the Pfr to Pr state due to increased thermal reversion (Legris *et al.*, 2016; Murcia *et al.*, 2021) (Figure 1.6). Due to its involvement in many developmental and physiological processes, increased temperatures over a longer term, leading to regular reductions in the pool of active phyB may have a greater impact on developmental processes in plants than the other phytochromes. Recently, a protein called PCH1 has been shown to bind to and stabilise the Pfr state in darkness, which allows phyB Pfr to persevere and hence, carry on regulating multiple pathways in darkness (Huang *et al.*, 2016). The closely related protein PCHL1 also directly binds the Pfr form and most likely carries out the same function as PCH1 (Enderle *et al.*, 2017). These studies show a more complicated reality of the activity of phyB under light and darkness. PCH1 transcript levels will be at their highest at sunset, therefore allowing the balance between Pr:Pfr to remain edged towards the Pfr having the greater presence at the beginning of the evening (Huang et al., 2016).

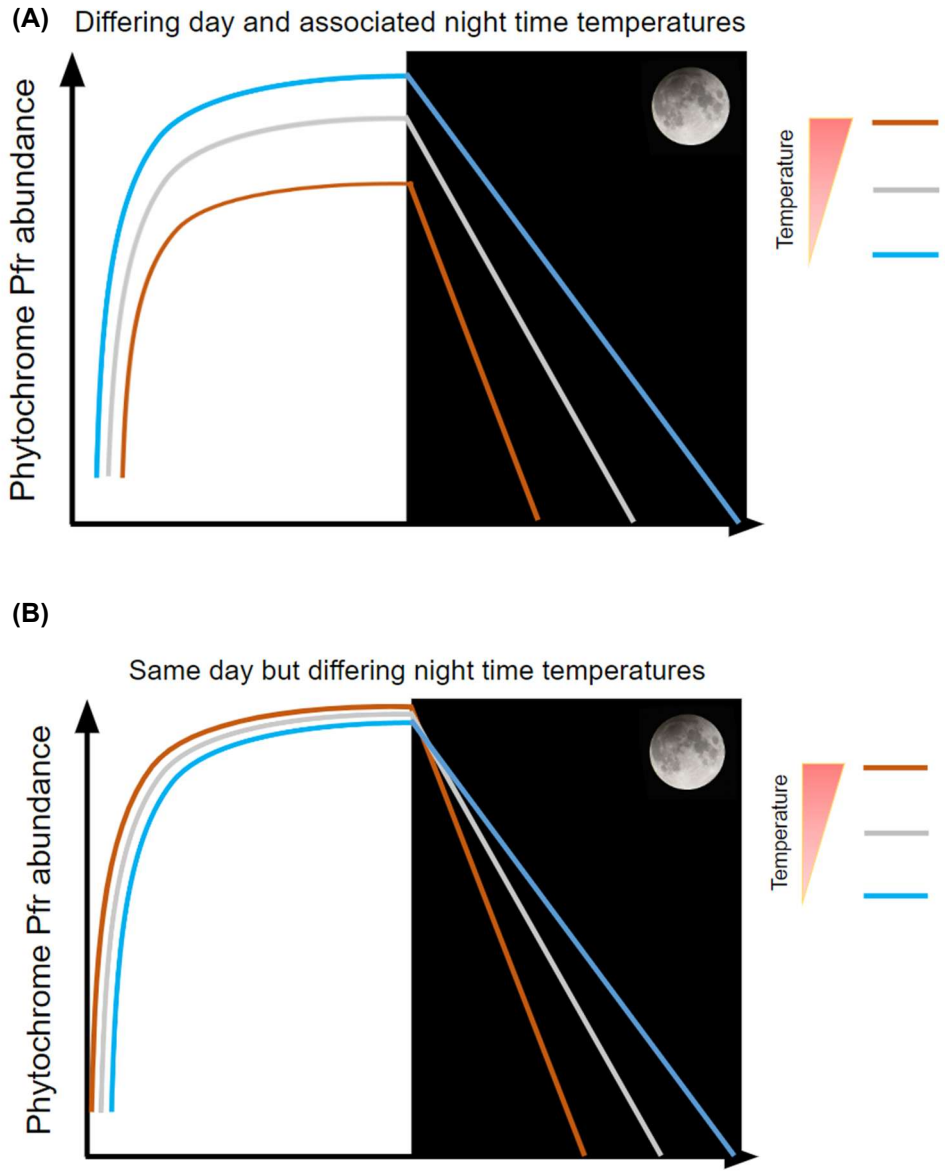

Figure 1.6 Levels of active phytochrome (Pfr) throughout 24 hours. (A) In a scenario where irradiance is constant but there are different day temperatures and night temperatures, there would be an increase in the levels of Pfr during the day due to light activation. Under a colder day (blue line) more Pfr would accumulate, ambient (grey line) intermediate levels would accumulate and warmer day (red line) fewer Pfr would accumulate. During the night thermal reversion would mean that the Pfr levels would decrease faster in a high night temperature case compared to cooler temperatures. **(B)** Example of the impact of thermal reversion on Pfr levels during the night, when the temperature is the same during the day. Adapted from (Klose, Nagy and Schäfer, 2020). Images created in Biorender.com

1.5.2 Phytochrome regulation of stomatal development

Phytochromes regulate stomatal development in several ways (Figure 1.7). One such way is via promoting the degradation of PIF4 within the photobodies, causing the likely co-degradation of both the PIF4 and the phytochromes and therefore preventing it from inhibiting the SPCH mediated entry of cells into the stomatal lineage in a temperature dependant manner (Lau *et al.*, 2018). PIF4 has been shown to be required for normal growth and development under elevated temperature and *pif4* mutants lack thermoresponsive phenotypes (Koini *et al.*, 2009). Higher temperatures lead to more PIF4 activity possibly due to enhanced thermal reversion of phyB. There have been suggestions that PIF4 may affect the kinetics of thermal reversion of phyB, possibly through the action of PIF6; however, this has only been shown in vitro (Smith *et al.*, 2017).

Another way phyB positively impacts stomatal development is the inhibition of the E3 ubiquitin ligase COP1, by preventing the interaction between COP1 and SUPPRESSOR OF PHYA-105 (SPA1). It does this by competitively binding to SPA1 (Sheerin *et al.*, 2015). The COP1/SPA1 complex, when active, is known to target ICE1 for degradation by the proteasome and as discussed earlier, ICE1 is a key regulator of stomatal development (Lee et al. 2017). Further evidence that COP1 levels are reduced when phyB is active is that COP1 activity is increased in darkness compared to when in light, showing a light mediated repression of its activity (Osterlund, Ang and Deng, 1999). As stated earlier, another E3 ubiquitin ligase HOS1 could be involved in temperature regulation of stomatal development through the degradation of ICE1 (Dong *et al.*, 2006).

As phyB regulates stomatal development, it would be expected that a mutation of phyB would lead to fewer stomata and more water use efficient plants as a result. Also, with the process of thermal reversion, higher temperatures could mimic a phy mutant and may reduce the number of stomata in a wild type. Previous work from the Casson lab in *phyB-9* and in *phyB-5* from a Ler background show that these mutants are more water use efficient over their lifetimes compared to wild-type under certain temperature conditions (Boccalandro *et al.*, 2009; Brown, 2018).

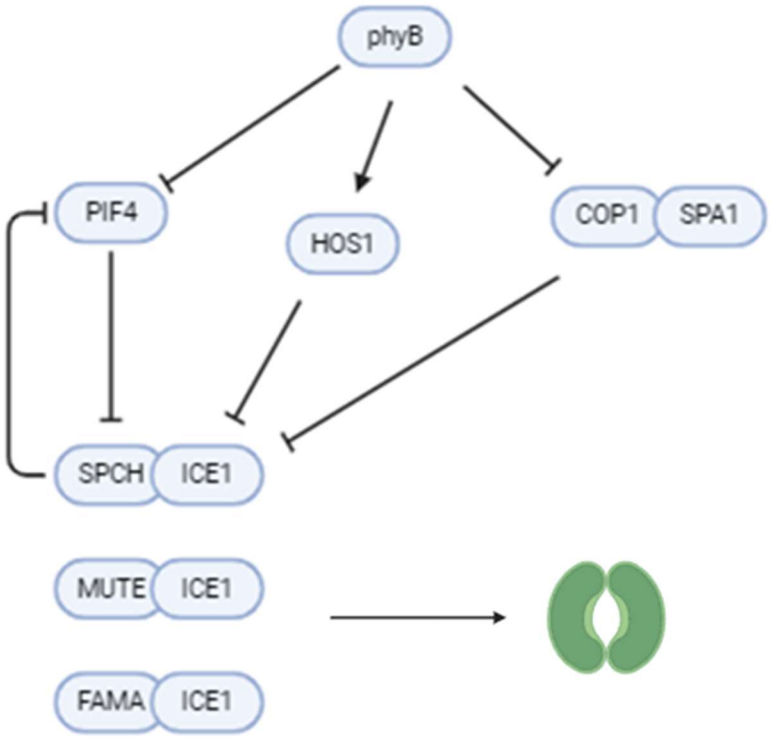

Figure 1.7 The genes involved in stomatal development regulation. Once phyB is activated by red light, it can inhibit PIF4 and COP1/SPA which are negative regulators of stomatal development by either inhibiting SPCH and degrading ICE1 respectively. HOS1 is activated by phyB to degrade ICE1 under certain environmental conditions. Made in Biorender.com.

1.5.3 Phytochromes and stomatal opening

Despite the general view that red light opening of stomata is mediated by photosynthetic signals, there is evidence that phyB is also important for stomatal opening in the presence of red light (Fang-Fang *et al.*, 2010). Therefore, collectively, *phyB* mutants have a reduced number of stomata but also reduced stomatal apertures compared to wild type plants. There seemed to be little influence of phyB opening stomata in darkness, most likely because of the reduction of active phyB Pfr due to dark reversion (Fang-Fang *et al.*, 2010). The stomatal opening is controlled along with the cryptochromes and phototropins, other light photoreceptors. The triple mutant of *cry1cry2phyB* opens less fully than the *phyB* and *cry1cry2* mutants respectively (Wang

et al., 2010). COP1 and PIF4 may act downstream of phyB to affect stomatal opening, with PIF4 preventing stomatal opening. ELONGATED HYPOCOTYL5 (HY5) targets PIF4 for degradation in the light and therefore could have an influence upon stomatal opening (Toledo-Ortiz *et al.*, 2014).

1.5.4 Phytochrome regulation of plant growth

The phytochromes feed in light information not just to help regulate stomatal development but also to influence growth. This can be seen with progressively higher order phytochrome mutants of Arabidopsis having reductions in biomass, and a phyQ (all five phytochromes mutated in Arabidopsis) generates only a few small leaves with extremely early flowering (Hu *et al.*, 2013). Seedlings exposed to light undergo a process called photomorphogenesis, which is presented during early seedling development by an inhibition of elongation of the hypocotyl and an initiation of leaf development. The phytochromes, namely phyB feed cues into transcriptional networks to enable photomorphogenic growth to occur, partially through the inhibition of inhibitors of photomorphogenesis, including PIF4. Under increased temperatures, PIF4 mRNA accumulates in part, due to the lack of binding of the evening complex proteins to the promoter of PIF4 (Nieto *et al.*, 2015; Li *et al.*, 2024). PIF4 activates auxin biosynthesis genes and growth promoting genes and other genes involved with the regulation of elongation of hypocotyls and hyponastic growth (Koini *et al.*, 2009). It has been shown that HOS1 will inhibit the transcriptional activity of PIF4 to prevent large amounts accumulating under light conditions. HOS1 does this when activated by phyB under light conditions (Kim *et al.*, 2017).

Plant architecture within a canopy also influences how much light neighbouring plants receive and angle of leaves could influence how much water is lost due to external factors such as wind. This is because in a hyponastic system with angled leaves, airflow can more easily remove water from the soil level if leaves are angled rather than flat. Increased temperatures lead to a lower biomass and often-smaller leaves, whereas lower temperatures often lead to greater biomass and larger leaves (Koini *et al.*, 2009).

1.6 Phytochrome regulation of flowering

Arabidopsis is a facultative long day flowering plant that will flower after perceiving day length through photoreceptors, primarily both the phytochromes and cryptochromes (Mockler *et al.*, 2003). Flowering in Arabidopsis is defined by the emergence of a bolt, which is the beginning of the stem from the rosette and marks the transition from vegetative to reproductive growth, with the shoot apical meristem converting to an inflorescence meristem (Jacqmard, Gadisseur and Bernier, 2003; Kinoshita *et al.*, 2020). Flowering is not only regulated by light cues contributing to day length but also temperature. Warmer temperatures will accelerate flowering and elongate growth of the hypocotyl and petioles (Gray *et al.*, 1998). There are several pathways leading to the control of flowering, including the temperature regulation of flowering is the process of vernalisation, whereby plants will flower after a prolonged period of cold (Lang and Nitsch, 1965). Another key component of flowering time is the circadian clock, a group of proteins that perceive light cues through photoreceptors and regulate key flowering genes such as CONSTANS (CO), which in turn regulates FLOWERING LOCUS T (FT) (Yanovsky and Kay, 2002; Halliday *et al.*, 2003). FT is also known as a florigen, and is a long-range signal expressed in leaves that integrates multiple flowering pathways (Mathieu *et al.*, 2007). Different ecotypes of Arabidopsis flower at different times of year and this is largely due to the presence of FLOWERING LOCUS C (FLC) and FRIDIGA (FRI). Vernalisation requires functional alleles of both FRI and FLC with FRI regulating the expression of *FLC* that inhibits the expression of flowering genes (Shindo *et al.*, 2005). Ecotypes such as Col-0 and Ler, have null or weak alleles of FRI or FLC respectively and hence do not require vernalisation in order to undergo the transition to flowering (Johanson *et al.*, 2000; Michaels *et al.*, 2003). FLC generates a MADS-box transcription factor that will repress FT and therefore prolong flowering (Michaels and Amasino, 1999; Searle *et al.*, 2006). Not only are the phytochromes key components of the stomatal development pathway, they are also involved in the flowering pathway. This can be seen in the mutation of phyB, which leads to accelerated flowering (Halliday *et al.*, 2003). phyB feed cues into the circadian clock, and directly regulates the flowering time pathway through interactions with FT (Endo *et al.*, 2013). The same interaction has been seen between phyB and FT orthologues in rice (Izawa *et al.*, 2002). Active phyB delays flowering by destabilising CO protein, allowing its degradation through the action of HOS1, preventing it from upregulating

FT which is required for earlier flowering (Lazaro *et al.*, 2012; Endo *et al.*, 2013). Equally, another E3 ubiquitin ligase, COP1 degrades CO during the night, in a process independent of light, unlike during the morning in which is likely to involve the action of phyB (Jang *et al.*, 2008). The exact mechanism for phyB regulation of CO stability in the morning is thought to include a role for the protein PHYTOCHROME-DEPENDENT LATE-FLOWERING (PHL) which will physically interact with phyB and inhibit downstream signalling (Endo *et al.*, 2013). Similarly, to that of CO protein levels, levels of PHL are decreased upon light exposure suggesting a role for photoreceptors in de-stabilising the protein during the day (Endo *et al.*, 2014). SPATULA (SPT) has a direct interaction with phyB and when mutated has a similar early flowering phenotype as phyB (Wu *et al.*, 2018).

PIF4 also regulates *FT* expression in a temperature dependent manner (Kumar *et al.*, 2012). Under higher temperatures, the chromatin around the *FT* promoter is de-repressed to allow DNA binding of PIF4, with PIF4 levels controlled in part by the action of the DELLA proteins and therefore influenced by gibberellin (Kumar *et al.*, 2012).

Similar pathways with many orthologues of the genes found in the flowering of Arabidopsis have also been found to be regulating flowering in rice plants. However, flowering in rice is complicated by the fact that it can flower under both short and long days using pathways that are integrated with each other although also independent (Ishikawa *et al.*, 2009). As there are three phytochromes in rice rather than the five found in Arabidopsis, the role of phytochromes in flowering may be different (Takano *et al.*, 2005). However, the role of phyB in the flowering time pathway is thought to be conserved across flowering plants (Cerdán and Chory, 2003). Related orthologues to FT and CO have been discovered in rice that carry out the same function as in Arabidopsis (Yano *et al.*, 2000; Kojima *et al.*, 2002).

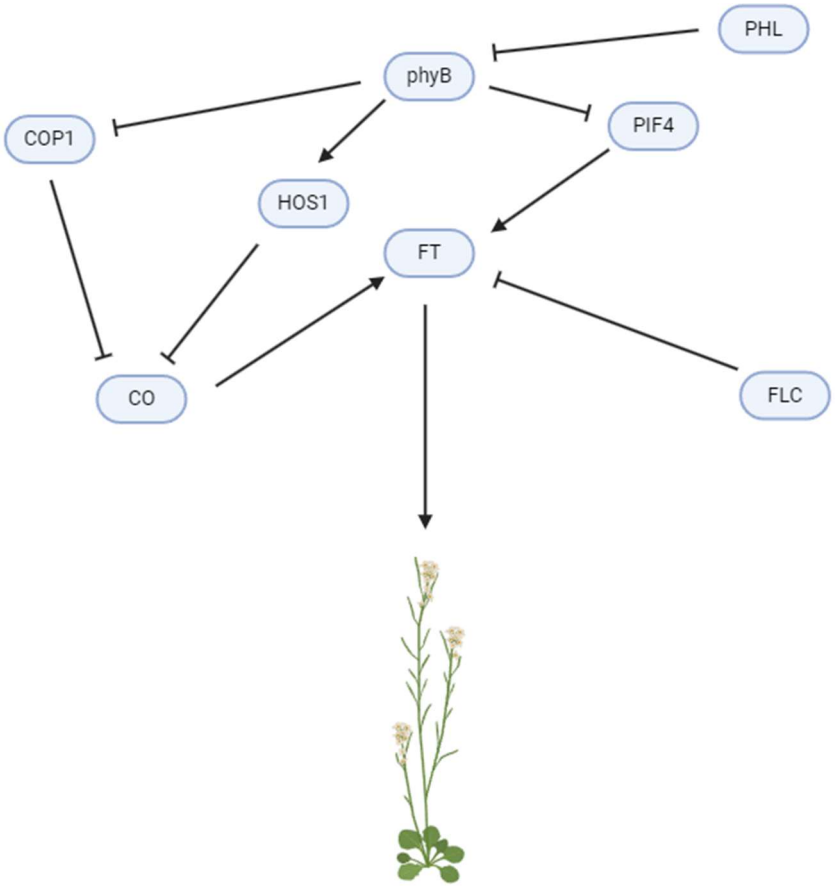

Figure 1.8. Genetic pathway showing the key genes involved in regulating flowering time. Phytochrome B is a key regulator of flowering time through its indirect targeted binding of FT and targeted degradation of CO through the E3 ubiquitin ligase. Created in Biorender.com.

1.6.1 Flowering time and water use

Flowering time has a positive correlation with water use, generally, the later a plant flowers, the better its lifetime water use efficiency (Kenney *et al.*, 2014; Kazan and Lyons, 2016; Ferguson *et al.*, 2019). This could be because more of the water taken up by the plant is being used in metabolic reactions during respiration or photosynthesis to improve plant growth and add greater biomass. An alternative could be that this is the case because plants that flower earlier are more likely to be grown under stressful environments such as drought, and flowering earlier is a way to escape stress and produce seed that is more likely to survive. From a genetic basis, the circadian clock genes contribute to lifetime WUE such as mutations in ELF3 contributing to a lower WUE than the background Col-0 (Simon *et al.*, 2020). High levels of expression of phyB over the lifetime of a plant increases the number of

stomata, which in turn should increase both the assimilation levels and stomatal conductance. However, considering most of the water taken up by the plant is lost through the stomata, an increase in the number of stomata could consequently reduce the WUE of a plant (Pei *et al.*, 1998).

1.7 Flowering and water use in rice

As rice is one of the most consumed crops across the globe, it is vital that these crops can be protected or enhanced to survive under growth conditions with higher temperatures and less water availability. In most cases, rice is grown in flooded paddy fields where large amounts of water is required for healthy growth and yield. Many growth practices have been developed to save water including alternate wetting and drying (Bouman and Tuong, 2001). Beyond water, there are many important nutrients to enable healthy growth. In all crops, nitrogen is vital for healthy plant growth and development, supporting growth and seed synthesis and is the most abundant macronutrient in plants (Frink, Waggoner and Ausubel, 1999; Crawford and Forde, 2002). However, because of the anaerobic conditions flood grown rice thrive under, there is limited nitrogen compounds available in the soil (Gu and Yang, 2022). Therefore, nitrogen-based fertilisers are used to supplement this lack of uptake and they play an important role in ensuring flowering occurs (Makino, 2011). While flowering in Arabidopsis is defined as the emergence of the bolt from the rosette, flowering in rice is defined as the appearance of the first panicle. High or low levels of fertiliser application in rice lead to accelerated flowering (Zhang *et al.*, 2021). Few studies have been undertaken to determine the role of phytochromes in regulating nitrogen responses in crops such as rice. Like in Arabidopsis, *phyB* mutants in rice flowers earlier and have visibly less chlorophyll content in their leaves (Reed *et al.*, 1993; Osugi *et al.*, 2011). Previous studies have suggested that the wild type ecotype in rice Nipponbare requires nitrogen in order to flower whereas *phyB* mutants flower regardless of whether fertiliser is added or not (Mawodza, 2019). This makes it intriguing to study the impacts of nitrogen combined with the impact of a *phyB* mutation. Stomata in rice are structurally distinct from their Arabidopsis counterparts, as they are arranged in files and have a different structure of stomatal complex as well by having flanking subsidiary cells. Recently, studies have shown that there is a link

between stomatal opening and nitrogen assimilation through the transcription factor drought and salt tolerance (DSR) (Han *et al.*, 2022). DSR has roles in regulating stomatal opening and nitrogen use efficiency (NUE) through the regulation of OsNR1.2, an NADH nitrogen receptor. When plants are under osmotic stress, there is stomatal closure to prevent any water that the plant uptakes being lost through transpiration, whereas when there is sufficient water, the stomata can be open. The more open the stomata the more carbon assimilation from the atmosphere and this directly relates to nitrogen assimilation as more carbon fixation requires a higher uptake of nitrogen from the soil to help generate tissues (Han *et al.*, 2022).

1.8 Phytochromes and photosynthesis

The phytochromes are the main ways in which red light information is fed to a plant. Therefore, they are important to photosynthesis which can be seen in the chlorophyll synthesis impact of *phyB* mutants which have a pale green leaf phenotype in both Arabidopsis and rice plants (Reed *et al.*, 1993; Inagaki *et al.*, 2015). PHYTOCHROME INTERACTING FACTOR 3 (PIF3) has been shown to be a negative regulator of chlorophyll biosynthesis and photosynthetic genes in etiolated seedlings, and on exposure to light, PIF3 is targeted for degradation in a phytochrome dependent manner (Stephenson, Fankhauser and Terry, 2009; Liu *et al.*, 2013; Dong *et al.*, 2017). However, the role of phyB in regulating these processes has been complicated by the fact that the specific phyB mutation *phyB-9,* which is used in most phytochromes studies, has a secondary mutation site in a gene called *VENOSA4*, which impacts upon leaf size and chlorophyll content (Yoshida *et al.*, 2018). The main damage caused by external stimuli, to the photosynthesis proteins and chaperones is due to increased levels of reactive oxygen species (ROS) under stressful conditions such as high light and ultraviolet radiation (UV) (Kreslavski *et al.*, 2018). The phytochromes, specifically phyB, have a key role in protecting the photosynthetic apparatus under damaging UV light. UV radiation degrades the amount of chlorophyll a and b pigments in a rapid fashion; however, the process is slowed under just a small illumination under red light, suggesting that the phytochromes may protect these pigments (Joshi, Biswal and Biswal, 1991). The mechanism behind this phytochrome mediated protection of the photosynthetic apparatus is believed to be due to an increase in the number of

protective proteins and antioxidant enzymes being produced which lowers the pool of ROS (Kreslavski *et al.*, 2018).

1.9 Research aims and objectives

The general aims of this project were as follows:

1. Investigate how temperatures affect the activity of phytochromes in regulating stomatal development, flowering, growth and water use.
2. To study the impact of increased temperatures on epidermal patterning in Arabidopsis.
3. To study the physiological effects of nutrient application upon both wild type and *OsphyB-1* mutants in rice.

To carry out these aims the following objectives were set out:

1. Analyse the stomatal density and water use efficiency of several phytochrome mutants with decreasing phytochrome activity that could be involved in a temperature-mediated response.
2. Analyse the molecular basis of stomatal and pavement cell patterning of the leaf epidermis under increased night temperatures using genetic approaches.
3. Use physiological methods such as thermal imaging, IRGA and fluorpen measurements to determine the impact of temperatures upon transpiration and photosynthesis.
4. Measure flowering time and photosynthetic parameters in rice under different nutrient regimes and determine yield impacts in rice wild type and *phyB* mutants.

Chapter 2: Materials and Methods

2.1 Seed and Chemical use

2.1.1 *Arabidopsis thaliana* and Rice (*O.sativa)*

Arabidopsis seed of background Columbia was used unless stated. Mutant lines are presented in Table 2.1. Rice seed of background Nipponbare was use in all experiments and mutant lines are presented in Table 2.2. Photos of individual lines both wild-type and mutant were taken (Figure 2.1).

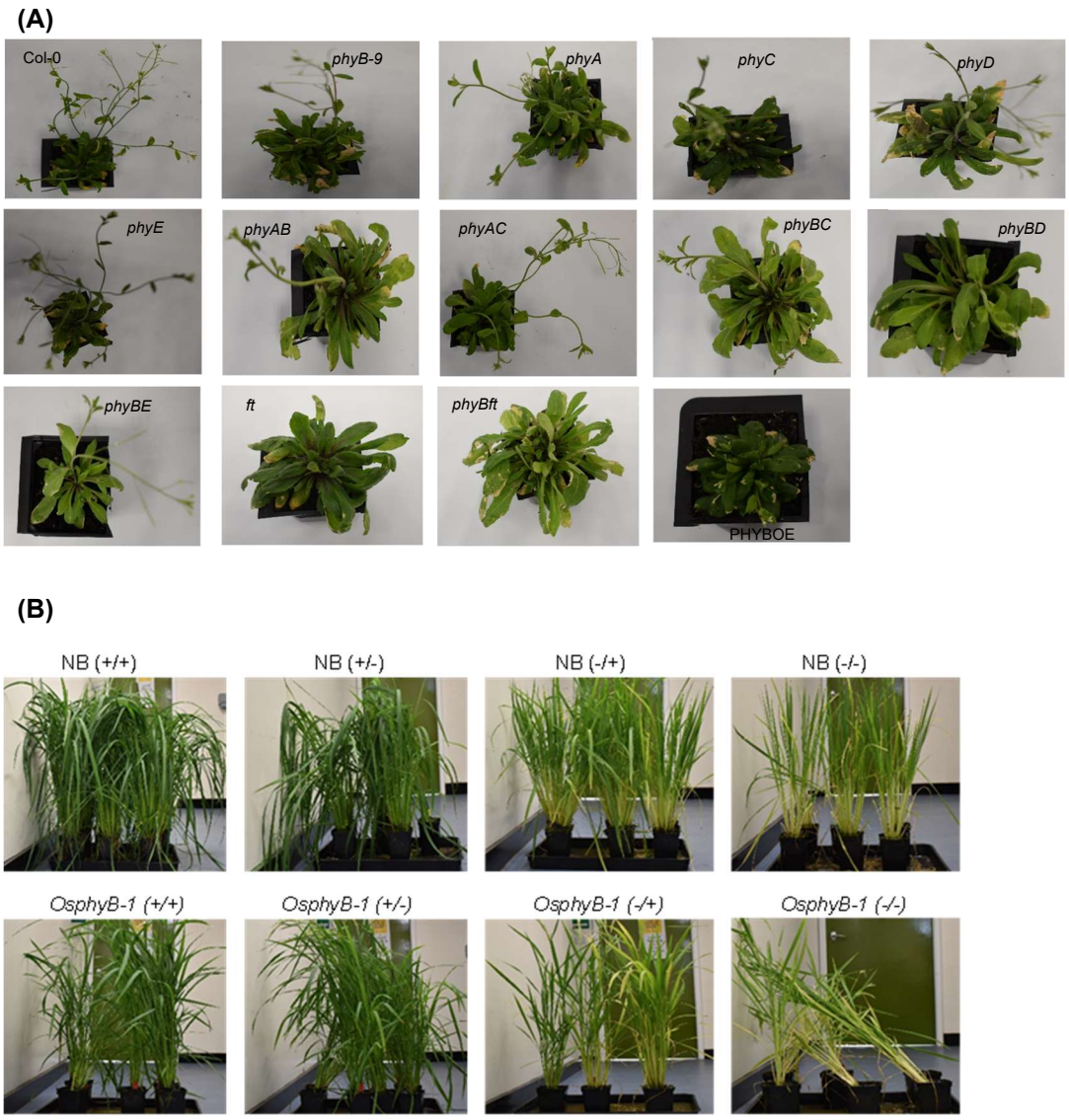

Figure 2.1. Photos taken of individual Arabidopsis and rice mutants used in this study. (A) Individual photos of Arabidopsis lines used in this study. **(B)** Photos of rice lines used in this study.

2.1.2 Laboratory chemical use

Unless stated otherwise, all chemicals used in these studies are either from Merck or Fisher Scientific.

2.2 Plant growth conditions

2.2.1 Arabidopsis plant husbandry and growth conditions

Arabidopsis thaliana seed, both wild type ecotypes and mutants, were either sown on Levington's F2+Sand®, Everris Professional compost or grown in tissue culture and allowed to stratify in darkness at 4°C for 2-3 days. Once stratified, they were either placed into a Sanyo-Gallenkamp SGC970/P/PLL with the following conditions: 11h photoperiod, 22°C day/night temperature, ambient CO_2 (~450ppm), relative humidity of 65% and a light level of photosynthetic active radiation (PAR) of 150 ± 20$\mu molm^{-2}s^{-1}$. Or transferred to a PGR15 Conviron (Controlled Environments Ltd, Winnipeg, MB, Canada) chamber with ambient CO_2 (~450ppm), 250$\mu molm^{-2}s^{-1}$ white light, a relative humidity of 65% and a 12h photoperiod. Light levels were checked periodically with a light meter (Apogee Model MQ-200 Quantum meter).

While the standard temperature used was 22°C/16°C (day/night) or 22°C, temperature conditions were dependent on experiments, and some had temperature regimes of 24°C day and 20°C night as well as the reverse 20°C day and 24°C night.

To carry out the far-red experiment, 50$\mu molm^{-2}s^{-1}$ far-red light (FR) was supplemented into the last 10 mins of the photoperiod on top of the 250$\mu molm^{-2}s^{-1}$. This amount of FR was chosen as it should be enough to cause reversion of the phytochromes from the Pfr form back to the Pr form, mimicking an HNT. However, different studies use differing levels of FR light (Devlin *et al.*, 1996; Devlin, Patel and Whitelam, 1998) and so the upper end of the range was used to ensure the FR had an impact.

Name	Ecotype/Allele	Notes
Col-0	Columbia-0	Casson Laboratory stocks
Ler	Landsberg erecta	Casson Laboratory stocks
phyB	Col-0/*phyB-9* (NASC_N6217)	(Reed et al., 1993)
phyA	salk_014575	
phyC	*phyC-2* (salk_057517)	
phyD	salk_027956	
phyE	salk_092529	
phyAB		
phyBC		
phyBD		This study
phyBE		This study
phyBft		
PHYBOE		Casson laboratory stocks
ft	GK-290E08	
pif4	*pif4-101* (SAIL_1288_E07)	
hos1	*hos1-3*	(Lazaro *et al.*, 2012)
hos1phyB	*hos1-3; phyB-9*	(Lazaro *et al.*, 2012)
cycd3;1	*SAIL_675_B08*	(Swaminathan *et al.*, 2000)
cycd5;1	*SALK_077898*	(Sterken *et al.*, 2012)
cycd7	GABI_496G06	
phyQ	*Phyabcde*	(Hu et al., 2013)

Table 2.1 *Arabidopsis thaliana* seed lines used in the present study.

2.2.2 Rice plant husbandry and growth conditions

Rice seeds of Nipponbare background were placed in a transparent container 1/3 filled with reversed osmosis (RO) water. These were allowed to germinate in a Sanyo growth chamber with the following conditions: 26°C day/ 24°C night temperatures, 12h photoperiod and a light level of 200µmolm^{-2}s^{-1} PAR. The seeds were left in the chamber for 7 days until germination when, they were transferred to a PGR15 Conviron growth chamber containing specialised Valoya NS1 broad spectrum LEDs and buried in soil in large 16cm in diameter pots. The soil mix consisted of: 71% sterilised Kettering loam (Boughton), 23.5% John Innes Number 3 compost, 5% sand and either with or without 200g of slow release fertiliser Osmocote (v/v) (Thomson and Morgan, Ipswich, UK). The growth conditions of the chamber the rice plants were grown in were the following: 600 µmolm^{-2}s^{-1} white light with no far-red irradiance, 12h photoperiod, a relative humidity of 60%, ambient CO_2 (~450ppm) and 30°C day/ 24°C night.

In order for optimum rice plant growth, the soil was kept saturated with water by filling at least 2/3 of the way up the pots. After 4 weeks of growth, plants were fertilised fortnightly with a water-based fertiliser (ChemPak high nitrogen feed number 2). All measurements were taken on the most photosynthetically active leaf, the flag leaf (Adachi *et al.*, 2017).

Name	Ecotype/allele	Notes
NB	Nipponbare	Donated by Tinashe Mowdza
OsphyB	*OsphyB-1*	(Takano et al., 2005)

Table 2.2 Rice lines used in the present study.

Name	Ecotype/allele	Notes
NB	Nipponbare	Donated by Tinashe Mowdza
OsphyB	*OsphyB-1*	(Takano et al., 2005)

For the fertiliser regime experiments, plants were either grown with a full fertiliser regime which included both a slow release osmocote fertiliser which is mixed in with the soil and the water-soluble Chempak fertiliser or without either of these two applications. There was also an intermediate of the two used, whereby only the slow release osmocote was used and the water-based fertiliser wasn't or vice versa. The

ingredients list for both fertilisers used in the study are in Tables 4.1 and 4.2 respectively.

2.3.1 Seed sterilisation

Arabidopsis seeds were sterilised for growth in tissue culture. To sterilise the seeds, they were mixed with 70% ethanol and allowed to dehydrate for a few minutes. The ethanol was then removed, and the seeds were washed with bleach mix (20% sodium hydrochlorite mixed with ethanol and 0.1% Tween-20). These were left on a rotating wheel for 20 mins before being aspirated. The seeds were washed 5 times with autoclaved RO water in a laminar flow hood before being plated out.

2.3.2 ½ MS media for tissue culture

1L of ½ MS media was made using 2.2g/L of Murashige & Skoog media (Sigma-Aldrich, M5519-50L) mixed with 800 ml of RO water in a Duran bottle. HCl was then added dropwise to the mix until the pH reached 5.7 before the more water was added to make the volume up to 1L. 6.4g of Plant agar (Duchefa Biochemie, 1100g/cm^2, P1001) was added to solidify the media for making plates. Before being able to use it, the media was autoclaved at 121°C for 30 minutes. Plates were then able to be poured using the mix.

2.4 Generation of double mutants

To develop the *phyBD* and *phyBE* double mutants, a cross was made between *phyB-9* as acceptor and *phyD/E* as donors (Table 2.1). To identify double mutants, individual F2 seedlings were genotyped (section 2.5.3) for wild-type genes or mutant genes with T-DNA insertions (Supplemental Figure 2.1).

2.5.1 DNA extraction

To check for homozygous mutants, a leaf disc (~1cm in diameter) was taken and ground in 400 µl Edwards (200mM Tris-HCl (pH 7.5), 250mM NaCl, 25mM EDTA, 0.5% SDS) buffer solution with a micropestle. The mix was then centrifuged at 17000rpm for 2mins and the supernatant removed and added to an equal volume of isopropanol (Propan-2-ol, Fisher Scientific 1067432) and mixed. After centrifugation

at 17000rpm for 5 mins, all liquid was removed and allowed to air dry for 5 mins before the pellet was re-suspended in water and stored at -20°C.

2.5.2 Genotyping

A PCR to determine if plants are homozygous for specific mutations used DreamTaq master mix. The PCR methodology has been adapted from the ThermoScientifc™ DreamTaq™ PCR master mix (2x) which upon the addition of primers and template, was ready to be used. This is because it contains the DNA polymerase, DreamTaq in a green buffer which is a ready made dye enabling the visualisation of PCR products on a agarose gel, $MgCl_2$ and dNTPS. The volumes of the master mix, primers and water used in each reaction is shown in Table 2.3.

Component	Concentration	Volume (Total 20µl)
Dream Taq polymerase mix	2x	10µl
Forward primer	10µm	0.5µl
Reverse primer	10µm	0.5µl
Molecular Biology grade H_2O		9µl

Table 2.3 Components required for genotyping PCR analysis and their volumes.

Component	Concentration	Volume (Total 20µl)
Dream Taq polymerase mix	2x	10µl
Forward primer	10µm	0.5µl
Reverse primer	10µm	0.5µl
Molecular Biology grade H_2O		9µl

Once the mix was created, it was gently mixed and briefly spun in a microcentrifuge before 18µl was added to a PCR tube. 2µl of the template DNA was then added to make a total volume of 20µl per reaction. The tubes were then loaded into a thermocycler and the settings for a 20µl reaction volume with 35 cycles is shown in Table 2.4. After the program had run, the samples were directly loaded onto a 1% agarose gel for analysis.

Stage		Temperature	Time
Initial denaturation		95°C	5mins
C1		95°C	30s
C2	x35	55°C	30s
C3		72°C	1min
Final		72°C	5mins

Table 2.4 Stages for a PCR required and their temperatures/times.

Stage		Temperature	Time
Initial denaturation		95°C	5mins
C1		95°C	30s
C2	x35	55°C	30s
C3		72°C	1min
Final		72°C	5mins

2.5.3 Gel electrophoresis

A 1% agarose gel was made using 1g of agar and 100ml of 1x TAE buffer and 5µl ethidium bromide. To make the gel, 50x TAE buffer was made with: 242g Tris Base, 57ml glacial acetic acid and 100ml 0.5M EDTA, made up to 1L with RO H_2O. Agarose powder was added to 100ml of 1x TAE and dissolved. 5µl of ethidium bromide (10mg/ml, Alfa Aesar) was mixed into the gel mix. This allows the DNA products to be viewed on the gel after running as it contains a fluorescent that binds to DNA. If the PCR product did not contain a dye element, a 6x loading dye (0.2% w/v bromophenol blue, 50% v/v glycerol) was added to samples. A DNA ladder (3µl GeneRuler, DNA Ladder mix ready-to-use 0.1µg/L, 50µg) was also loaded into the first well of the gel as a reference for size and quantification of the PCR product. The gel was run at 110V for 30mins before being visualised using a GelDoc-It^{TM} machine with a VisionWorks® LS analysis software (UVP LLC).

2.6 Stomatal impressions

Once the plants were mature (approximately 5 weeks or upon flowering), 3 fully expanded leaves from 5 plants were taken and Impression Plus dental resin (ImpressPLUS Wash, Perfection Plus, UK) was used to coat the abaxial surface of the

leaves and allowed to set. Once set, the mould was removed from the leaf material and nail varnish was coated onto the leaf mould and allowed to dry. Tape was used to remove the dried nail varnish coating from the mould and applied to a microscope slide for visualisation.

2.6.1 Visualisation and stomatal density/index

The microscope slides were viewed at 20x magnification under a Brunel 300-M microscope fitted with a Moticam 5 camera and a Prior ES10ZE Focus Controller. Each impression was imaged using the Micro-manager software 1.4 three times; once at the tip, mid and base of the leaf. Z-stacks were created at a resolution of 1296 x 972 in the software ImageJ.

The ImageJ software was also used to count the number of stomata and pavement cells in each image. A 400µm x 400µm counting square was created. Stomata and cells which had more than 50% of their area inside the square were included in the counts, the opposite being true if 50% was outside.

Stomatal density and index were calculated using the following equation:

Stomatal density = Number of stomata/mm^2

Stomatal index (%) = (Number of stomata / Total number of cells)*100

2.6.2 Stomatal length and width

Stomatal length and width were measured in ImageJ software using the measuring tool after the image was calibrated by measuring a known distance with the tool. Stomatal length was defined as the distance from the top of the joining of the two guard cells to the bottom. The width was defined as the distance from the edge of one side of the stomatal complex to the other edge of the opposite side.

2.6.3 Epidermal patterning counts

Using the same images from stomatal counts, the number of stomatal complexes, defined as a primary stoma with a corresponding satellite stoma, lone stomata without a satellite stoma and the number of symmetrical meristemoid divisions were counted. A representative image of each counted phenotype is shown in Figure 4.1.

2.7 Carbon isotope discrimination

Once the plants had flowered, 5 were cut at the rosette level and placed in tin foil cases before being dried over 2-3 days in an oven at 60°C. Once dried, the leaves were ground and 1-2µg of powder was weighed into tin capsules. Four replicate air samples were also collected from chambers as references. The capsules containing the tissue powder was then sent for combustion at 1800°C and separation by a gas chromatograph, before undergoing magnetic field ionization in an ANCA GSL 20-20 Mass Spectrometer (Sercon PDZ Europa) to separate the two C^{12} and C^{13} ions. The data received from this was in the form of δC, with the following calculations needed to determine the ΔC^{13} values (Farquhar and Ehleringer, 1989):

$$\delta = R/R_{standard} - 1$$

Where R is the sample carbon isotope ratio from individual plants and R standard is the Vienna Peedee Belemnite (VPBD) reference that is defined as the point where the stable carbon isotope scale is zero. This can then be used to determine the relative abundance of the two isotopic forms.

$$\Delta C^{13} = (\delta a - \delta p)/(1 + \delta p)$$

Where δ a refers to the atmospheric CO_2 from the reference air samples and the δ p is the δC^{13} of the plant sample.

Although CID was performed in many of the experiments, it is not possible to compare between the different results for different experiments. This is because the carbon in the cabinet air is influenced by external factors and the scale of CID can therefore vary across different time points, depending on the external environment.

2.8 Thermal imaging

An infrared (IR) thermal imaging camera (FLIR T650SC; FLIR Systems Inc., Boston, MA, USA) was used to image 6x4 trays of plants, half of which were one genotype and the other half a second genotype. The camera settings used were the default, with images taken once every 1min. The camera was set up using a tripod to be positioned directly above the tray of Arabidopsis plants in the chamber and the door was kept closed for the duration of the experiment. To allow the camera to adapt to the

conditions of the chamber, the first half hour of images taken were removed from analysis to allow for adaptation of plants and the thermal imaging camera to cabinet conditions. Images were taken over a time period of 1h 30mins between the hours of 09:00 am and 17:00 pm and analysed. Plants were measured at the stage of bolting. Replicate measurements of the same trays were taken at the same time every day to ensure consistency.

ResearchIR software (FLIR Systems, https://www.flir.com/) was used to analyse the thermal imagery. Four regions of interest (ROIs) were selected as temperature measurements. The regions selected were on outer leaves and away from the main vein to ensure that the reading of temperature was not affected by the vein or the larger densities of inner leaves of the plant. The numerical output of the regions of interest from the images was then plotted over time.

2.9 Plant physiology

2.9.1 Flowering time

Flowering time was recorded as days post germination and flowering were defined as the first appearance of the bolt from the rosette.

2.9.2 Rosette area

Regular photographs of *Arabidopsis* plants at different stages throughout their life cycle were taken. These photographs were taken at a regular height from the trays and one photo was taken every 2-3 days from when they were moved into the 6x10 insert trays which was 16 days post germination (d.p.g). These photos were taken until 40 d.p.g when the plants in the trays had become too large and their leaves started overlapping so it became difficult to give accurate rosette measurements (Supplementary Figure 2.3). The images were loaded into ImageJ and using a known distance, the scale was calibrated, the line-measuring tool was calibrated to this length. The images were then converted to 8-bit images. These images were then transformed by converting the image to a black and white 8-bit and manually adjusting the threshold until the rosettes were clearly delineated from the compost background. Noise was removed manually and using the de-speckling tool. The wand-tracing tool

was then able to differentiate between different rosettes and was used to calculate the total area (Figure 2.2).

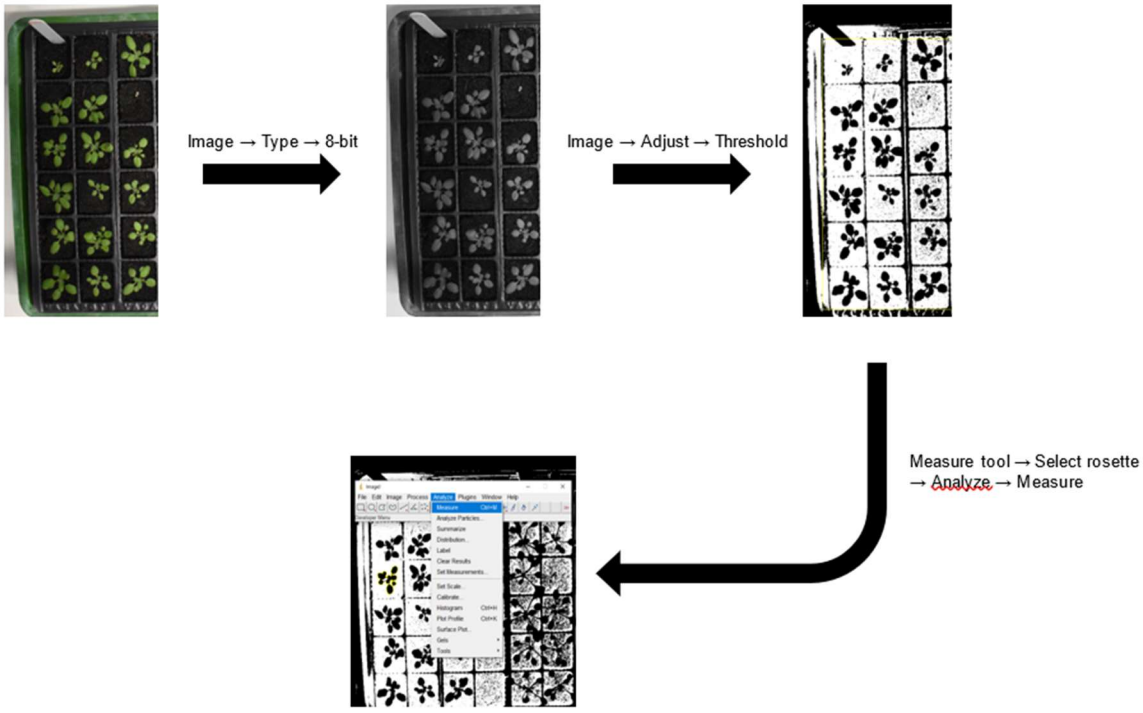

Figure 2.2. Workflow of calculation of rosette area from photographs. Photographs with a scale of known size are loaded into ImageJ software before being converted to an 8-bit image and the threshold adjusted to give clear edges of the rosettes. The measuring tool was then used to measure the area of a rosette.

2.9.3 Biomass

Both dry and wet biomass were measured by weighing the above ground tissue on a tabletop analytical balance (0.001 decimal place) once the rosette had been removed from the soil and before drying for carbon isotope discrimination.

2.10 Measurement of Photosynthetic parameters

2.10.1 Non-Photochemical Quenching

Before measurements were taken, the plants were dark adapted for 30 mins. A handheld PAM fluorometer; FluorPen FP 110 (Photon System Instruments, Drásov,Czech Republic) was clamped onto a region of the leaf that did not include a vein and two programs were run. A handheld PAM fluorometer; FlourPen FP 110 (Photon System Instruments, Drásov,Czech

Republic) was clamped onto a region of the leaf that did not include a vein. Non-photochemical quenching (NPQ) was measured using the parameters shown in Table 2.5.

Phase	Duration	# of pulses	1st pulse	Pulse interval
Light	60s	5	7 s	12 s
Dark recovery	88s	3	11 s	26 s

Table 2.5. The protocol of NPQ measurements taken by the FlourPen after dark adaptation (Photon System Instruments, Drásov,Czech Republic).

The protocol includes following measured and calculated parameters:

Abbreviation	Explanation
F_0	minimum fluorescence in dark-adapted state
F_m	maximum fluorescence in dark-adapted state, measured during the first saturation flash after dark adaptation
F_p	fluorescence in the peak of fast Kautsky induction
F_m_L, Lss, D, Dss[1]	maximum fluorescence
QYmax[2]	maximum quantum yield of PSII in dark-adapted state - F_v/F_m
QY_L, Lss, D, Dss[1,3]	effective quantum yield of PSII
NPQ_L, Lss, D, Dss[1,4]	non-photochemical chlorophyll fluorescence quenching
Qp_L, Lss, D, Dss[1,5]	coefficient of photochemical quenching, an estimate of open PSII reaction centers

Figure 2.3. The measured and calculated outputs of the FluorPen NPQ 1 program (Photon System Instruments, Drásov,Czech Republic).

2.10.2 OJIP curve

Similarly to the NPQ protocol, before measuring the OJIP parameters (Figure 2.4) the plants were dark-adapted. This was done on a separate day to that of the NPQ to make sure that the previous fluorescence program did not influence any results from the OJIP. However, the time of day that the results were collected was kept consistent across the two programs.

Abbreviation	Explanation
Bckg	Background
F_0	$F_0 = F_{50\mu s}$, fluorescence intensity at 50 µs
F_J	F_J = fluorescence intensity at J-step (at 2 ms)
F_I	F_I = fluorescence intensity at i-step (at 30 ms)
F_m	F_m = maximal fluorescence intensity
F_v	$F_v = F_m - F_0$ (maximal variable fluorescence)
V_J	$V_J = (F_J - F_0) / (F_m - F_0)$
V_I	$V_I = (F_I - F_0) / (F_m - F_0)$
F_m / F_0	
F_v / F_0	
F_v / F_m	
M_0 or $(dV/dt)_0$	$M_0 = TR_0 / RC - ET_0 / RC = 4 (F_{300} - F_0) / (F_m - F_0)$
Area	Area between fluorescence curve and F_m (background subtracted)
Fix Area	Area below the fluorescence curve between $F_{40\mu s}$ and F_{1s} (background subtracted)
S_M	S_M = Area / $(F_m - F_0)$ (multiple turn-over)
S_s	S_s = the smallest S_M turn-over (single turn-over)
N	$N = S_M . M_0 . (1 / V_J)$ turn-over number Q_A
Phi_P_0	$Phi\_P_0 = 1 - (F_0 / F_m)$ (or F_v / F_m)
$Psi\__0$	$Psi\__0 = 1 - V_J$
Phi_E_0	$Phi\_E_0 = (1 - (F_0 / F_M)) . Psi\__0$
Phi_D_0	$Phi\_D_0 = 1 - Phi\_P_0 - (F_0 / F_m)$
Phi_Pav	$Phi\_Pav = Phi\_P_0 (S_M / t_{fm})$ t_{fm} = time to reach F_m (in ms)
ABS / RC	$ABS / RC = M_0 . (1 / V_J) . (1 / Phi\_P_0)$
TR_0 / RC	$TR_0 / RC = M_0 . (1 / V_J)$
ET_0 / RC	$ET_0 / RC = M_0 . (1 / V_J) . Psi\__0$
DI_0 / RC	$DI_0 / RC = (ABS / RC) - (TR_0 / RC)$

Figure 2.4. The parameters that the OJIP protocol measures from the Fluorpen FP110 (Photon System Instruments, Drásov,Czech Republic).

2.11 Gas exchange analysis

To determine gas exchange analysis for rice, an infrared gas analyser (IRGA; LI-6800 Portable Photosynthesis System, LI-COR Biosciences, Lincoln, NE, USA) was used, a leaf was placed into a 6cm^2 chamber which contains a fluorometer (6800-01A, LI-COR Biosciences). In this sealed chamber, measurements such as carbon assimilation and stomatal conductance can be measured. Fully expanded mature flag leaves were used on rice plants and the width of these leaves were measured and entered into the machine. All other values were either the default or matched to the conditions of the chamber unless stated. For Arabidopsis, fully expanded healthy

leaves were used at the stage of flowering with 6 plants being used per genotype. Once the leaf had been clamped into the chamber, it was allowed to adapt to the conditions in the chamber for at least 30 mins before any programs were run.

All measurements were taken at least one hour after the photoperiod started and ended at least one hour before the end of the photoperiod.

2.11.1 Steady state and saturating light measurements

Leaf chamber conditions for steady and saturating light measurements are shown in Table 2.6. Steady state measurements were taken by logging the carbon assimilation and stomatal conductance every 5 mins. Once clamped to the leaf, the assimilation and stomatal conductance were allowed to settle for at least 30 mins before collecting data. The conditions used for Arabidopsis were different to rice to account for the different growth conditions of the two plants. These conditions are shown in Table 2.7.

Settings	Values
RH	60%
Fan speed	10000 rpm
Leaf temperature	27°C
Light (Steady/Saturating light)	600/2000µmol$m^{-2}s^{-1}$
Flow set-point	500µmols^{-1}
CO_2 level	450ppm

Table 2.6. Settings in the leaf chamber of Licor measurements for rice.

Settings	Values
RH	60%
Fan speed	10000 rpm
Leaf temperature	27°C
Light (Steady/Saturating light)	600/2000µmol$m^{-2}s^{-1}$
Flow set-point	500µmols^{-1}
CO_2 level	450ppm

2.12 Rice measurements

Due to mortality of some of the rice plants before maturity, there is a variable n number across genotypes and treatments in some cases. These will all be noted in the figure legends for clarity. Ambient CO_2 conditions were also different between chambers

(~50ppm difference) and so the intermediate fertiliser and extreme fertilisers cannot be directly compared.

2.12.1 Flowering time

Rice flowering time was measured as the time from the germination to the appearance of the first panicle separated from the stem.

2.12.2 Rice stomatal impressions

Stomatal impressions were taken in a similar fashion to Arabidopsis, using dental resin on the tip, mid and base of the flag leaf. This was allowed to set, and the mould covered with nail varnish which was again allowed to set. Tape was then used to peel the varnish from the leaf mould at the three points and then added to a microscope slide. Peels were viewed at 20x magnification under a Brunel 300-M microscope fitted with a Moticam 5 camera and a Prior ES10ZE Focus Controller. Each impression was imaged using the Micro-manager software 1.4 three times; once at the tip, mid and base of the leaf. Z-stacks were created at a resolution of 1296 x 972 in the software ImageJ.

The ImageJ software was also used to count the number of stomata and pavement cells in each image. A 400µm x 400µm counting square was created. Stomata and cells which had more than 50% of their area inside the square were included in the counts, the opposite being true if 50% was outside.

2.12.3 Rice yield measurements

Once panicles had stopped being produced, watering of the plants was stopped to allow them to dry out before seed was collected. The number of panicles at the end of the rice life cycle were counted, this included those that were unfilled.

2.12.4 Rice panicle weight

Panicles, both filled and unfilled were weighed and then the number recorded. Seed weight was not attempted due to the large number of unfilled panicles that were present in a *OsphyB-1* mutant.

2.13 Statistical analysis

Statistical analysis was carried out in GraphPad Prism (9.0.2). Unless stated, a two-way ANOVA was used to test the significance of differences between genotypes and treatments. For multiple comparisons, unless stated, Tukey's multiple comparisons test was used, this test takes into account potential differences in the number of replicates (n). Significance, defined as a p-value ≤0.05, are denoted by the p-value shown. Whereas, values of non-significance, defined as p>0.05 are not shown.

The majority of graphs are represented as box-and-whisker plots where the median is shown as well as the 25th to 75th percentile at either end of the box. The highest and lowest values are also shown extending above and below the box as the whiskers. Bar graphs generated for epidermal patterning have the statistical analysis shown in tables.

2.14 Primer sequences

Below is a table of all the forward, reverse and T-DNA insertion primers used in this study. All primers were ordered from and synthesised by Sigma-Aldrich.

Primer name	Sequence (5'-3')	Notes
phyB-9 fwd 2	TGGACTGCATTATCCTGCTAC	Genotyping
phyB-9 rev 2	TGCCATACCGCACACAGCATC	Genotyping
phyB-9 WT for	CTATGTGCTTGGTTGGTTCTAC	Sequencing
Lba1	TGGTTCACGTAGTGGGCCATCG	Genotyping for T-DNA insertion
SAIL_LB	GCCTTTTCAGAAATGGATAAATAGCCTTGCTTCC	Genotyping for T-DNA insertion
CYCD3_LP	CTCCCCTGCTAAGCTAACCAC	Genotyping
CYCD3_RP	TGGTAAAACGAAATGGAGTGG	Genotyping
CYCD5_LP	GAGAATCTCCGATTCGAAACC	Genotyping
CYCD5_RP	CAAAAGACAATCGGCGTTTAG	Genotyping
CYCD7_LP	CACTGTTCCGAGAGTGAGGAG	Genotyping
CYCD7_RP	TATCAGTTCCCGTTTCACGTC	Genotyping
GABI_LB	ATAATAACGCTGCGGACATCTACATTTT	Genotyping
phyA_LP	GGGAGTATGGAAAGGCTTTGTG	Genotyping

phyA_RP	TCCCTATCATCTGGATCATGC	Genotyping
phyC_LP	CATAAGCGACTCAGACATAGAGG	Genotyping
phyC_RP	GCAACTCACATCAAGGTGCATAC	Genotyping
phyD_LP	GGATTCACTCTAACAACACTGG	Genotyping
phyD_RP	CGGTAGAATCAGAATGGTTAGC	Genotyping
phyE_LP	CGCAGTTCAGTCTCAGAAGC	Genotyping
phyE_RP	CTCCAAGTGAGATGGCACCAG	Genotyping

Table 2.7. Primer sequences used throughout this study.

Chapter 3: The impact of temperature on plant water use via the phytochromes

3.1 Introduction

Climate change is leading to more frequent temperature spikes over longer periods of time which have a huge impact on the health and productivity of land plants (Janni *et al.*, 2024). Therefore, plants need to adapt to these temperature increases to maximise water use and minimise water losses. In a world of increasing atmospheric carbon dioxide levels, a fine balancing act is required. This is because the pores on the epidermis of the leaf, the stomata, open to allow carbon dioxide into the leaf and into the mesophyll for metabolic processes such as photosynthesis and water is lost through evapotranspiration as a consequence (Lee and Bowling, 1995). Therefore, increased levels of CO_2 due to climate change could lead to greater carbon fixation and improve biomass accumulation but at the cost of increased water losses, which are exacerbated with increased temperatures (Dusenge, Duarte and Way, 2019). This will create a trade-off and so development of technologies to improve water retention while increasing assimilation are important (Lefebvre *et al.*, 2005; Zhu, de Sturler and Long, 2007; Franks and Beerling, 2009). The red-light photoreceptors, the phytochromes, are proposed to be required for determining not only stomatal opening in the short term but also the development of stomata over a longer period of time (Casson *et al.*, 2009; Wang *et al.*, 2010; Murata, Mori and Munemasa, 2015). These changes in development lead to differing numbers of stomata depending on the environment the plants are grown in; for example, plants grown at higher irradiances have increased stomatal density and indices than those grown at lower irradiances as long as there is not a significant difference in temperature (Schoch, Zinsou and Sibi, 1980; Beerling and Chaloner, 1993). The main phytochrome involved in stomatal development is phyB, which when mutated leads to a reduced number of stomata on the leaf epidermis (Boccalandro *et al.*, 2009; Casson *et al.*, 2009). Reductions in the stomatal density can correlate with increased lifetime water use efficiency because fewer stomata mean less water is lost through them via transpiration. phyB mutants were shown to have improved lifetime WUE when compared to the Landsberg erecta WT control under constant temperature condition (Boccalandro *et al.*, 2009) (Figure 3.1A). Further evidence from the Casson lab for improved WUE in a *phyB* mutant was shown when Col-0 and *phyB-9* were grown under 20°C day and 16°C night for an 11 hour day, *phyB-9* was significantly more water use efficient than Col-0 (Figure 3.1B) (Brown, 2018). However, this improved WUE was conditional and was only the case

when *phyB-9* were grown under 500ppm CO_2 and not decreased or elevated levels of CO_2. Therefore, this suggests that while *phyB* is more water use efficient under certain conditions, this can also be changed depending on environmental factors.

Along with its role in regulating stomatal development and WUE, phyB also regulates flowering through its interaction with FT (Endo and Nagatani, 2008). FT expresses a florigen protein in the leaf phloem and moves into the shoot apical meristem to regulate flowering (Corbesier *et al.*, 2007; Jaeger and Wigge, 2007; Mathieu *et al.*, 2007; Tamaki *et al.*, 2007). It has recently been shown to upregulate transcription of a sugar transporter, SWEET10 and so may be involved in carbon metabolism (Andrés *et al.*, 2020). As flowering is accelerated in phytochrome mutants, there may be a link between FT driven carbon metabolism and the phytochromes (Reed *et al.*, 1993). Little has been studied regarding the impact of temperature and particularly the timing of temperatures on WUE. With increased prolonged periods of high temperatures due to climate change, including regular spikes in night time temperatures (Peng *et al.*, 2004), it is important to determine the extent of the temperature dependency upon the phytochromes water use efficiency state.

Temperature influences physiological traits such as biomass accumulation, with lower temperatures resulting in small plants, with compact rosettes which increase in stem elongation and increased biomass with increasing temperatures up to a point (Atkin *et al.*, 2006; Franklin, 2009; Xia *et al.*, 2009). Flowering time is also influenced, by both the phytochromes and temperature, with higher temperatures typically resulting in earlier flowering plants (Endo and Nagatani, 2008; Osugi *et al.*, 2011; Jagadish *et al.*, 2016). Beyond this, high temperatures lead to hyponastic growth characterised by elongated petioles and more angled leaves as well as reduced leaf size and earlier flowering (Gray *et al.*, 1998; Koini *et al.*, 2009). Therefore, higher temperatures are likely to impact plant canopy architecture which could further affect their WUE.

The role of the other phytochromes beyond phyB in temperature related is less well characterised, however, should be considered because increases in temperature affect the Pfr state of all the phytochromes which will affect multiple developmental and physiological pathways.

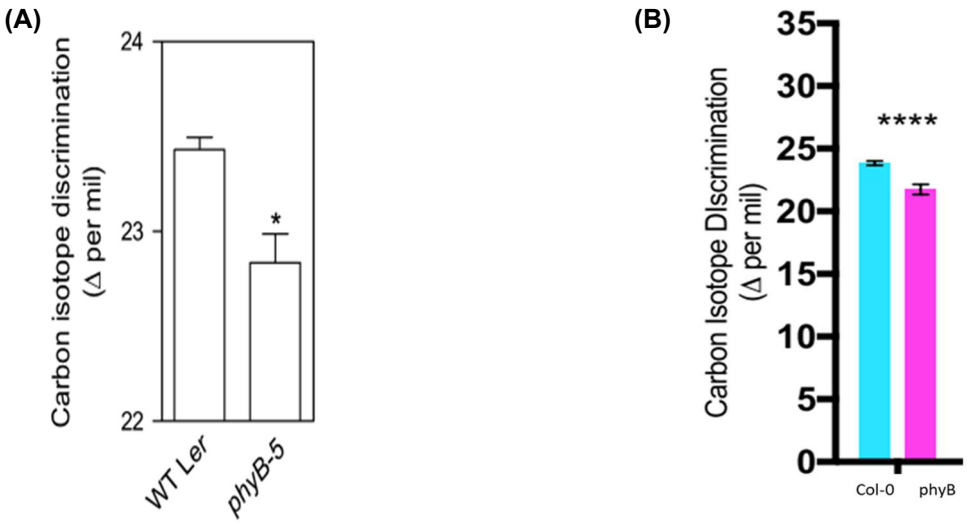

Figure 3.1. *phyB-9* is more water use efficient than Col-0 under certain temperature conditions. (A) Carbon isotope discrimination for Col-0 and *phyB-9* grown under 23°C±1°C, adapted from (Boccalandro *et al.*, 2009). **(B)** Carbon isotope discrimination for Col-0 and *phyB-9* grown under 20°C day and 16°C night, adapted from (Brown, 2018).

3.1.2 Aims and objectives

phyB is known to regulate stomatal and photosynthetic traits, as well as plant morphology including elongation growth and hyponasty (Kim, Lee and Park, 2021). Collectively, these traits trade-off to impact WUE. An increase in temperature leads to faster thermal reversion of phyB from the active Pfr to the inactive Pr states (Legris *et al.*, 2016; Klose, Nagy and Schäfer, 2020). The hypothesis of this chapter is that higher temperature corresponds to a decreasing gradient of phytochrome activity, affecting the trade-off in traits influencing WUE. I therefore predict that changes in the temperature load experienced by a plant improves plant WUE up to an optimum point beyond which there is a decrease due to the trade off with multiple other traits being affected (Figure 3.2).

The aim of this chapter is to investigate how temperature and phytochromes interact to regulate plant WUE.

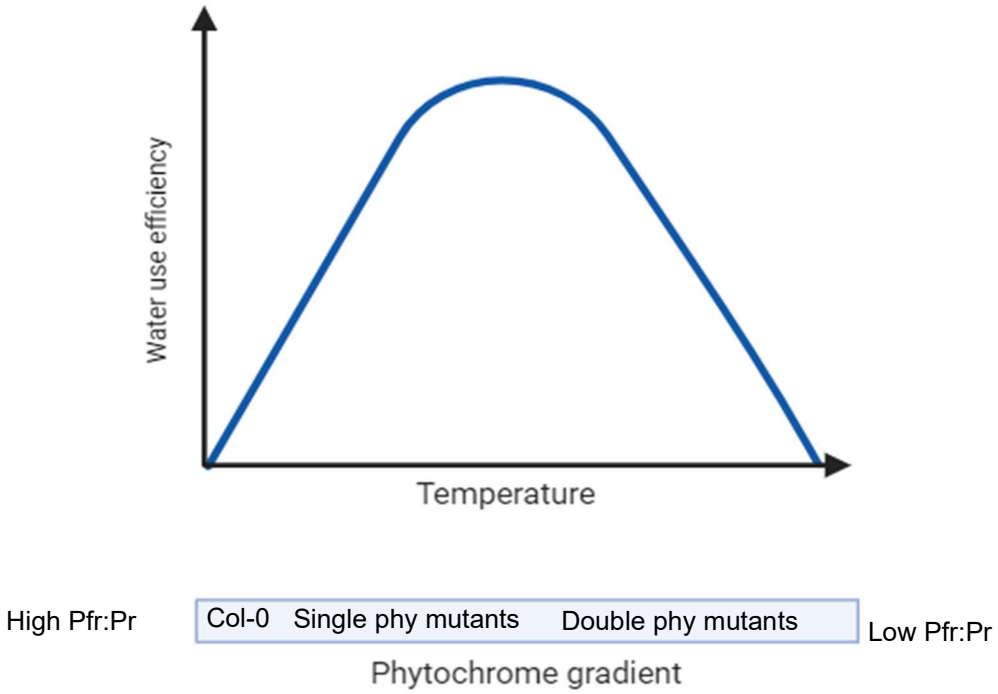

Figure 3.2 Hypotheses investigated in the present study. (A) Temperature influences phytochrome thermal reversion and so the balance of Pfr:Pr. Temperature mediated changes in the Pfr:Pr ratio are predicted to lead initially to improvements in WUE due to changes in stomatal traits before trade-offs in photosynthetic performance and plant morphology mitigate these at higher temperature loads. This study utilises a *PHYB* overexpressing line and single and higher order phytochrome mutants to generate plants with differences in the PFr:Pr ratio.

To achieve this aim and test the hypothesis, the objectives of this chapter were as follows:

1. To examine the impact of different temperature regimes and the timing of increased temperatures on the water use efficiency state of phy mutants.
2. To determine if the other phytochromes contribute to water use at 22°C/16°C.
3. To investigate the relationship between flowering and water use in the phytochromes.
4. To evaluate the potential impact of temperatures upon carbon assimilation and plant biomass accumulation.

The aims and objectives of this chapter were achieved through the following strategies:

1. Using multiple tools to measure the water use and transpiration of a range of phytochrome mutants.

2. Investigating the correlations between different factors that influence WUE.
3. Studying the impact of Pfr activity on photosynthetic traits and biomass.

3.2 Hotter days lead to reductions in plant WUE in a phy dependant manner

To investigate the impact of increased day or night temperature on plant WUE and the role of phyB in regulating this trait, plants were grown under different temperature regimes but with the same overall temperature load. Temperature load is here defined as the overall average temperature that a plant perceives over a 24-hour period. To differentiate the impact of day and night time temperature from overall changes in temperature load, experiments were designed where the temperature load that the plants perceived over the 24-hour averaged to 22°C. Three growth conditions were used: A high day temperature (HDT; 24°C day and 20°C night), 22°C constant and a high night temperature (HNT; 20°C day and 24°C night). As the overall temperature that the plants perceived over the 24-hour averaged to 22°C, any changes that are seen between the WUE of the plants should be due to the timing of the temperature increase and not other external factors as all environmental factors were controlled to be equal. Once the plants had flowered, mature leaves were taken for stomatal impressions from which the stomatal density was calculated (Figure 3.3B). Stomatal indices (SI) were also determined and are discussed in Chapter 4. After this, the plants were dried before other leaves were taken for carbon isotope discrimination to determine a proxy of lifetime water use efficiency (Figure 3.3A). For delta carbon, the closer to zero the number, the less discrimination between the two isotopes of carbon and therefore the more water use efficient a plant is. As expected, Col-0 had significantly more stomata than *phyB-9* under all three temperature regimes (Figure 3.3B). However, in contrast to previous studies (Boccalandro *et al.*, 2009; Brown, 2018), the carbon isotope discrimination data indicated that *phyB-9* plants were less water use efficient than the Col-0 plants regardless of temperature regime (Figure 3.3A). Within the Col-0 genotype, the plants grown under HDT were the least water use efficient although there was variation in this dataset, the most water efficient were the plants grown under HNT. A similar trend occurred in the *phyB-9* mutants with the

least water efficient being the plants grown under HDT and the most efficient being those grown under 22°C, with little difference between 22°C and HNT.

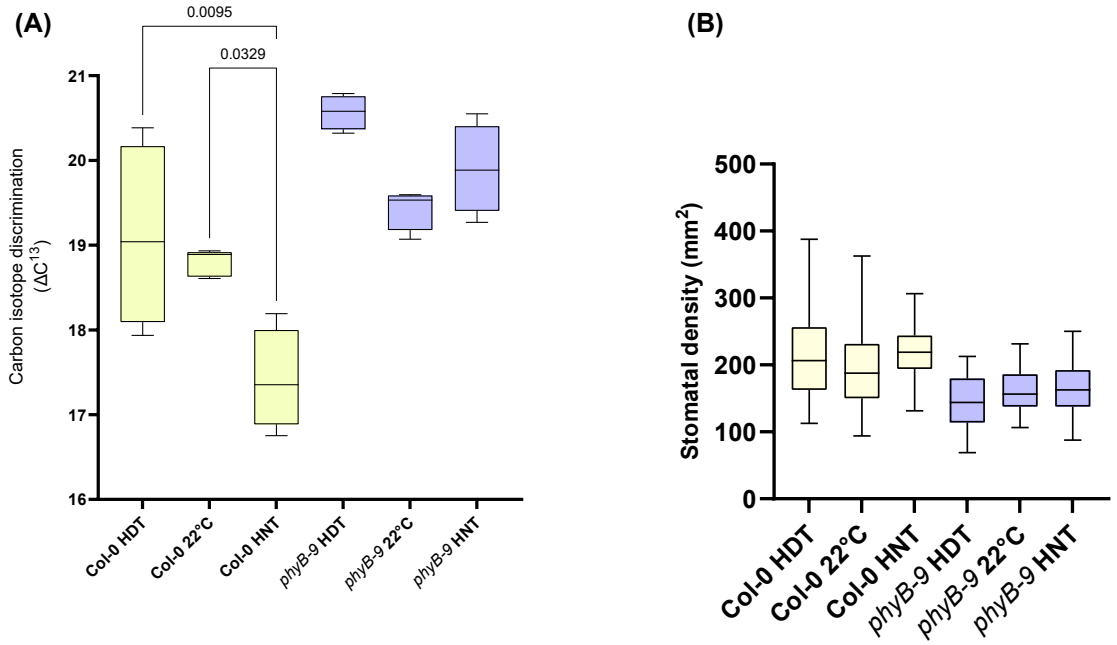

Figure 3.3. Carbon isotope discrimination and stomatal density of Col-0 and *phyB-9* under different temperature regimes. (A) Carbon isotope discrimination of Col-0 and *phyB-9* plants grown under high day temperature (HDT), 22°C and high night temperature (HNT). Plants were dried after flowering and material was taken for IRMS analysis to determine the ratio of the two carbon isotopes (C^{12} and C^{13}), n=5. **(B)** Stomatal density per mm^2 was calculated from impressions of mature leaves after plants had flowered, n=36. Box-plot graphs were made in GraphPad prism, the line shows the median value, the boxes represent the 95% interval and the whiskers the highest and lowest value in the dataset. Statistical analysis was carried out in GraphPad prism using a two-way ANOVA and Tukey's multiple comparisons test. Significant p-values ≤0.05 are shown whereas non-significant values >0.05.

To determine how the carbon isotope discrimination and stomatal density were related for this experiment, a correlation of the average stomatal density from 4 plants and the carbon isotope discrimination from the same plants was generated for each temperature regime (Figure 3.4). Col-0 HDT plants had a stronger relationship (r^2 = 0.5841) between CID and stomatal density, with increased density there was increased CID and hence a loss of WUE, which would be expected. However, with decreased day temperatures or increased night temperatures, there was a loss of a correlation between SD and CID in Col-0 suggesting under these conditions, they are not related (r^2 = 0.0396 for 22°C and r^2 = 0.0407 for HNT). There was a weak positive correlation in the *phyB-9* HDT plants (r^2 = 0.1297), and this weak trend continued at

the other temperature regimes, with the r^2 values are closer to 0 (0.0624 and 0.0071 for 22°C and HNT respectively) and so these trends are less positive and hinting at a lack of a correlation between the two traits. A reduction in day temperatures or increases in night temperatures impact the positive relationship between lower SD and higher WUE.

The SD of *phyB-9* is lower than Col-0 but the CID is higher, this contrasts with other studies as phyB is required for improved WUE. In addition to this, the timing of the temperature and not the SD has a greater impact on CID. In both Col-0 and *phyB-9*, HDT has the most detrimental impact on WUE and in Col-0 there is a clear trend that the lower the day temperature (or the higher the night temperature), the more WUE. This relationship does not hold as much in *phyB-9* as 22°C has a higher CID than HNT suggesting that improved CID under HNT is especially sensitive to and requires the presence of phyB (Pfr). However, these results do not clearly distinguish between whether it is a lower day time or higher night time that causes the improvement in WUE. The fact that phyB has a lower WUE in these experiments at HDT does not discount that other phytochromes are responsible for the differences in WUE.

The flowering time of these plants also showed an interesting result. With both Col-0 and *phyB-9* having significantly accelerated flowering when grown under increasing night temperatures. *phyB-9* flowers earlier than Col-0 under all temperature regimes and the *phyB-9* plants grown under HNT have the fastest flowering of all. However, this could be due to a cooler day and not necessarily a warmer night (Supplementary Figure 3.1).

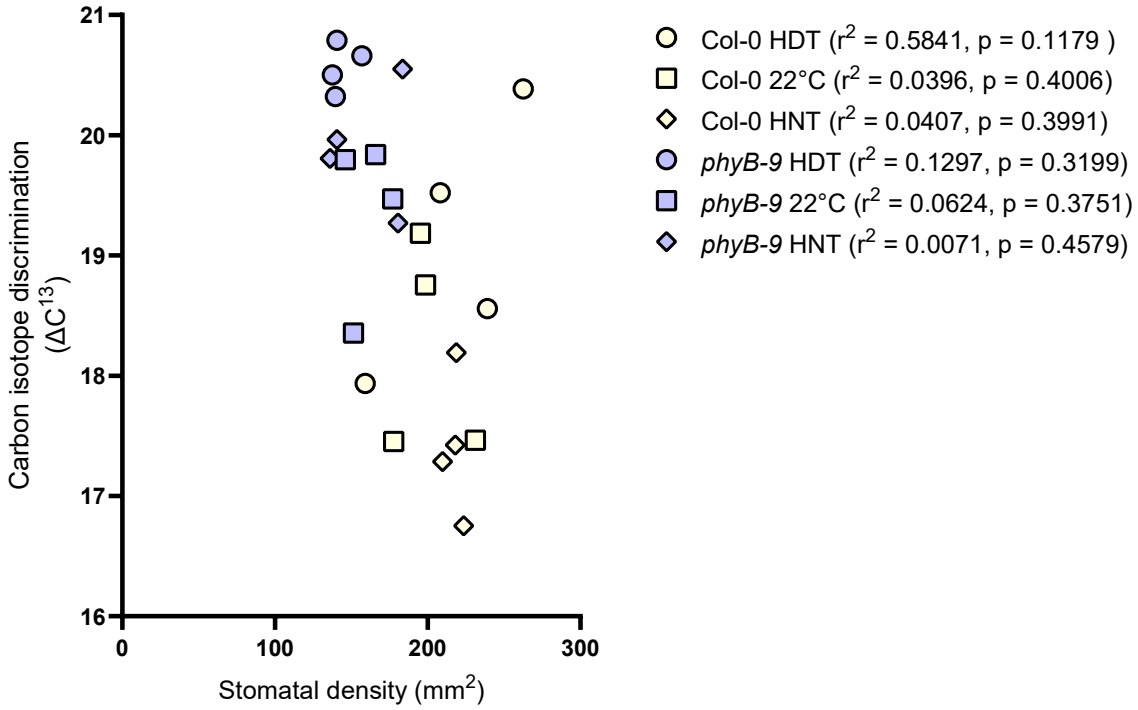

Figure 3.4. Correlations between stomatal density and carbon isotope discrimination from Figure 3.3. Col-0 and *phyB* had their stomatal density and carbon isotope discrimination compared under HDT, 22°C and HNT. Each point represents an individual plant, n=4. The graphs were generated in GraphPad prism. r^2-values and p-values are shown in the key next to their corresponding treatment.

3.3 Addition of end of day far-red suggests that higher night temperatures are important for determining water use efficiency

The increase in CID for all *phyB-9* temperature regimes suggests that temperature is an important factor in determining WUE and the timing of the increase in temperature could also be a significant factor. My previous experiments indicate that warmer days coupled to cooler nights lead to lower WUE than cooler days and warmer nights. phyB impacts on WUE under these different temperature loads and in particular is required for improved WUE at HNT.

HDT temperatures would be expected to cause a lower Pfr:Pr ratio during the day than either the 22°C and HNT conditions. However, the lower night time temperature would mean a slower thermal reversion at night and potentially greater Pfr activity. Collectively, these data coupled to the fact that these are different to previous results regarding phyB, meaning that it is difficult to determine whether Pfr activity during the

day or accelerated thermal reversion of Pfr to Pr in the night (or both) is associated with improvements in WUE.

To try and address this question, Col-0 and *phyB-9* were grown under 22°C constant conditions. In addition to the new temperature regime, these plants were either grown with or without the addition of 50µmol$m^{-2}s^{-1}$ far-red (FR) light at the last 10 minutes of the photoperiod over their lifetime. Far-red light causes reversion of the active phytochromes from their Pfr state to the inactive Pr state. Therefore, the strong pulse of far-red light at the end of the photoperiod should be sufficient to revert the majority of active phytochromes to be inactivated (Devlin *et al.*, 1996; Devlin, Patel and Whitelam, 1998). This was used to act as a proxy for increased night temperatures, as thermal reversion under warmer temperatures reverts the active phytochromes to be inactive in a rapid way.

Once again, Col-0 and *phyB* with or without far-red light supplementation had leaves removed for stomatal impressions and stomatal density was measured (Figure 3.5A) and whole plants were removed at the rosette level to determine the ratio of C^{12} to C^{13} (Figure 3.5B). Similarly to the previous experiment, Col-0 had significantly more stomata than *phyB-9* when they were grown under 22°C and the addition of far-red light did not impact this (Figure 3.5A). End of day (EoD) far-red did not impact the stomatal density of *phyB-9* compared to absence of the FR. As per the previous experiments, the CID of Col-0 at 22°C compared to *phyB-9* was significantly reduced and the addition of EoD FR led to further reductions, although not significant to the 5% level, making Col-0 more WUE under these conditions. The same trend was observed in *phyB-9* with EoD FR reducing the CID compared to when there was no FR addition (Figure 3.5B). These results suggest that thermal reversion rates and hence Pfr persistence during the night likely does impact WUE and that fast thermal reversion does improve the WUE of plants, however this is not due to stomatal numbers, but possibly due to changes in stomatal activity or structure of the stomata. The improvement of WUE in *phyB-9* plants with FR supplementation suggests that other phytochromes may be having an impact.

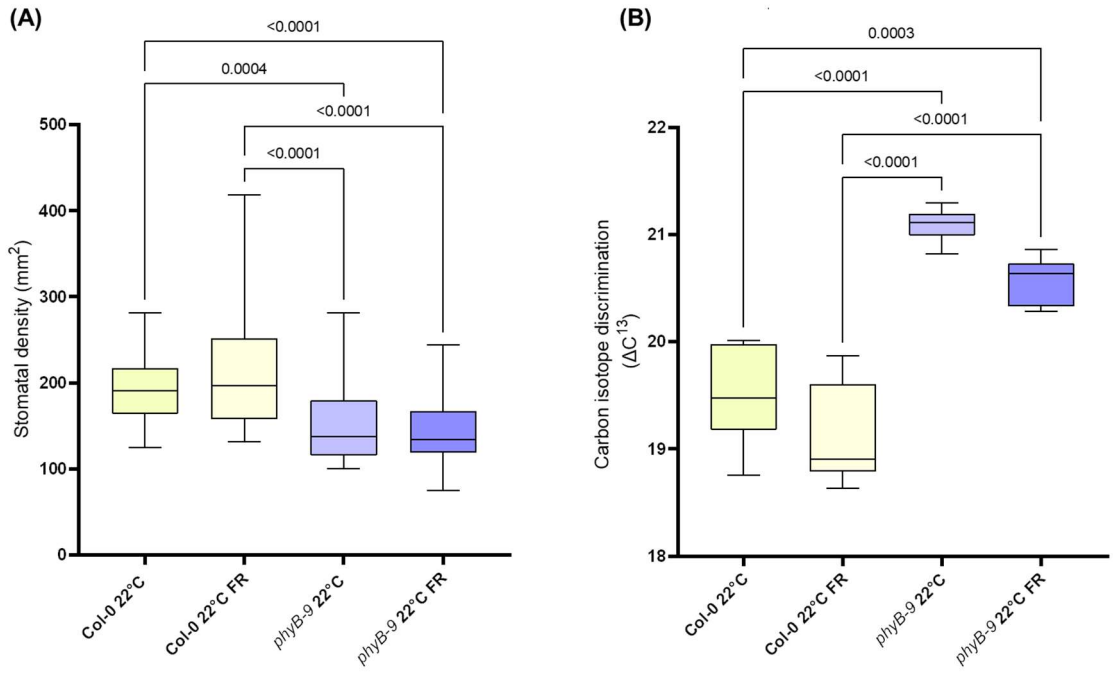

Figure 3.5. Stomatal density and carbon isotope discrimination under different temperature/far-red regimes. (A) Col-0 and *phyB-9* plants either grown with or without EoD FR had leaves removed and impressions taken before the stomatal density was calculated, n=36. **(B).** Plants were dried after flowering and material was taken for IRMS analysis to determine the ratio of the two carbon isotopes (C^{12} and C^{13}), n=5. Box-plot graphs were made in GraphPad prism, the line shows the median value, the boxes represent the 95% interval and the whiskers the highest and lowest value in the dataset. Statistical analysis was carried out in GraphPad prism using a two-way ANOVA and Tukey's multiple comparisons test. Significant p-values ≤0.05 are shown whereas non-significant values >0.05.

Once again, correlations between the stomatal density and CID were carried out for the previous experiment. While there is a strong correlation between density and CID for the plants grown without the EoD FR, this is mainly being driven by *phyB-9* which has an r-value of 0.8850 which is a negative relationship between increasing density and reduced CID, whereas Col-0 has no correlation (Figure 3.6A). The plants that had the addition of EoD FR had no significant relationship between CID and density, and both Col-0 and *phyB-9* had weak relationships between CID and density (Figure 3.6B)

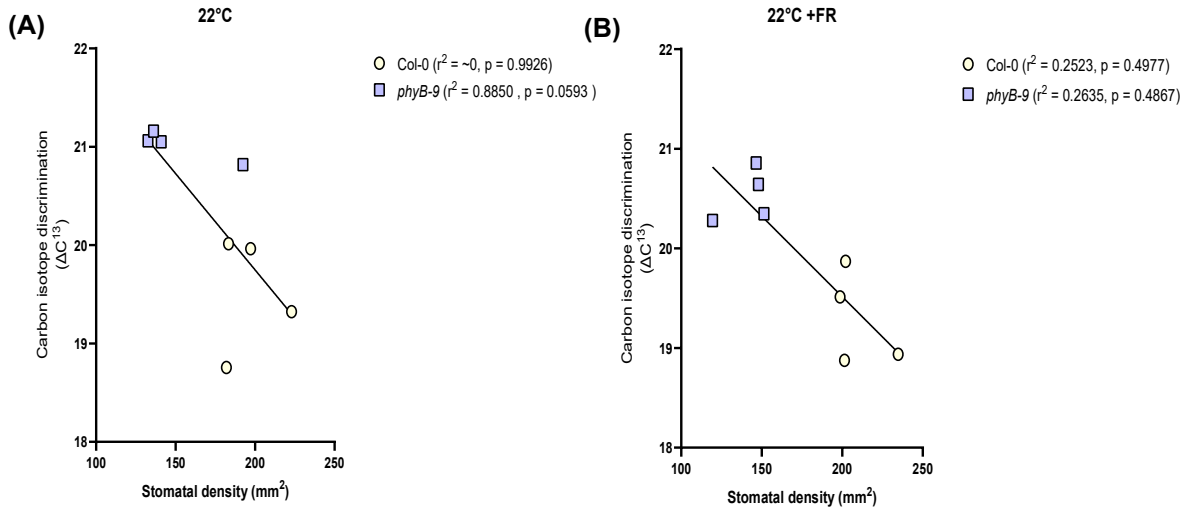

Figure 3.6. Correlations between stomatal density and carbon isotope discrimination from Figure 3.5. (A) Col-0 and *phyB-9* grown at 22°C without the addition of EoD FR. **(B)** Col-0 and *phyB-9* grown at 22°C with the addition of EoD FR. Each point represents an individual plant, n=4. The graphs were generated in GraphPad prism and the line of best fit was a non-linear regression plot with one curve for all datasets for a particular temperature and far-red condition. A correlation analysis was carried out and the r-values and p-values for each dataset are shown next to their respective datasets.

3.4 Col-0 has cooler leaf temperatures than *phyB-9* regardless of temperature regime

Carbon isotope discrimination is a proxy for lifetime water use and improvements in WUE have been shown to be correlated with lower stomatal densities, which is in contrast to the data seen in Fig 3.6 (Masle, Gilmore and Farquhar, 2005; Boccalandro *et al.*, 2009). Decreases in the number of stomata would be expected to reduce the amount of water being lost via evapotranspiration, while increases would be expected to have the opposite effect. The use of thermal imaging is a useful tool to allow the investigation to see if the leaf temperature was similar to what would be expected in the data from stomatal densities during growth. Evapotranspiration impacts on leaf temperature and therefore, leaf temperature as determined by thermal imaging can be used as a proxy for evapotranspiration (Leinonen *et al.*, 2006). Thermal imaging gives an average leaf temperature for a plant; warmer leaves typically mean less water is being lost through transpiration whereas cooler leaves suggest more evaporative cooling is occurring. To see the impact of growing Col-0 and *phyB-9* under both 22°C

and 22°C/16°C, thermal images were taken at regular intervals (1 per minute), and the average leaf temperature was calculated using FLIR thermal imaging software. To consider possible cabinet air flow effects, the trays were rotated daily and where possible the temperature was only recorded from the plants in the centre of the trays to prevent edge effects. However, the impact of canopy architecture on leaf temperature is more difficult to control for. The 22°C/16°C regime was introduced as it represents more of a typical temperature regime that a plant would experience in the wild.

For Col-0, the leaves of those plants grown at 22°C/16°C were significantly cooler than those plants grown at 22°C. Given that the chamber temperature was 22°C during thermal imaging measurements, this suggests that there was less transpiration occurring when Col-0 was grown under the higher temperature load. *phyB-9* had significantly higher leaf temperatures than Col-0 at both 22°C and 22°C/16°C. *phyB-9* grown at 22°C/16°C showed a small but significant decrease in the leaf temperature when compared to those plants grown at 22°C (Figure 3.7C). For reference, still images from the two trays are included (Figure 3.6A-B). For both Col-0 and *phyB*-9, leaf SD was higher at 22°C/16°C than at 22°C and this reflects the cooler leaf temperatures at 22°C/16°C suggesting that these plants have greater levels of transpiration than those grown at 22°C (Figure 3.7D).

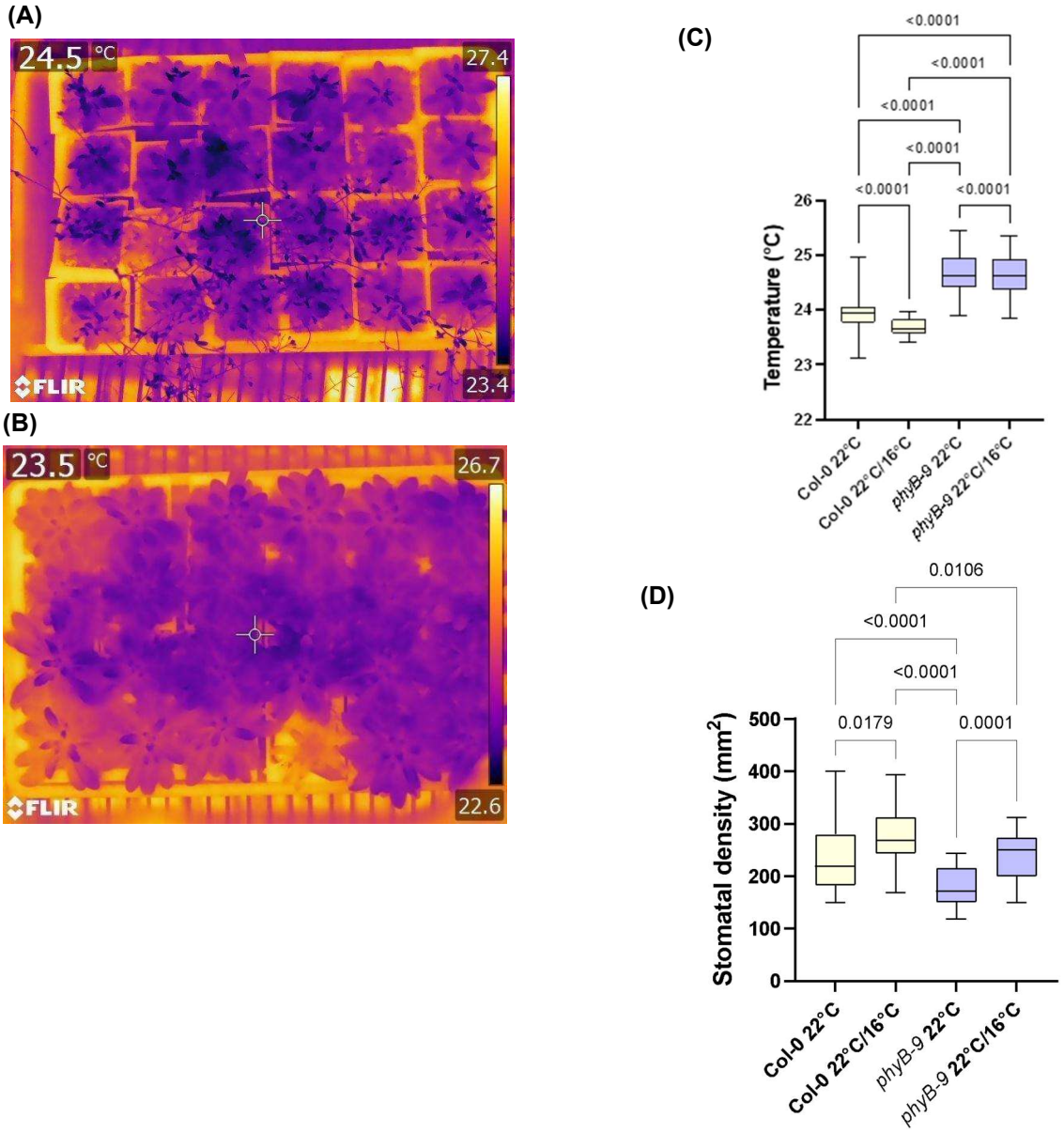

Figure 3.7. Increased temperature loads lead to *phyB-9* having more transpiration than Col-0. **(A-B)** Representative temperature images for Col-0 and *phyB-9* plants grown under 22°C **(A)** and 22°C/16°C **(B)**. **(C)** Col-0 and *phyB-9* were grown under 22°C or 22°C/16°C and temperature measurements were taken regularly (1 per minute) for 1 hour before the first 30 mins of images were removed to account for acclimatisation to cabinet conditions, n=5. **(D)** Stomatal density of Col-0 and *phyB-9* 3 leaves were taken from 4 plants for impressions, n=36. Graphs were generated in GraphPad prism, box and whisker plots show the median value (line) and the boxes represent the 95% interval with the whiskers being the highest and lowest value in the dataset. Statistical analysis was carried out in GraphPad prism, a two-way ANOVA with Tukey's multiple comparisons test was used. Significant p-values ≤0.05 are shown and insignificant p-values >0.05 are not.

phyB has warmer leaf temperatures than Col-0 under both conditions, which aligns with the stomatal density data. Given that this difference in leaf temperature is likely

to reflect reduced transpiration, this would suggest that these *phyB* plants are more WUE but this was not supported by the carbon isotope discrimination data for the plants grown at 22°C (Figures 3.3 & 3.5). This could indicate that under these conditions any positive impact of reduced SD on WUE in *phyB* mutants, is being mitigated by changes in other traits such as photosynthesis and morphology.

To provide further analysis for the relationship of CID and WUE, IRGA measurements were carried out in Col-0 and *phyB* at 22°C/16°C. Unfortunately, due to leaves being too small to fill the chamber, IRGA was not able to be accurately used to measure the iWUE of plants grown at 22°C. Under cabinet conditions, steady state IRGA measurements indicated that both stomatal conductance and assimilation rates were significantly higher in Col-0 compared to *phyB* (Figures 3.8A and 3.8B). However, using these values to calculate iWUE, it was found that *phyB* mutants had significantly higher iWUE than Col-0. As carbon isotope discrimination data was not available for these plants it is not possible to determine if this does reflect longer term WUE however, this IRGA data does correlate with the thermal imaging data in Figures 3.7C and D. This data could therefore suggest that at lower temperature loads, *phyB* is more WUE than Col-0 but that this is reversed at higher temperature loads.

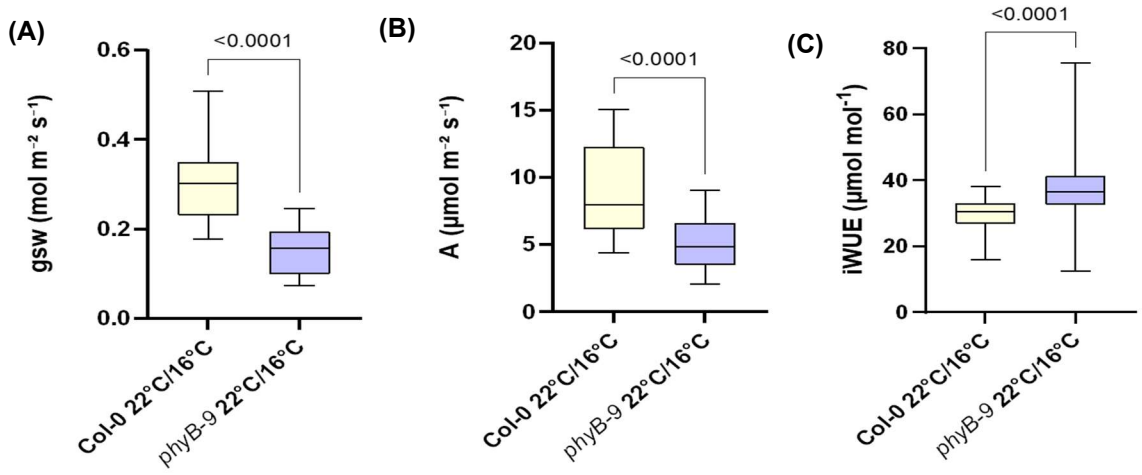

Figure 3.8. IRGA data from Col-0 and *phyB-9* at 22°C/16°C. (A) Stomatal conductance (gsw) and **(B)** Carbon assimilation were used to calculate **(C)** Instantaneous WUE (iWUE) of 6 plants at cabinet conditions. Graphs were generated in GraphPad prism box and whisker plots show the median value (line) and the boxes represent the 95% interval with the whiskers being the highest and lowest value in the dataset. Statistical analysis was carried out in GraphPad prism, an unpaired, two-tailed t-test was carried out. Significant p-values ≤0.05 are shown and insignificant p-values >0.05 are not.

3.5 A phytochrome gradient could give an insight into the role of temperatures and the phytochromes with water use

For WT plants, higher temperatures would be expected to reduce the total Pfr:Pr ratio during the day and lead to faster Pfr:Pr conversion at night. I hypothesised that higher temperatures would initially increase the WUE of WT plants due to reductions in stomatal density before further increases in temperature lead to detrimental impacts on photosynthetic processes, which counter the initial benefits of reduced stomatal densities. However, it is unlikely from the data so far that the SD is influencing the changes in CID that are seen, and so other factors may be involved such as the other phytochromes. To test this and further investigate the role of phytochromes in regulating the water use of plants, experiments were performed with both single and higher order phytochrome mutants. This was predicted to phenocopy the impact of increasing temperature on a WT plant as these genotypes represent a gradient of phytochrome activity, genetically altering the Pfr:Pr ratio without the need to change temperature or light conditions. Several phytochrome mutants were used to create a phytochrome gradient; wild-type Col-0, single mutants *phy*(*A*-*E*), as well as combinations of double mutants: *phyAB, phyAC, phyBC, phyBD* and *phyBE.* The inclusion of a *PHYB* overexpressor (*PHYB*OE) was included as a high Pfr control which, if the water use responses that were being seen are due to decreased levels of Pfr activity, should show an opposing result to *phyB-9.* Unfortunately, due to the time constraints, it was not possible to include higher order mutants in the Col-0 background. In a separate experiment, a *phyQ* mutant, in which all 5 phytochromes are mutated in the Ler background (Hu *et al.*, 2013), was grown under the same conditions. Finally, a mutant of the flowering time regulator FT was included because of the direct correlation of flowering time to WUE and its role in mobilising carbon from the leaves during the floral transition. If the impact of phyB on WUE is through its delay of flowering time this in turn could increase the carbon mobilisation by FT and so a *phyBft* mutant was also included (Halliday *et al.*, 2003; Andrés *et al.*, 2020). Individual plant images from all these lines were taken (Supplementary Figure 3.2).

As for previous experiments, once mature and flowering, leaves were taken for both carbon isotope discrimination via IRMS and impressions were taken of the

abaxial surface for stomatal density calculations (Figure 3.8). While all other mutants were not significantly different from Col-0, the double mutants *phyAC* and *phyBC* had reductions in their WUE, suggesting that multiple phytochromes could be acting to regulate water use under 22°C/16°C. The *phyA* and *phyC* mutants do not show this trend and so this could be an additive effect. There was large variation in the carbon isotope of both *phyBE* and *PHYBOE*, although not significant (Figure 3.9A). Although not significant at the 5% level, *phyB-9* plants were less WUE than Col-0; although a different experiment this was different to the results for iWUE determined by IRGA (Figure 3.8). IRGA gives a snapshot of WUE for that moment in time during the day when the measurements were taken and therefore what is happening during the rest of the time is not accounted for.

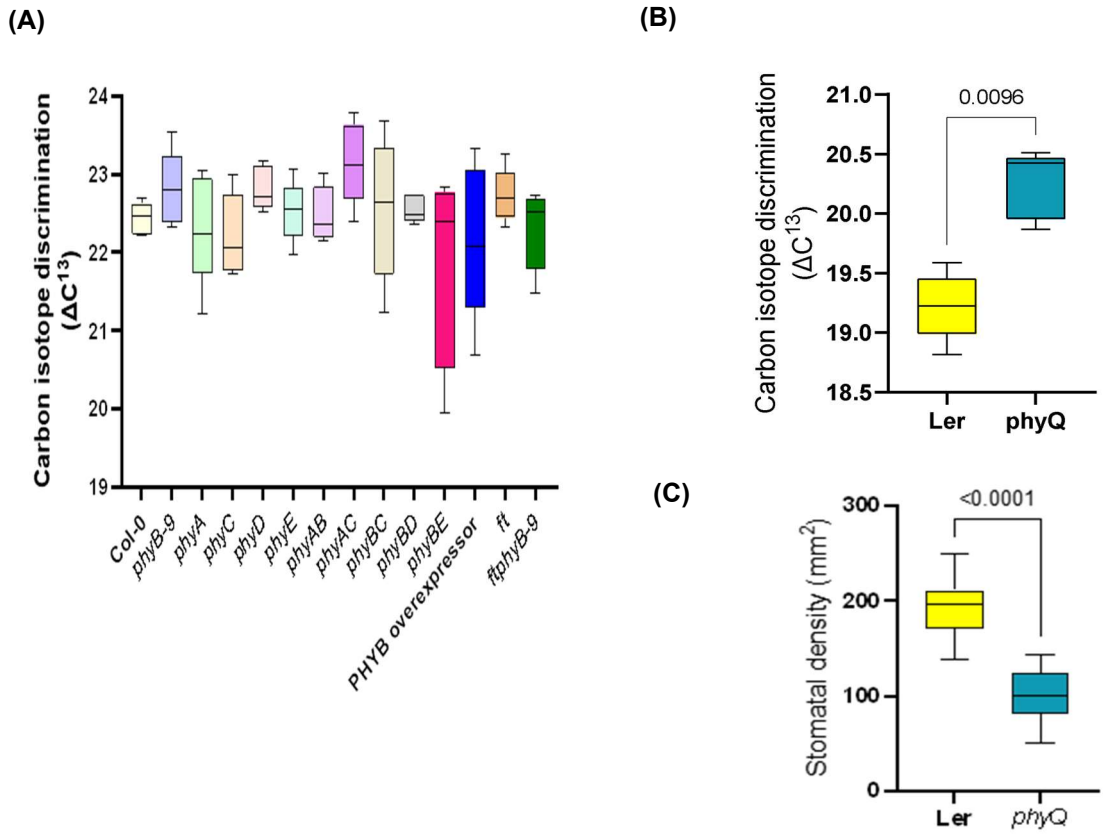

Figure 3.9. A phytochrome gradient was generated to study the impact of decreased Pfr levels on water use. A range of phytochrome mutants were grown under a temperature regime of 22°C/16°C alongside Col-0, these included all 5 phytochrome single mutants (A-E), *phyAB, AC, BC, BD* and *BE,* along with the PHYBOE. **(A)** Carbon isotope discrimination of Col-0 and the mutants material was sent for IRMS. n=4-5. **(B)** Carbon isotope discrimination of Landsberg-*erecta* and *phyQ,* n=5. **(C)** Stomatal density of Ler and *phyQ*. Stomatal density per mm2 was calculated from impressions of mature leaves after plants had flowered, n=36. Carbon isotope discrimination of

Landsberg-*erecta* and *phyQ,* n=5. Box-plot graphs were made in GraphPad prism, the line shows the median value, the boxes represent the 95% interval and the whiskers the highest and lowest value in the dataset. Statistical analysis was carried out in GraphPad prism using a two-way ANOVA and Tukey's multiple comparisons test. For **(B)** and **(C)** an unpaired, two-tailed t-test was carried out. Significant p-values ≤0.05 are shown whereas non-significant values >0.05.

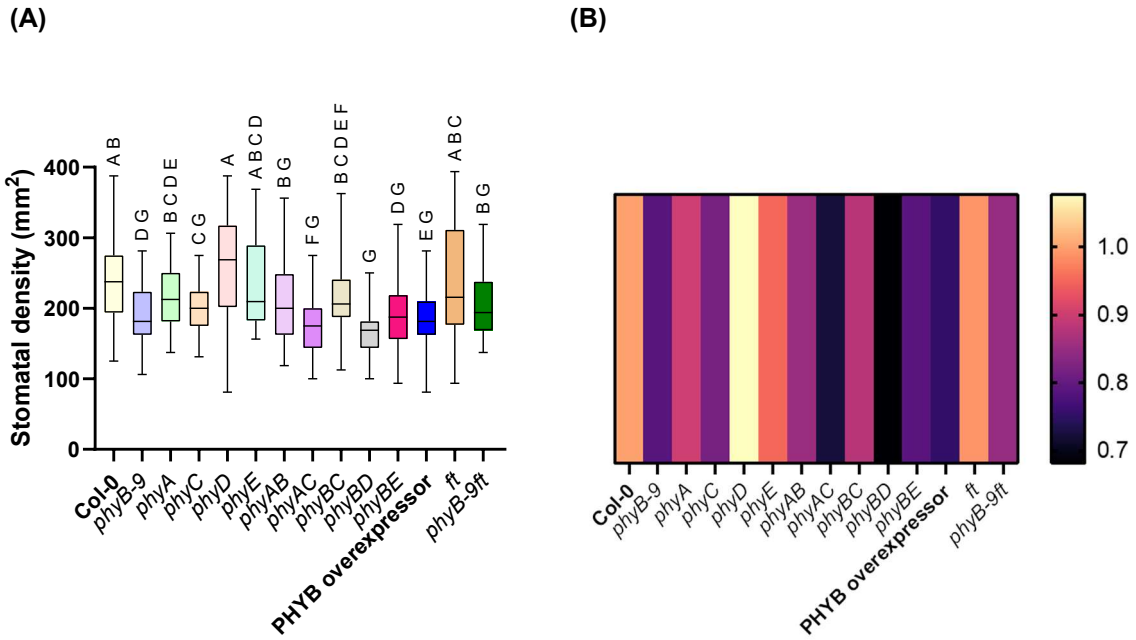

Figure 3.10. Stomatal density of Col-0 and the phy mutants. (A) Three leaves from four mature plants were taken for impressions, n =4. **(B)** Average stomatal density data aligned to Col-0 (=1) to compare densities. Box-plot and heat map graphs were made in GraphPad prism, the line shows the median value, the boxes represent the 95% interval and the whiskers the highest and lowest value in the dataset. Statistical analysis was carried out in GraphPad prism using a two-way ANOVA and Tukey's multiple comparisons test. Significant p-values ≤0.05 are shown by changes in letters.

Despite there not being major differences in CID between the phytochrome mutants there were differences in stomatal density. Interestingly, the stomatal density between Col-0 and *phyB-9* was not significantly different in this experiment. The biggest impact on density between the single mutants was in the *phyD* mutant that had a significant increase in density, which could explain its poorer WUE (Figure 3.10A-B). The double mutants, *phyAB, phyBC* and *phyBE* all had similar densities to Col-0 and *phyB-9*, whereas *phyAC, phyBD* and the *PHYBOE* had significantly fewer stomata than the wild-type (Figure 3.10). Carbon isotope discrimination of both Ler and *phyQ* were lower overall than the other mutants, however Ler was significantly more WUE than *phyQ* (Figure 3.9C). However, *phyQ* had significantly fewer stomata than Ler (Figure 3.9C). Collectively, without higher order mutants within the same background, it is not possibly to fully test my hypothesis regarding the relationship between WUE and a phy gradient. Whilst some single mutants (phyA and phyC) do have non-significant improvements in WUE, a clear trend is not obvious, however, the phenotypes of the double mutants do not show clear epistatic effects compared to their respective single mutants, which may support additive roles of the phytochromes.

Although there were no significant differences within the phytochrome gradient for WUE, there were large differences between the stomatal density. As carbon isotope discrimination is a proxy for lifetime WUE, the use of thermal imaging on these plants may provide more instantaneous transpiration properties during growth and hint at the water use state of these plants during growth.

3.6 phyB in combination with phyD/E are most important for regulating leaf temperature through transpiration

As before, thermal imaging was performed on Col-0 and the phytochrome mutants to determine leaf temperature and by inference, transpiration levels. To keep consistency, replicate imagery was taken at the same time of day for individual trays. As per the previous thermal imaging experiment, *phyB* had a higher leaf temperature than Col-0, as did *phyC* and *phyD*. The *PHYBOE* had a leaf temperature that was between Col-0 and *phyB*. By way of contrast, *phyA* and *phyE* mutants had cooler leaves than Col-0. The double mutant of *phyAB* negated this reduction in leaf

temperature of *phyA* as this mutant had a significantly higher temperature. All of the double phy mutants had significantly higher leaf temperatures than Col-0 (Figure 3.11). The two phytochrome mutant combinations that seem to be impacting this the most are *phyBD* and *phyBE* and it seems that this relationship is an additive one as the single mutants for phyD and phyE do not show significantly increased leaf temperatures. This could mean that phyD/E may have a role in regulating stomatal development when they form heterodimers with phyB. This suggests that the additive removal of Pfr is contributing to a higher leaf temperature and therefore likely, less transpiration, which in general aligns with what might be predicted from the SD data, except for *phyA*. The fact that the carbon isotope discrimination data (Figure 3.9A) only partially correlates, again suggests that non-stomatal traits are likely being impacted and that these negate any positive impact on WUE of reductions in transpiration.

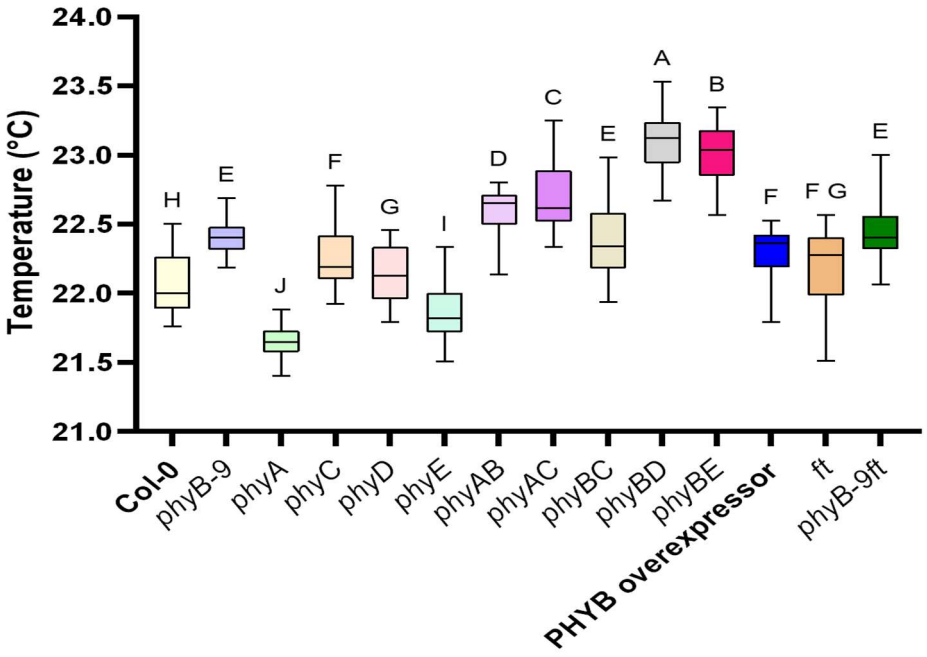

Figure 3.11. Thermal imagery of Col-0 and phytochrome mutants. Plants were grown under 22°C/16°C and temperature measurements were taken regularly (1 per minute) for 1 hour before the first 30 mins of images were removed to account for acclimatisation to cabinet conditions, n=4. Graphs were generated in GraphPad prism, box and whisker plots show the median value (line) and the boxes represent the 95% interval with the whiskers being the highest and lowest value in the dataset. Statistical analysis was carried out in GraphPad prism, a one-way ANOVA with Tukey's multiple comparisons test was used, and significant differences are denoted by letters.

3.7 Flowering time, rosette area and biomass

The amount of time a plant takes to flower is often an indication of the stress that plant is under and reducing the time to flowering time may be a strategy to increase the probability that a plant can pass on its genes before dying (Qiu *et al.*, 2023). Higher temperatures typically speed up flowering time and drought has a similar effect (Balasubramanian and Weigel, 2006; Su *et al.*, 2013). Therefore, it is of little surprise that there is a strong positive correlation between flowering time and WUE. The less WUE the plant, the earlier it flowers (Kenney *et al.*, 2014). To see the impact of reducing the phytochrome pool upon this correlation, the flowering time of the phytochrome mutants along with *ft* and *phyB-9ft* was measured (Figure 3.12A). Here, flowering time is defined as the emergence of the bolt from the rosette. All the phytochrome single mutants had a similar flowering time to each other and to Col-0, which had a mean flowering time of 42.1 ± 1.57 d.p.g, though *phyB* (39.3 ± 1.38 d.p.g) and *phyE* (40.0 ± 1.07 d.p.g) mutants did flower slightly earlier, though this was not significant under these conditions. There were, however, variations in the flowering time of the double mutants with *phyAC* (38.7 ± 2.94 d.p.g) and *phyBC* (38.1 ± 2.04 d.p.g) having an accelerated flowering time compared to Col-0. The double mutant with the fastest flowering time was *phyBE* (35.5 ± 0.58 d.p.g), which was significantly faster than most other mutants.

(A)

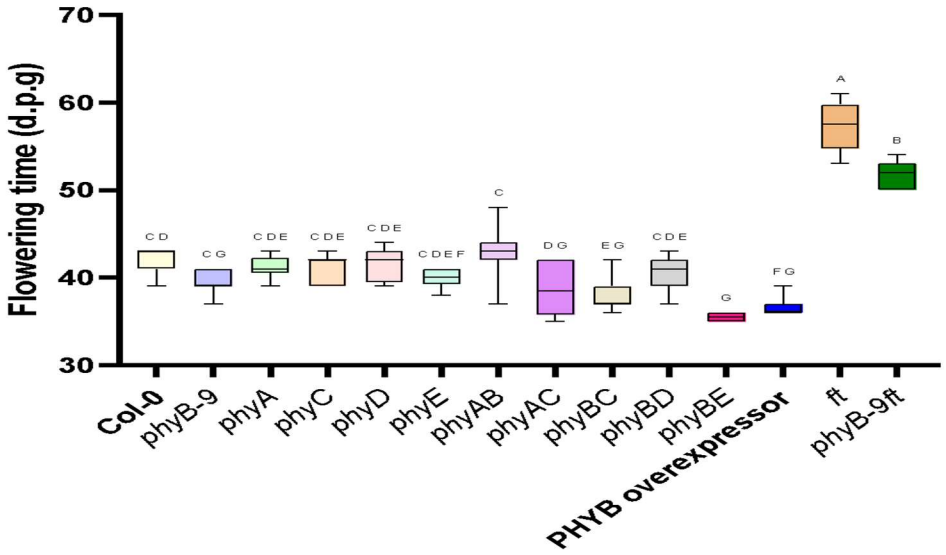

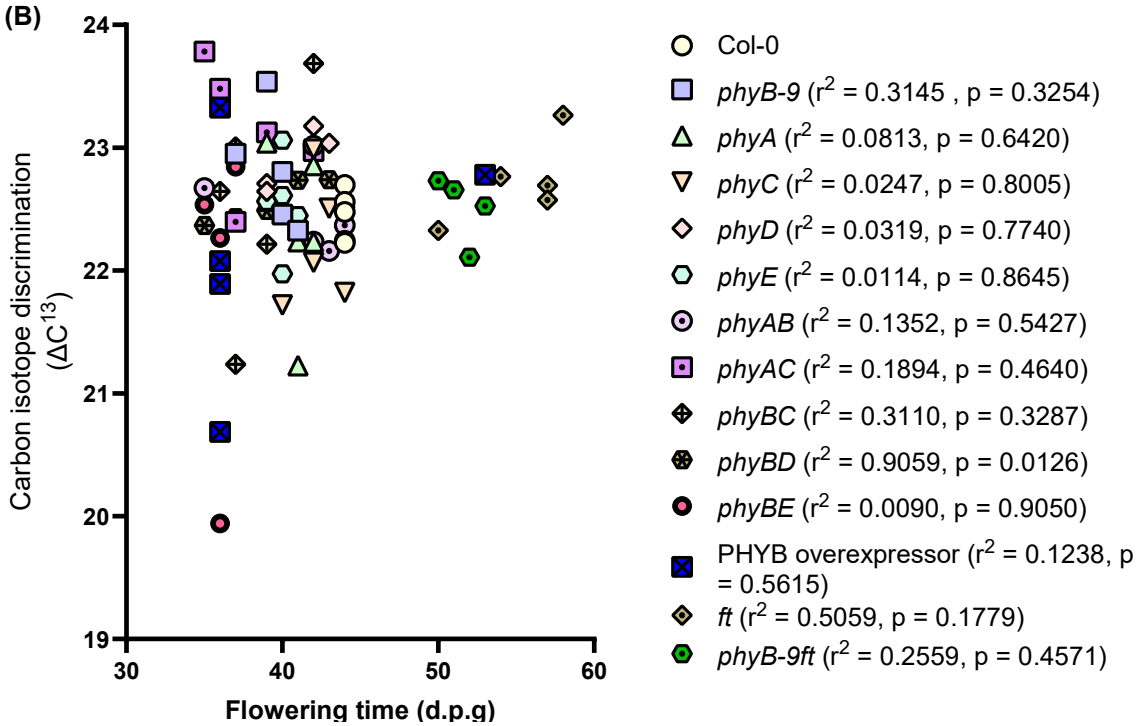

Figure 3.12. Flowering time of Col-0 and phytochrome gradient mutants along with the flowering mutant *ft* and *phyB-9 ft.* (A) Col-0 and a range of phytochrome mutants with *ft* and *phyBft* were grown at 22°C/16°C and the number of days post germination before the emergence of the bolt from the rosette was recorded, n=6-8. Box-plot graphs were made in GraphPad prism, the line shows the median value, the boxes represent the 95% interval and the whiskers the highest and lowest value in the dataset. Statistical analysis was carried out in GraphPad prism using a one-way ANOVA and Tukey's multiple comparisons test. Significant p-values ≤0.05 are designated by letter changes. **(B)** Correlation between carbon isotope discrimination and flowering time. r^2-values and p-values are shown in the key next to their corresponding treatment.

The *PHYBOE* also had a reduced flowering time compared to Col-0 although not as pronounced. As expected, *ft* had a significantly delayed flowering time. Interestingly, the *phyB-9 ft* mutant also had a significantly delayed flowering but to a lesser extent than *ft* suggesting a possible additive interaction. To see how these results correlated with WUE, they were compared to the carbon isotope discrimination from Figure 3.9A. There were a range of correlations between flowering time and CID, with some positive and some negative (Figure 3.12B). However, the only significant correlation was *phyBD* which had a r^2-value of 0.9059. This shows a strong positive correlation between increased flowering and increased CID, the opposite of the expected outcome. The single *phyB* mutant had a low correlation (r^2 = 0.3145), while *phyD* had

little correlation (r^2 = 0.0319). Therefore, functional phyB and phyD are required for improved WUE with delayed flowering but they are not adequate individually to improve WUE through flowering time. As the *ft* and *ftphyB-9* mutants did not show improved CID compared to *phyB-9*, the delayed flowering is not sufficient to improve WUE.

To investigate the impact of a phytochrome gradient on biomass accumulation the plants in the phytochrome gradient had their wet biomass weighed after the plants were cut at the soil level (Figure 3.13A). Most of the mutants showed no significant differences in fresh weight biomasses. The exceptions were *phyBE* and *PHYBOE* which had a significantly lower wet biomass than Col-0 and the other phytochrome mutants. A similar trend was seen in the dry weight measurements (Figure 3.13B), with *phyBE* and *PHYBOE* having a lower biomass than the single phy mutants but not the double mutants and the wild type.

The plants used in the phytochrome gradient had their rosette area measured regularly and a rosette growth curve of average size per line was produced (Figure 3.13C). Individual photos of plants were taken regularly up to 40 days post germination to determine the changes in rosette size over time. The images were not taken beyond this point because of overlapping canopies (Supplementary Figure 3.3). Due to some of the plants not surviving to maturity there is a variation in n number between datasets. As with the biomass results, *phyBE* and the *PHYB*OE also had a small rosette in comparison to the other mutants and Col-0, with a reduced rate of growth compared to the other lines between 25-30 days post germination. All the other lines had similar rosette sizes, although all the phytochrome mutants and *ft* were larger than Col-0. The mutant with the largest rosette size was *phyBC.* These results combined with the biomass data suggest that different phytochrome combinations are having an impact upon the growth and biomass.

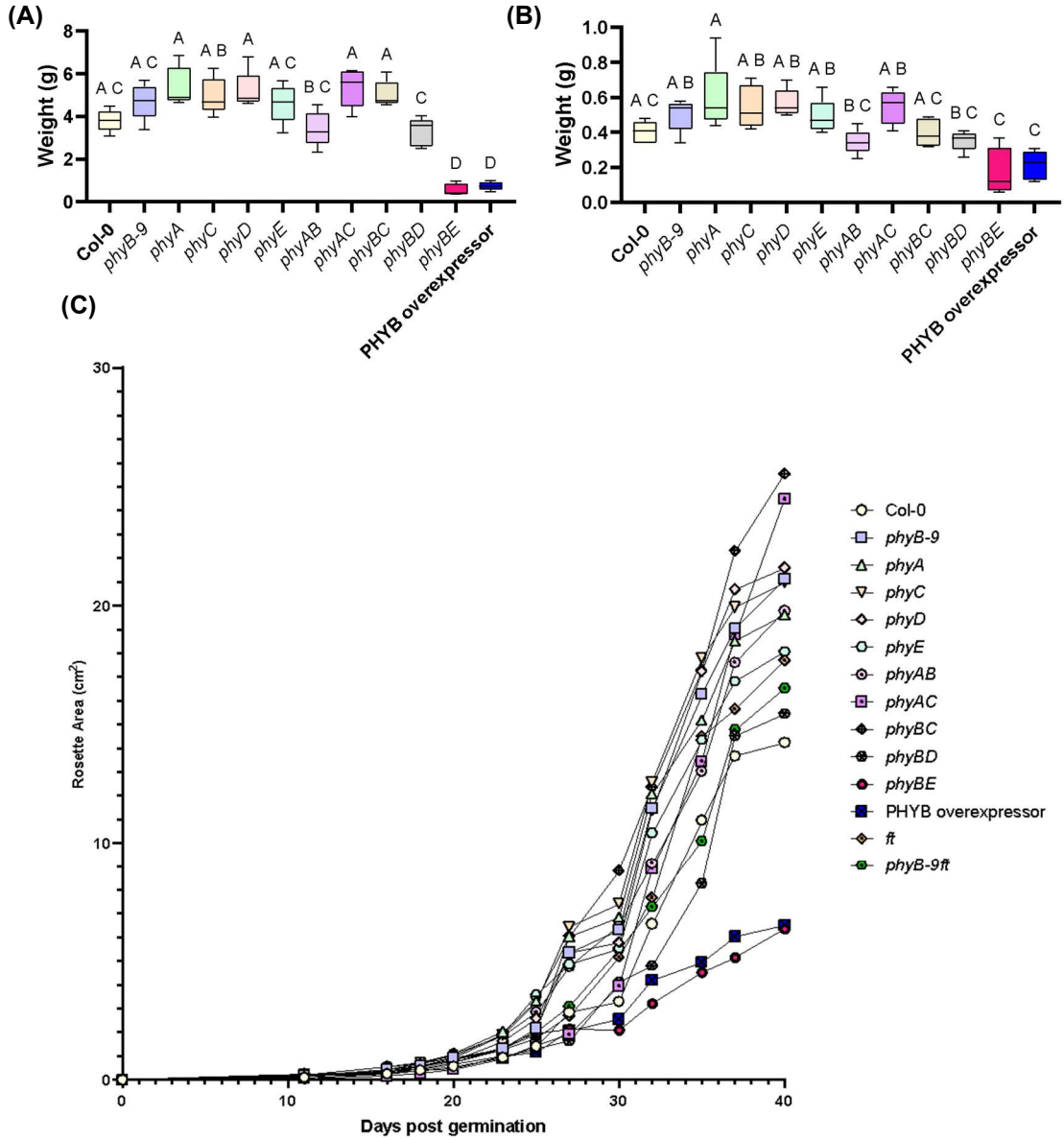

Figure 3.13. Growth properties of phytochrome gradient plants. (A) Average wet biomass of plants in the phytochrome gradient. Before being dried for carbon isotope discrimination, the fresh weight of each plant was weighed. **(B)** Average dry biomass of the plants from the phytochrome gradient. After being dried for carbon isotope discrimination, plants were weighed for their dry weight. Box-plot graphs showing the 95% interval range were generated in GraphPad prism and the median is represented as the average line and the whiskers represent the largest and smallest values, n=5. Statistical analysis was carried out in GraphPad using a one-way ANOVA and Tukey's multiple comparisons test. Significant p-values ≤0.05 are shown and non-significant p-values <0.05 are not. **(C)** Average rosette area from 0 days post germination to 40 d.p.g. Rosette area's were calculated from photographs in ImageJ. Growth curve was generated in GraphPad prism, n=5.

3.8 The combination between phyB and phyE is important to regulate correct photosynthetic function at 22°C/16°C

WUE is directly related not only to stomatal conductance but also to assimilation. In fact, *phyB-9* mutants have a distinctive yellow-green leaf colour which is due to decreased chlorophyll synthesis (Inagaki *et al.*, 2015). Therefore, it was important to study the impact of the different phytochrome mutants in the gradient of activity on photosynthetic parameters to see if the efficiency of photosynthesis was impaired. Due to the difficulty using IRGA to carry out these measurements, a FlourPen Fp110 was used, which measures fluorescence output from a leaf in a dark-adapted state to determine non-photochemical quenching (NPQ) state of the chlorophyll and a number of parameters in a OJIP curve to determine photosynthetic efficiency. Both these measurements were carried out on each of the lines in the phytochrome gradient and selected parameters were analysed. These included the Fv/Fm which is the maximum quantum yield of photosystem II (PSII), Qymax, which is the maximum quantum yield of PSII in dark adapted plants, NPQLss, which determines the amount of NPQ occurring within the chlorophyll and ET/RC which determines the number of electrons transferring per reaction centre. All these parameters give a good indication of the efficiency of a plant's photosynthesis, although not assimilation.

The only significant difference between lines in measuring Fv/Fm was that *phyBE* had a decreased Fv/Fm compared to all other lines (Figure 3.14A). The same line had a significant decrease in maximum QY (Figure 3.14B). However, with both measurements there were large variations in *phyBE*, similar to the CID observation (Figure 3.9A). The measurement of NPQ showed a significant increase in a *phyAB* mutant compared to a *phyA* mutant with no significant differences between all other comparisons (Figure 3.14C). There were more differences between the values of electron transfer per reaction centre with significantly increased transfer in *phyD* and *phyAC* and a significant decrease between *phyAC* and *phyBE* (Figure 3.14D). The largest changes in the photosynthetic efficiency were in the higher order phytochrome mutants, particularly in *phyBE*. Therefore, because the double mutants are a proxy for what could occur in a wild type under higher temperature loads, this could suggest poorer photosynthetic performance under these temperatures, although these plants had an overall smaller size which would have impacted performance. The changes in

photosynthetic activity were only the case in the *phyBE* plants suggesting that the combination of phyB and phyE has the most significant impact on photosynthetic parameters under these conditions. As there are different factors that contribute and influence water use, it was useful to generate correlations between different factors to see which one's influence WUE the most.

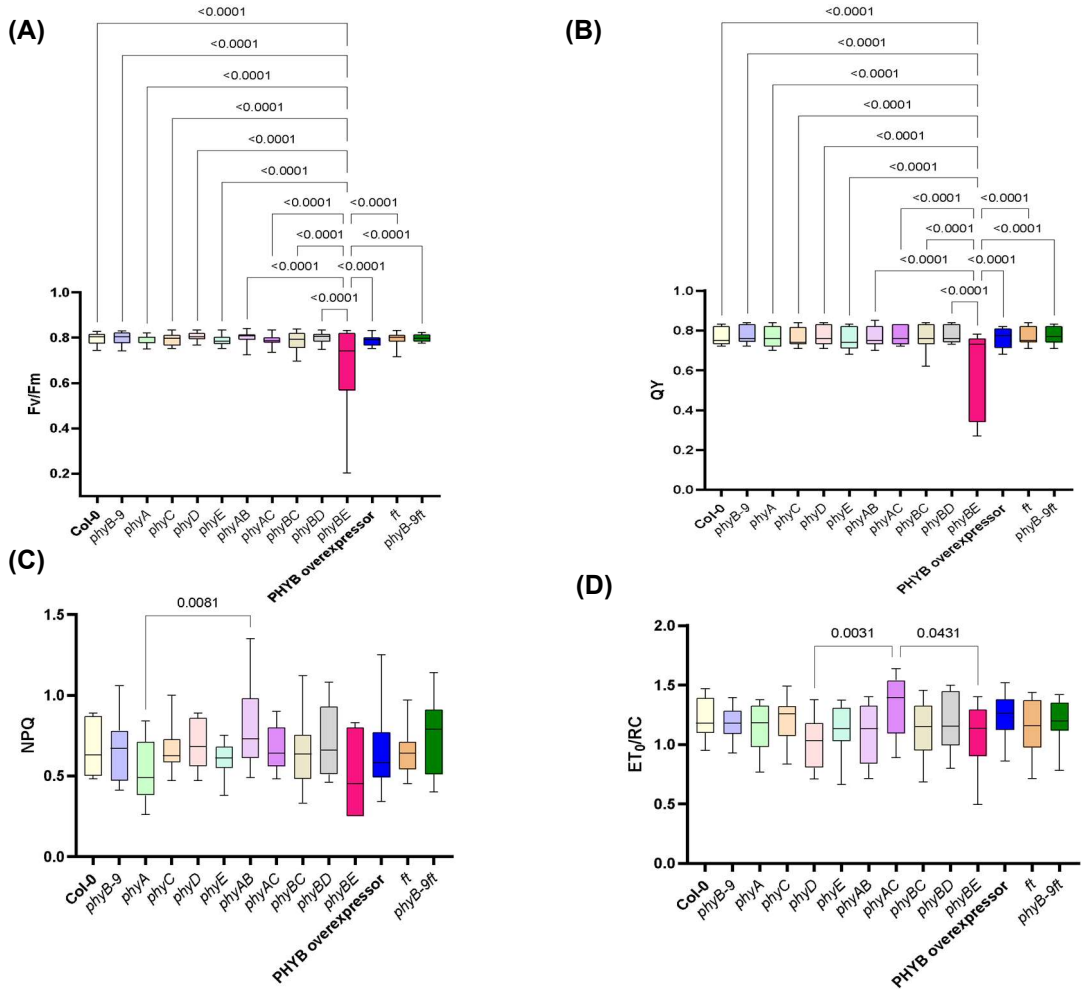

Figure 3.14 . Photosynthetic efficiency of Col-0 and the mutants that are part of the gradient. Col-0 and the phytochrome mutants were grown at 22°C/16°C and their average photosynthetic parameters measured using either the NPQ protocol or generation of an OJIP curve from a Flourpen FP110 sensor. **(A)** Fv/Fm was measured using the OJIP curve, **(B)** Maximum quantum yield was measured from the NPQ protocol, **(C)** The extent of NPQ was measured from the NPQ protocol and **(D)** The number of electron transfers per reaction centre from PSII was measured from the OJIP curve. For all parameters n=4-5. Box-plot graphs were made in GraphPad prism, the line shows the median value, the boxes represent the 25-75% interval and the whiskers the highest and lowest value in the dataset. Statistical analysis was carried out in GraphPad prism using a two-way ANOVA and Tukey's multiple comparisons test. Significant p-values ≤0.05 are shown whereas non-significant values >0.05.

3.9 phyB and phyD in combination regulate improved WUE in an additive manner.

The most interesting mutants in the phytochrome gradient are the *phyBD* and *phyBE* double mutants and the *PHYBOE*. This is because they have the greatest responses in growth, density and photosynthetic parameters, as well as differences in leaf temperature, with *phyBE* also having architectural differences by looking more like a phyQ mutant (Supplementary Figure 2.2). Therefore, correlations of some of these parameters against carbon isotope discrimination were generated along with Col-0 and *phyB-9* to see if the trends were similar to those that were observed for *phyB-9* and Col-0 under a higher temperature load (Figures 3.4A-C). The strongest correlation between SD and CID was Col-0 which had an r^2-value of 0.6948. Once again, *phyB* had a r^2-value that was close to 0 (0.0052) and so it can be inferred that for *phyB* there is no relationship between CID and SD at 22°C/16°C. With increased Pfr removal, there was more of a negative correlation between SD and CID. The strongest of these trends was in *phyBD* (r^2 = 0.3342), *phyBE* had a weak correlation (r^2 = 0.0631). The *PHYBOE* had a slight negative trend, although again a weak correlation, r^2 = 0.02954 (Figure 3.15A). There is a trend of decreasing stomatal density relating to higher CID values and hence, less WUE plants and this trend is more extreme in phy double mutants. The combination of phyB and phyD is important for the regulation of WUE, possibly through stomatal pore size.

A correlation between CID and flowering time was not possible for Col-0 and the *PHYBOE*, this was because the values were in a straight line for both. However, the three other phytochrome mutants were able to be correlated. *phyB* had a negative correlation with a r^2 value of 0.1127, suggesting that these plants were more WUE the later they flowered. When phyD is mutated alongside phyB, there is a strong positive correlation (r^2 = 0.8636) suggesting the opposite trend; that the earlier flowering plants have the most improved WUE. Meanwhile *phyBE* was between the two other mutants with an r^2-value of 0.090 suggesting no correlation. Therefore, *phyB* single mutants that flower later are more WUE. When phyD and to a lesser extent phyE mutants is added in combination with *phyB-9* there is a loss of this trend. This implies that phyD has a strong role in maintaining a positive relationship between WUE and flowering (Figure 3.15).

Col-0, *phyB* and *phyBE* have positive correlations between wet biomass and CID, with *phyB* being a stronger relationship (r^2 = 0.2534, 0.8064 and 0.0.3045). This suggests that with greater biomass there is also an increase in CID and therefore a decrease in WUE. On the other hand, *phyBD* has a negative relationship, r^2 = 0.3911 and along with PHYBOE (r^2 = 0.2908) has this trend of improved WUE with increased biomass.

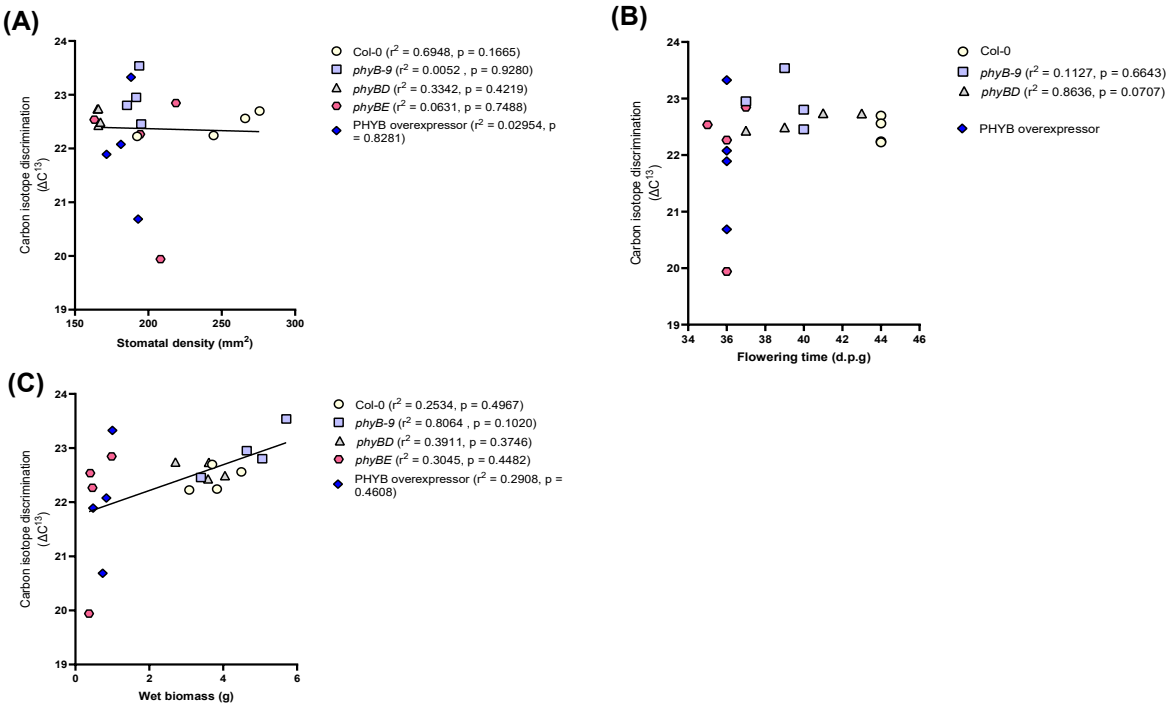

Figure 3.15. Correlations between carbon isotope discrimination and several parameters. Col-0, *phyB-9, phyBE* and the PHYBOE were compared between carbon isotope discrimination and **(A)** Stomatal density, **(B)** Wet biomass, **(C)** Dry biomass and **(D)** Flowering time. Graphs were generated in GraphPad prism and the line represents a non-linear regression line of best fit for all of the data, r^2-values and p-values are shown where applicable.

3.10 Discussion

Due to climate change causing increased temperatures, particularly at night, there is a need to study the impact of these on the ability of plants to use water, otherwise known as their water use efficiency (WUE). phyB is a key regulator of stomatal development and when this gene is mutated the plant produces fewer stomata and offers an improved WUE in Arabidopsis. This coupled with the recent discovery that it could be a temperature sensor, makes it an important candidate to be studied in relation to water use (Boccalandro *et al.*, 2009; Legris *et al.*, 2016; Brown, 2018). Therefore, Col-0 and phyB-9 mutants were grown under different temperature

regimes including a higher night temperature regime. The temperature treatments used in this study are unlikely to be realistic in the environment but coupled with EoD FR treatments, I felt that this allowed for the impacts of higher night time temperatures to be studied in isolation. Most published experiments ultimately have major changes in overall temperature load and so arguably, any differences cannot be directly attributed to when the actual change is applied, but with a standard temperature load, this has been attempted to be negated. The different temperature regimes in this experiment included three which had the same temperature load across the 24 hour day (22°C and HNT), this was to ensure that any changes that were seen in development were due to the timing of the temperature changes and not due to the temperature load perceived by the plant. The inclusion of the 22°C day and 16°C night was because this more accurately reflected the natural environment and provided a normal day baseline from which mutations in the phytochrome could additively represent higher temperature loads. Upon growing both Col-0 and *phyB-9* under three temperature regimes that had an overall temperature load of 22°C, unlike previous studies, *phyB-9* was less WUE than Col-0 under all three temperature regimes (Boccalandro *et al.*, 2009; Brown, 2018) (Figure 3.3A). Even though the CID data indicates that *phyB* mutants have reduced lifetime WUE, their stomatal density was lower than Col-0 under all three conditions, which would be expected to lead to reduced evapotranspiration (Figure 3.3B). The correlations between stomatal density and carbon isotope discrimination under the three temperature regimes for Col-0 and *phyB-9* showed that the timing of the increased temperature impacted the trend of water use. Strangely, the r numbers for the correlation of Col-0 CID and SD suggest that under increased night temperatures (or reduced day temperatures) there is a switch from a positive correlation between CID and density, as would be expected, to a negative correlation. Therefore, it is likely that increased night temperatures or reduced day temperatures are impacting upon CID through means that are not related to stomatal conductance such as photosynthesis or canopy structures (Figure 3.16). The trend in *phyB* is similar, with less positive correlations occurring with increased night temperature, however these correlations do not become negative like Col-0. End of day far-red light was used to mimic a HNT scenario because FR light causes reversion of Pfr to Pr. Addition of EoD FR to Col-0 did indeed mimic the response of a HNT in both CID and the negative correlation

trends without changes in SD (Figures 3.5 and 3.6). In both the temperature and FR experiment, *phyB* was consistently less WUE than Col-0 and hence, functional phyB is required for improved WUE. A higher ratio of Pfr:Pr may be required for improved lifetime WUE although this is impacted by HNT. phyB Pfr appears to be required for improved WUE at higher temperature loads and it is the total Pfr:Pr pool at night and its faster reversion that dictates the improved WUE determined by the EoD FR.

The trend of functional phyB being required for improved WUE at higher temperature loads was tested at reduced temperature loads to see its impact. The stomatal density of Col-0 and *phyB* both increased at 22°C/16°C compared to the same genotypes at 22°C. This was reflected in the thermal imagery which showed that although *phyB* was significantly warmer than Col-0 under both temperature regimes, the plants grown at 22°C/16°C were cooler within genotypes, most likely due to the increased number of stomata leading to more evapotranspiration (Figure 3.7). The iWUE data from the IRGA of Col-0 and *phyB* at 22°C/16°C showed that *phyB* was more WUE than Col-0 at this temperature regime. This was despite *phyB* having reduced assimilation under these conditions. In this case, compared to Col-0, the reduction in stomatal conductance of *phyB* mutants had proportionally more of an impact on the iWUE. However, thermal imaging and IRGA measurements were taken during the day for limited period and do not examine the impact at night when phyB possibly has more of an impact on WUE (Figure 3.8).

A phytochrome gradient of Pfr activity was developed to mimic the levels of Pfr under different temperatures to determine if thermal revision of the other phytochromes are important for regulating improved WUE and how lower ratios of Pfr:Pr in higher order mutants would impact this. A mutant of the flowering time gene FT and *phyBFT* were included in the study due to the potential link between FT and carbon assimilation (Andrés *et al.*, 2020). While there were no significant differences between the CID for the mutants, *phyB* had lower WUE compared to Col-0, despite the decreased SD (Figures 3.9 and 3.10), contradicting the previous IRGA data (Figure 3.8). This could be due to differences in canopy structure between Col-0 and *phyB. phyB* plants undergo more hyponastic growth, characterised by elongated petioles and angled leaves compared to Col-0 (Figure 3.16). Notably, the two double mutants *phyBD* and *phyBE* had reduced stomatal

densities but increased CID much like the *phyB* mutant. Interestingly, a *phyQ* mutant in a Ler background was also significantly less WUE than the WT even though it had fewer stomata, again this could be due to canopy impacts as a phyQ mutant has an extremely open canopy when compared to Ler.

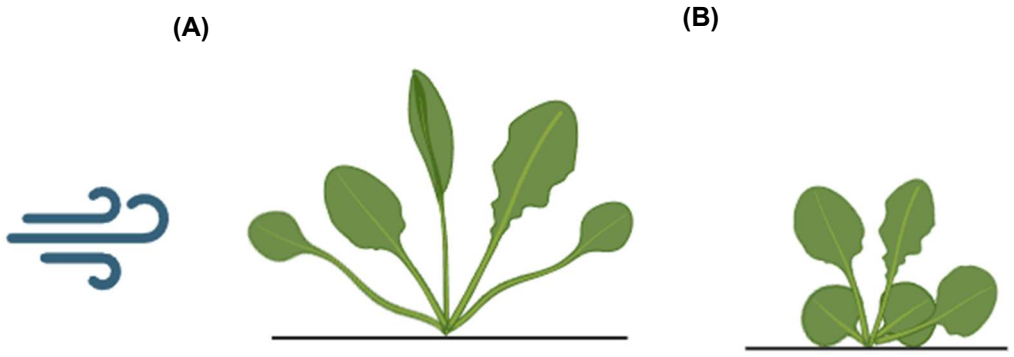

Figure 3.16 Plant architecture and canopy effects may be important in determining lifetime WUE. (A) Higher temperatures (less active Pfr) induce hyponastic growth characterised by elongated petioles and more angled leaves away from the surface and so air flow through the canopy could be more likely to remove water. This growth is more prevalent in *phyB-9* and higher order phy mutants **(B)** Under lower temperatures (more active Pfr) the rosette is more bunched together and more of the leaves are flatter, meaning that air flow through the canopy is less likely to remove water and have potential impacts on lifetime WUE.

When plants were analysed via thermal imaging. *phyB* was significantly warmer than Col-0 and so was likely to have less transpiration occurring (Figure 3.11). The *phyBD* and *phyBE* mutants had the highest average leaf temperatures, with *phyBD* being more significantly warmer than any other mutant. This is possibly an additive effect of phyB and phyD mutations, because the single mutants both have warmer leaves than Col-0 and so in combination wild-type versions of these genes could be required for increased transpiration. To a lesser extent, the same trend could be observed in *phyBE.* In general, the higher order phy mutants had warmer leaf temperatures and so increased levels of Pfr activity are required for evaporative cooling to occur, this can be seen in Col-0 having a cooler average leaf temperature, but the *PHYBOE* bucks this trend, possibly due to its tight rosette structure meaning it cannot cool as

easily (Figure 3.13). Much like *phyB* at higher temperature loads, it is possible that the combination of phyB and phyD/E is required for improved WUE. These proteins are known to bind to each other to form heterodimers and so this could be the method of action (Sharrock and Clack, 2004). The major significant differences in flowering were seen in *phyBE* and *PHYBOE* which flowered significantly earlier than other lines and *ft* and *phyBft* which flowered significantly later (Figure 3.12A). Although there is a positive correlation between improved WUE and later flowering in the literature, this was not seen for these lines (Kenney *et al.*, 2014). In fact, the only significant correlation between flowering time and CID for the mutants was in *phyBD* which had a strong positive relationship between increased CID and delayed flowering (Figure 3.12B). Therefore, the ability to be able to correlate flowering time and CID in phytochrome mutants is questionable.

Due to the lack of correlations between flowering time and CID, it was decided that the biomass accumulation and photosynthetic parameters of these lines should be measured to see if the impact on WUE was due to assimilation via photosynthesis. All the phytochrome mutants had a greater wet biomass than Col-0 except for *phyBE* and the *PHYBOE* and this was reflected in the rosette sizes with these two lines having the smallest (Figure 3.13A and C). In the case of *PHYBOE*, this suggests that too much Pfr:Pr ratio causes plants to be inhibited in their leaf growth, whereas in the case of the phy mutants, reduced Pfr:Pr promotes rosette growth. PhyB and phyE single mutants both had increased biomass and rosette size compared to Col-0, however when they were both mutated the size decreased dramatically, and so phyB and phyE functionally combine to regulate growth. The only significant differences to all mutants in photosynthetic parameters were the *phyBE* plants for Fv/Fm and QY (Figure 3.14). However, there was large variation in the data for *phyBE* and so whether this is a true reflection, or an outlier is questionable. Due to the lack of differences in photosynthetic outputs, it is unlikely that the changes in WUE that were seen were because of carbon assimilation. However, the discovery of a second site mutation in *phyB-9* that mutates the VENOSA4 gene, has been shown to reduce photosynthetic parameters such as chloroplast size and leaf growth (Yoshida *et al.*, 2018) and so this may be having a larger impact on *phyBE* than would be expected in a double mutant without this second site mutation.

The hypothesis that Pfr levels decrease and hence WUE increases with increasing temperature up to an optimum point before there is a decrease in WUE cannot be proven from this data. Any gains in WUE by phy mutants is not robust in comparison to the SD or leaf temperatures from thermal imagery. However, if the plants in the phytochrome gradient were grown at lower temperatures, this could provide more insight into the impact of the phys on WUE in a temperature dependant manner. At higher temperature loads and increased day temperatures, functional phyB is required to improve WUE. This is likely to not be occurring through its regulation of stomatal development as the number of stomata remained equal under all temperature regimes. Thermal imagery and IRGA further showed that transpiration is not likely to account for decrease in WUE in a *phyB* mutant. There are several other avenues that could be explored to determine the relationship between WUE and temperature loads, namely further research into how carbon assimilation is impacted under these temperatures, a possibility that could be studied in a smaller leaf chamber attached to an IRGA and the impact on more photosynthetic parameters. Further to this, the link between phys B/D/E needs to be studied further to dissect their impact on temperature driven flowering, biomass and WUE. Finally, plant architecture is likely to have had an impact on WUE and so uncoupling a canopy from these studies going forward would be useful, however this would require a large amount of growth space.

3.11 Key findings

1. Functional phyB is required for improved WUE at higher temperature loads, particularly during warmer days.
2. Changes in photosynthesis or plant architecture are more likely to account for increased CID and not transpiration.
3. phyB and phyD/E combine to regulate stomatal density, flowering and biomass.

Chapter 4: How does temperature driven thermal reversion affect epidermal patterning?

4.1 Introduction

Development of leaves occurs from a group of pluripotent cells on the flanks of the shoot apical meristem (SAM) (Cho *et al.*, 2007). The leaf epidermis of plants is a vital contact between the environment and the internal leaf surface and consists of a number of different cell types. These include the guard cells that make up the stomata, which are specialised for gas exchange, the hairlike trichomes that protect against herbivores and the jigsaw puzzle arranged pavement cells (Glover, 2000; Pechan *et al.*, 2002; Javelle *et al.*, 2011). In Arabidopsis, the development of stomata happens through a series of asymmetric divisions before the final symmetric division to form guard cells (Pillitteri *et al.*, 2007) (Section 1.3). The patterning of the plant epidermis is spatially and environmentally regulated, which together with changes in internal leaf development are proposed to generate an organ with optimal traits for the environment under which it developed (Hara *et al.*, 2009; Casson and Hetherington, 2010; Kim *et al.*, 2020). For optimal gas exchange, a one cell spacing mechanism ensures that stomata cannot develop immediately adjacent to each other (Sachs, 1991). Together with mechanisms that regulate the number of cells that enter into the stomatal lineage, this allows the optimum arrangement of stomata to balance carbon uptake with water loss. As discussed in section 1.4 the main regulators of epidermal patterning are the EPFs and the cell cycle regulators, notably CYCD3;1 and CYCD5;1 (Harashima, Dissmeyer and Schnittger, 2013; Lau *et al.*, 2014; Han *et al.*, 2022; Zuch *et al.*, 2023). CYCD3;1 is upregulated by SPCH to allow the first division of the lineage to occur, the asymmetric MMC to M and SLGC division (Lau *et al.*, 2014). Meanwhile, CYCD5;1 is upregulated by MUTE binding to its promoter and allows the terminal symmetric division to occur in the lineage (Han *et al.*, 2022) (Figure 4.1).

All the specialised cells mentioned above are derived from protodermal cells. The selection of which protodermal cells go on to produce stomata, pavement cells and trichomes is not well understood. It is thought that a family of homeodomain leucine zipper IV (HD-ZIP IV) including ATML1 and PDF2 may direct the cells towards particular epidermal cell fates. Another member of the family, HDG2 interacts with MUTE in a positive fashion and may help to direct the cells to become stomata (Peterson *et al.*, 2013). There may be a relationship between the development of trichomes and stomata, with ICE1 being shown to be involved in the development of

both; gain-of-function mutants in ICE1 have fewer trichomes and an increase in the number of stomata where trichomes would usually be produced (Kanaoka *et al.*, 2008). TMM, the peptide receptor that when mutated leads to stomatal clustering and increased number of stomata, also suppresses trichome development when overexpressed, suggesting the potential links between stomatal and trichome development (Yan *et al.*, 2014). A *spch* mutant has only interlocked pavement cells which shows that they are the default epidermal cell type that protodermal cells will form in the absence of specialised cell signals. It was shown that through the production of stomatal lineage ground cells, the stomatal lineage contributes to around 48% of the pavement cells in mature leaves (Geisler, Nadeau and Sack, 2000).

Figure 4.1. The role of the cyclins and SMR4 in the stomatal lineage. SMR4 interacts with MUTE and the cyclins to progress the stomatal lineage. CYCD3;1 is inhibited by SMR4 directly to prevent asymmetric divisions during cell proliferation, while MUTE and SMR4 interact to upregulate CYCD5;1 which progresses symmetric cell divisions during differentiation. Taken from (Han *et al.*, 2022).

phyB helps to shape the epidermal surface and in part, this is through interaction with PIF4. PIF4 is able to bind to the *SPCH* promoter and inhibit *SPCH* transcription. As a negative regulator of PIF4¸ phyB antagonises PIF4 mediated inhibition of SPCH but

this is impacted by temperatures as PIF4 accumulates under higher temperatures, likely in part to a reduced pool of phyB Pfr (Lau *et al.*, 2018). This means it is likely that under increased temperatures less cells are being committed to enter the stomatal lineage as SPCH controls entry into the lineage. phyB also physically interacts with and promotes activity of HOS1 mediated inhibition of PIF4 (Lazaro *et al.*, 2012; Kim *et al.*, 2017). HOS1 itself has dual roles in regulating stomatal development, with the inhibition of both PIF4 and ICE1; in the case of ICE1, this inhibits stomatal development (Dong *et al.*, 2006).

Under increased temperature loads, functional phyB was required to improve WUE (section 3.3). This functional phyB is likely to have impacts upon the epidermal patterning of plants under higher temperature loads as well. This is because phyB is a negative regulator of PIF4 and positive regulator of HOS1 which both in turn influence the activity of SPCH and ICE1 respectively, both of which are required for stomatal patterning of the epidermis (Dong *et al.*, 2006; Lau *et al.*, 2018).

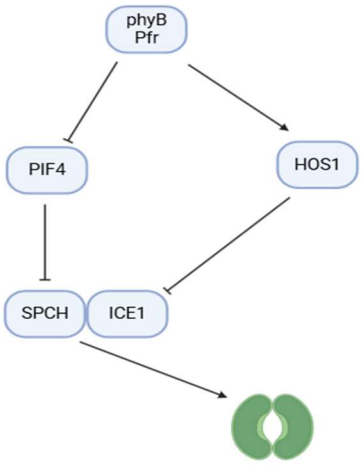

Figure 4.2. Schematic showing the interaction of phyB with PIF4 and HOS1 to regulate stomatal development. Functional phyB interacts with PIF4 to target it for ubiquitination which prevents the inhibition of SPCH by PIF4. Functional phyB activates HOS1 which targets ICE1 for ubiquitination and prevents the interaction between ICE1 and SPCH, inhibiting stomatal development.

4.1.1 Aims and objectives

The aim of this chapter is to investigate the effect of higher temperatures, particularly at night, on epidermal patterning of stomata and other cells

To achieve this aim, I proposed the following objectives:

1. To determine the impact of night time temperature on the patterning of the epidermis
2. To analyse the role of phyB in the temperature regulated epidermal patterning phenotype

4.2 HNT increase S.I. of *phyB-9*, independent of PIF4.

Following on from the work in chapter 3 looking at the impact of temperature on WUE and SD, to determine whether different day and night temperature regimes impact on epidermal cell patterning, genotypes were grown under three different temperature regimes used previously; a high day temperature (HDT) (24°C/ 20°C), 22°C constant throughout the day and a high night temperature (20°C/24°C). As with the previous chapter, experiments were performed with *phyB-9* mutants, given the role of this photoreceptor in regulating stomatal development (Casson and Hetherington, 2010). Mutants in *pif4* were also included as this has been shown to regulate stomatal development in response to temperature, via regulation of *SPCH* and has also been shown to be relatively insensitive to elevated temperatures in other aspects of development (Franklin *et al.*, 2011; Lau *et al.*, 2018). The *PHYB*OE line was also included with the enhanced levels of PHYB hypothesised to mimic *pif* mutants given its antagonism of the PIFs. Given that PIF4 and phyB are antagonistic, any differences between the *pif4* mutant and the *PHYB*OE would point to gene specific roles.

Stomatal index was measured again in the same manner as above (Figure 4.3). Col-0 had a SI of 25.7% (+/- 1.74 SEM) under the high day temperature (HDT); although this is higher compared to both 22°C and HNT, this was not significant. Interestingly, the SI of *phyB* increased with increasing night temperature (or lower day temperature). Under HDT, the SI of *phyB-9* leaves was significantly lower than that of Col-0 under these conditions, but this was reversed at HNT, with *phyB-9* leaves having a higher SI. The *PHYB*OE shows an opposite trend with the SI decreasing as the night temperature increases. Unlike the other genotypes, the SI of the *pif4* mutant does not change under these different temperature treatments and, in general, has higher SIs compared to the other genotypes.

To understand why the SI of *phyB-9* increases with increasing night temperature, the stomatal density was also examined; this is the same density data from section 3.2 and is shown in Figure 4.3B. Although *phyB-9* has a lower stomatal density under all treatments compared to Col-0, there is no significant change in the density data for *phyB-9* within the genotype under the three temperature regimes. Similarly, the SD of the *PHYB*OE does not show any significant difference across the three treatments despite showing a significant decrease in the SI with increasing night temperature, opposing the trend observed for *phyB-9* (Figure 4.3B). Therefore, these changes in SI are likely due to either larger/fewer pavement cells (for increased SI) and decreases are due to smaller/more pavement cells making the percentage of stomata reduced.

In order to investigate how these changes in SI were occurring in some genotypes in the absence of changes in SD, epidermal patterning was examined. In particular, analysis of images identified a subset of divisions, often associated with stomatal lineage cells, that were symmetrical rather than being asymmetrical, as is expected for divisions with the stomatal lineage. Therefore, the number of stomatal complexes, lone stomates and symmetric divisions were counted (as represented in Figure 4.4).

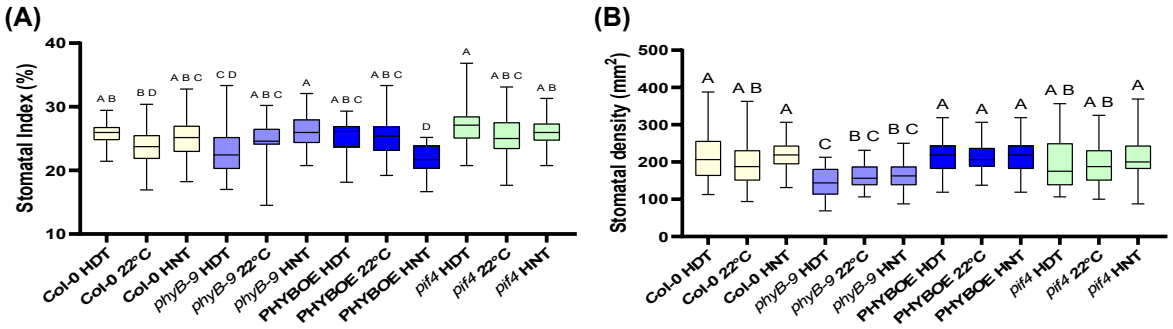

Figure 4.3. **(A)** Stomatal index of Col-0, *phyB*-9, PHYB overexpressor and *pif4*. Plants were grown under different temperature regimes: HDT (24°C day and 20°C night), 22°C day and night and HNT (20°C day and 24°C night). Impressions were made from leaves from each genotype and the number of stomata and epidermal cells counted before a percentage of stomata compared to the total number of cells in the image was calculated. **(B)** Stomatal density calculated from the number of stomata per mm^2. Graphs were made and statistical analysis were carried out in GraphPad prism and Two-way Avona's with Tukey's multiple comparisons test were used, n=35. Box and whisker plots are shown with the centre line being the median value and the boxes representing the 25-75% interval. The whiskers extend out to the highest and lowest values respectively. Significant p-values ≤0.05 are designated by letter changes.

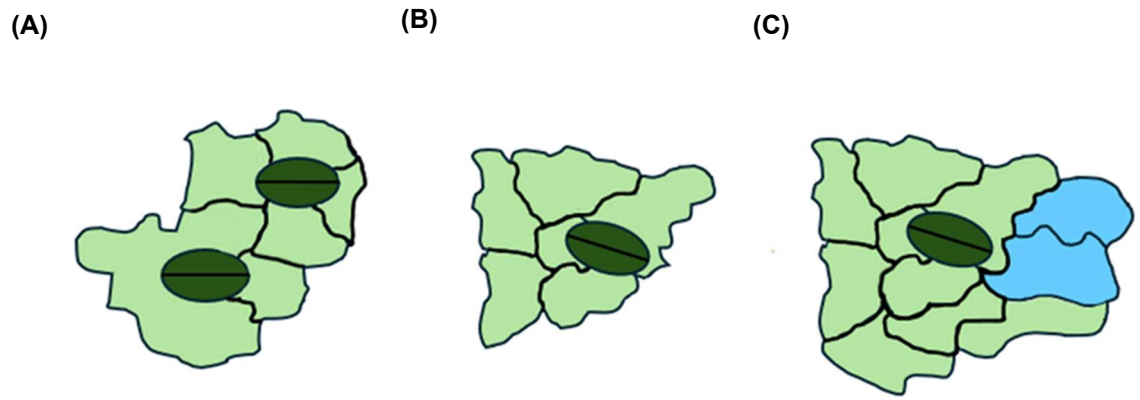

Figure 4.4. Schematic images of stomatal patterning. (A) Stomatal complexes are defined by the primary stomata that have a satellite stomata associated with them. **(B)** Lone stomates do not have associated satellite stomata. **(C)** Symmetrical divisions (blue) in association with a primary stomate. Stomata are coloured darker green, while pavement cells are coloured lighter.

Col-0 grown under all temperature conditions had similar numbers of stomatal complexes and lone stomates. The number of symmetrical divisions increased with increasing night temperature. In comparison, *phyB-9* had a large reduction in the number of stomatal complexes compared to Col-0 under all temperature regimes, however the number of complexes increased with increasing night temperature. This increase in the number of complexes coincided with a reduction in the number of symmetrical divisions, suggesting that under HNT more meristemoids are going on to form stomata, and more of these stomata are forming complexes rather than lone stoma. Whereas at lower night temperatures, more M's could be forming SLGC rather going on to produce stomata (Figure 4.5). *pif4* shows a similar number of complexes to Col-0 and these and the number of lone stomas are not impacted by the different temperature regimes. There is a slight decrease in the number of symmetrical divisions at 22°C, however both the HDT and HNT temperature did not have significant changes. The *PHYB*OE had a decrease in the number of complexes with increased night temperatures, and although the number of lone stoma were not impacted, there was an increase in the number of symmetric divisions at a HNT compared to 22°C, which was the opposing result of *phyB-9*. Therefore, the HNT response in *phyB-9* is likely due to the absence of phyB.

In a WT plant, a change in the distribution of the temperature load, does not lead to appreciable differences in patterning or stomatal density. Mutation in *phyB* however, leads to plants that are sensitive to how temperature load is distributed, and this mainly presents as changes in the number of satellite stomata being generated and termination of cell divisions with the stomatal lineage. Mutations in *pif4* upshift the SI of the plant but they still behave more like a WT in terms of epidermal patterning and so it's unlikely that the phyB mediated sensitisation of patterning is down to PIF4 transcriptional repression of SPCH. Due to the epidermal changes seen in *phyB*, it suggests that functional phyB has a role in buffering cell fate decisions in the epidermis in response to against temperature differences.

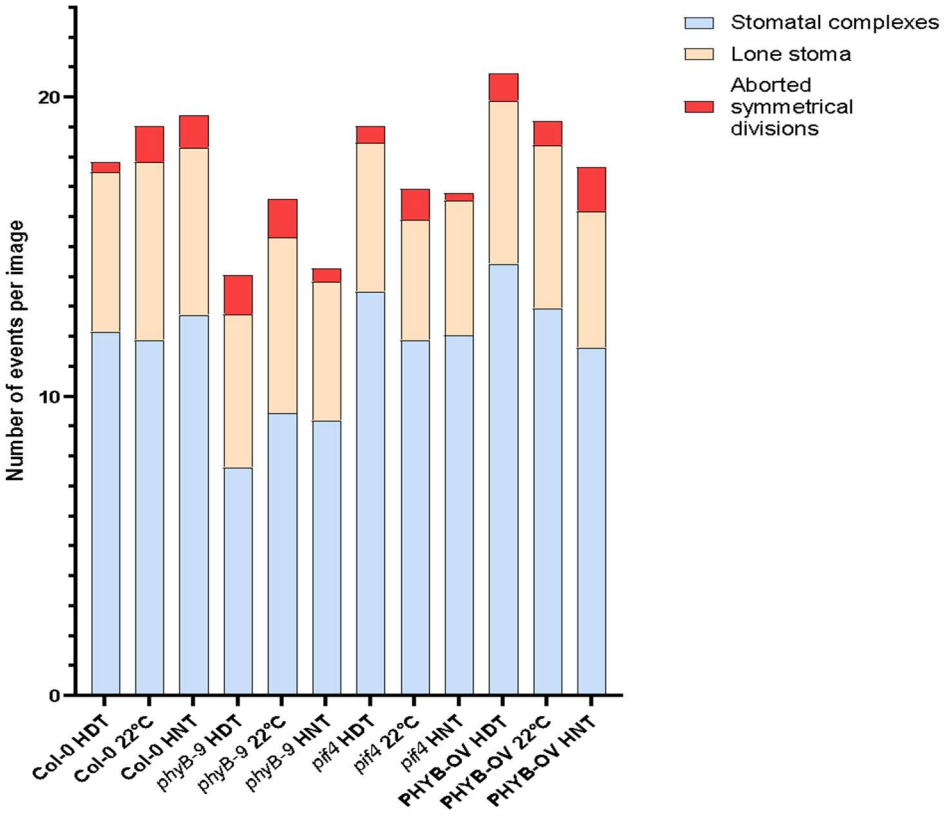

Figure 4.5. Number of stomatal events on average in the epidermis. (A) Col-0, *phyB-9*, *pif4* and *PHYB* overexpressor (PHYB-OV) were grown under HDT, 22°C or HNT and the number of stomatal complexes, lone stomata and aborted symmetrical divisions were counted. Graphs were generated in GraphPad prism, n=35. Statistical analysis was carried out in GraphPad Prism using a two-way Anova and Tukey's multiple comparisons test, p-values are shown in Table 4.1.

Stomatal complexes	Col-0 HDT	Col-0 22°C	Col-0 HNT	*phyB-9* HDT	*phyB-9* 22°C	*phyB-9* HNT	*pif4* HDT	*pif4* 22°C	*pif4* HNT	PHYBOE HDT	PHYBOE 22°C
Col-0 HDT	N/A	>0.9999	0.9995	<0.0001	0.0022	0.0005	0.6422	>0.9999	>0.9999	0.0266	0.9874
Col-0 22°C	>0.9999	N/A	0.9814	<0.0001	0.0114	0.0028	0.3412	>0.9999	>0.9999	0.0058	0.8913
Col-0 HNT	0.9995	0.9814	N/A	<0.0001	<0.0001	<0.0001	0.9874	0.9814	0.9968	0.2689	>0.9999
phyB-9 HDT	<0.0001	<0.0001	<0.0001	N/A	0.2068	0.4222	<0.0001	<0.0001	<0.0001	<0.0001	<0.0001
phyB-9 22°C	0.0022	0.0114	<0.0001	0.2068	N/A	>0.9999	<0.0001	0.0114	0.0046	<0.0001	<0.0001
phyB-9 HNT	0.0005	0.0028	<0.0001	0.4222	>0.9999	N/A	<0.0001	0.0028	0.0010	<0.0001	<0.0001
pif4 HDT	0.6422	0.3412	0.9874	<0.0001	<0.0001	<0.0001	N/A	0.3412	0.5091	0.9630	0.9995
pif4 22°C	>0.9999	>0.9999	0.9814	<0.0001	0.0114	0.0028	0.3412	N/A	>0.9999	0.0058	0.8913
pif4 HNT	>0.9999	>0.9999	0.9968	<0.0001	0.0046	0.0010	0.5091	>0.9999	N/A	0.0142	0.9630
PHYBOE HDT	0.0266	0.0058	0.2689	<0.0001	<0.0001	<0.0001	0.9630	0.0058	0.0142	N/A	0.5091
PHYBOE 22°C	0.9874	0.8913	>0.9999	<0.0001	<0.0001	<0.0001	0.9995	0.8913	0.9630	0.5091	N/A
PHYBOE HNT	0.9997	>0.9999	0.8913	<0.0001	0.0394	0.0114	0.1552	>0.9999	>0.9999	0.0013	0.6851
Lone stoma	Col-0 HDT	Col-0 22°C	Col-0 HNT	*phyB-9* HDT	*phyB-9* 22°C	*phyB-9* HNT	*pif4* HDT	*pif4* 22°C	*pif4* HNT	PHYBOE HDT	PHYBOE 22°C
Col-0 HDT	N/A	0.9990	>0.9999	>0.9999	0.9997	0.9948	>0.9999	0.6581	0.9814	>0.9999	>0.9999
Col-0 22°C	0.9990	N/A	>0.9999	0.9814	>0.9999	0.6851	0.9337	0.1333	0.5537	0.9997	0.9997
Col-0 HNT	>0.99999	>0.99999	N/A	0.9999	>0.9999	0.9499	0.9982	0.4222	0.8913	>0.9999	>0.9999
phyB-9 HDT	>0.9999	0.9814	0.9999	N/A	0.9917	0.9999	>0.9999	0.8913	0.9990	>0.9999	>0.9999
phyB-9 22°C	0.9997	>0.9999	>0.9999	0.9917	N/A	0.7653	0.9630	0.1797	0.6422	>0.9999	>0.9999
phyB-9 HNT	0.9948	0.6851	0.9499	0.9999	0.7653	N/A	>0.9999	0.9990	>0.9999	0.9874	0.9874
pif4 HDT	>0.9999	0.9337	0.9982	>0.9999	0.9630	>0.9999	N/A	0.9630	>0.9999	0.9999	0.9999
pif4 22°C	0.6581	0.1333	0.4222	0.8913	0.1797	0.9990	0.9630	N/A	0.9999	0.5982	0.5982
pif4 HNT	0.9814	0.5537	0.8913	0.9990	0.6422	>0.9999	>0.9999	0.9999	N/A	0.9630	0.9630
PHYBOE HDT	>0.9999	0.9997	>0.9999	>0.9999	>0.9999	0.9874	0.9999	0.5982	0.9630	N/A	0.9630
PHYBOE 22°C	>0.9999	0.9997	>0.9999	>0.9999	>0.9999	0.9874	0.9999	0.5982	0.9630	>0.9999	N/A
PHYBOE HNT	0.9874	0.5982	0.9142	0.9995	0.6851	>0.9999	>0.9999	0.9997	>0.9999	0.9734	0.9734

Symmetric divisions	Col-0 HDT	Col-0 22°C	Col-0 HNT	*phyB-9* HDT	*phyB-9* 22°C	*phyB-9* HNT	*pif4* HDT	*pif4* 22°C	*pif4* HNT	PHYBOE HDT	PHYBOE 22°C
Col-0 HDT	N/A	0.9734	0.9917	0.9337	0.9499	>0.9999	>0.9999	0.9948	>0.9999	0.9990	0.9999
Col-0 22°C	0.9734	N/A	>0.9999	>0.9999	>0.9999	0.9917	0.9982	>0.9999	0.9499	>0.9999	>0.9999
Col-0 HNT	0.9917	>0.9999	N/A	>0.9999	>0.9999	0.9982	0.9997	>0.9999	0.9814	>0.9999	>0.9999
phyB-9 HDT	0.9337	>0.9999	>0.99999	N/A	>0.9999	0.9734	0.9917	>0.9999	0.8913	>0.9999	0.9997
phyB-9 22°C	0.9499	>0.9999	>0.99999	>0.9999	N/A	0.9814	0.9948	>0.9999	0.9142	>0.9999	0.9999
phyB-9 HNT	>0.9999	0.9917	0.9982	0.9734	0.9814	N/A	>0.9999	0.9990	>0.9999	0.9999	>0.9999
pif4 HDT	>0.9999	0.9982	0.9997	0.9917	0.9948	>0.9999	N/A	0.9999	>0.9999	>0.9999	>0.9999
pif4 22°C	0.9948	>0.9999	>0.9999	>0.9999	>0.999	0.9990	0.9999	N/A	0.9874	>0.9999	>0.9999
pif4 HNT	>0.9999	0.9499	0.9814	0.8913	0.9142	>0.9999	>0.9999	0.9874	N/A	0.9968	0.9995
PHYBOE HDT	0.9990	>0.9999	>0.99999	>0.9999	>0.9999	0.9999	>0.9999	>0.9999	0.9968	N/A	>0.9999
PHYBOE 22°C	0.9999	>0.9999	>0.9999	0.9997	0.9999	>0.9999	>0.9999	>0.9999	0.9995	>0.9999	N/A
PHYBOE HNT	0.8349	>0.9999	>0.9999	>0.9999	>0.9999	0.9142	0.9630	>0.9999	0.7653	0.9995	0.9968

Table 4.1. Statistical p-values for a Two-way ANOVA with Tukey's multiple comparisons test for the data from Figure 4.4. Significant p-values ≤ 0.05 are highlighted in green.

4.3 HOS1 may act with *phyB* to regulate epidermal patterning under high night temperature

The E3 ubiquitin ligase HOS1 targets the bHLH transcription factor ICE1 for degradation and therefore affects stomatal development through the inhibition of interactions between ICE1 and SPCH, MUTE and FAMA (Dong *et al.*, 2006; Kanaoka *et al.*, 2008) . The relationship between HOS1 and ICE1 has been characterised as a temperature mediated response. HOS1 has been demonstrated to target ICE1 for degradation under colder temperatures but the role of HOS1 under the temperature regimes used here, have not been investigated (Dong *et al.*, 2006). HOS1 was used in this study as a proxy for the role of ICE1, which was not available in this study (Chinnusamy *et al.*, 2003). Col-0, *phyB-9*, *hos1* and *phyB-9hos1* double mutant were grown under both 22°C and HNT. Inclusion of the *phyB-9hos1* double mutant would allow me to distinguish between epistatic and additive interactions, if indeed HOS1 (and potentially ICE1) is involved. As before, SI, SD and patterning phenotypes were determined (Figure 4.5).

The wild-type Col-0 had a small but not significant decrease in the SI when grown under a HNT compared to 22°C, which followed the previously seen results. The *phyB-9* mutant grown under 22°C had a similar index to Col-0, however when compared to those grown under a HNT, there was a significantly higher SI compared to all other genotypes except the Col-0 22°C, which again followed the previous results (Figure 4.6A). The *hos1* single mutant grown under 22°C had a similar SI to both the *phyB-9* and the Col-0 grown under the same conditions and there was little change when compared to the plants grown under an HNT. However, the response compared to *phyB-9* was slightly more pronounced compared to the WT. The response of the *phyB-9hos1* double mutant was similar in trend to that of *phyB*, with an increase in SI at HNT. However, the SI of the *phyB-9hos1* double mutant was lower than that of either parental line, though this was only significant when compared to *phyB-9*. The fact that the trend for SI changes between plants grown at 22°C versus HNT was similar to both parents but the SI is lower, could suggest an additive impact on SI but an epistatic relationship cannot be ruled out.

In terms of density, Col-0 had a decrease in the number of stomata when grown under an HNT compared to those grown under 22°C. There is minimal difference between

the *phyB-9* mutants under both temperature regimes, however *phyB-9* grown under the HNT had a significantly lower density compared to Col-0 at 22°C. The single *hos1* mutant grown under a HNT had an increased density and similarly, the double mutant had the same trend, although the plants grown under 22°C had a lower density overall compared to the other genotypes. This SD data again does not clarify any additive or epistatic interactions between phyB and HOS1, though the double mutant is more similar in response to *hos1*.

The epidermal patterning of stomata and pavement cells was also studied (Figure 4.7). The number of stomatal complexes typically decreased when plants were grown under a HNT compared to those grown under 22°C, however this was not the case for the *hos1* and *phyB-9hos1*. Independent of the genotype or temperature that the plants were grown under, there was minimal change between the numbers of lone stoma. When examining the number of symmetrical divisions, the major differences were in genotypes that included *phyB-9*. There was a large decrease in the number of these aborted divisions in the *phyB-9* single mutant when grown under HNT compared to those under 22°C and this same trend can be seen in the *phyB-9hos1* double mutant. All other genotypes had similar numbers of symmetric divisions regardless of temperature regime.

Collectively, between these different analyses it is therefore difficult to establish any clear genetic relationship between the phenotypes of the single mutants and the double. However, the trend in stomatal index of both *hos1* (although not significant to the 5% level) and *phyBhos1* bears greater similarity to that of *phyB-9* than Col-0 and suggests that HOS1 and hence potentially ICE1, may have a role in buffering epidermal decisions against temperature changes.

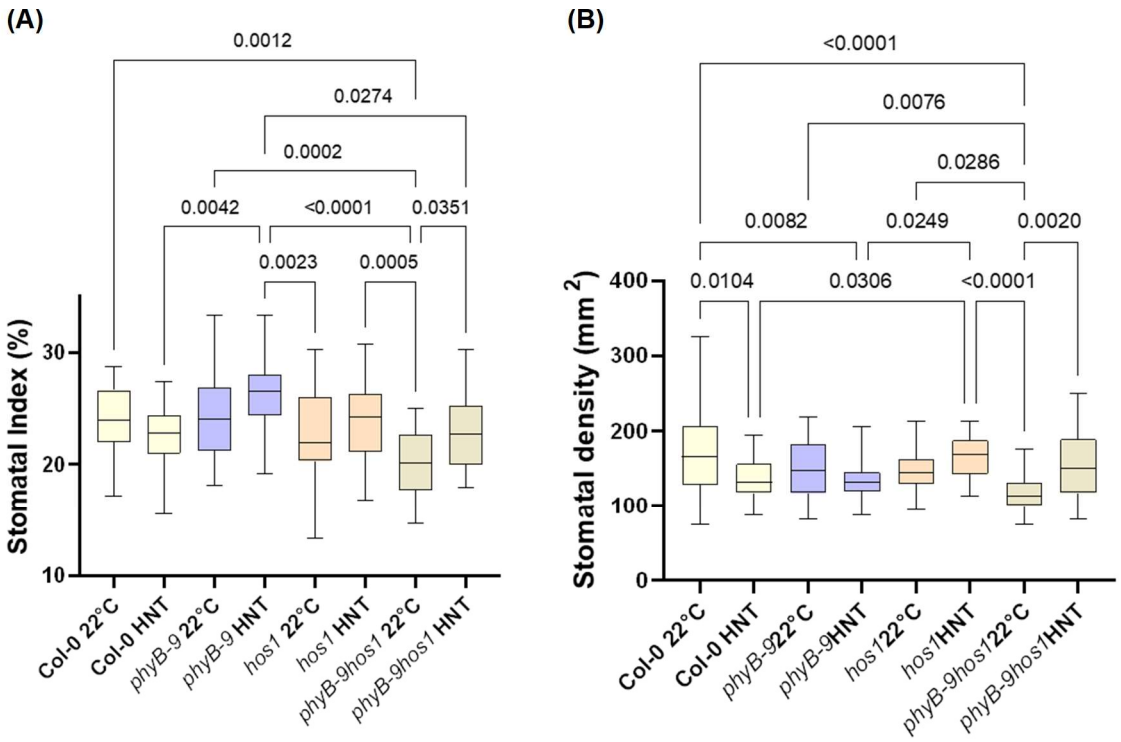

Figure 4.6. The role of HOS1 in stomatal development and epidermal patterning under different temperature regimes. Col-0, *phyB-9, hos1* and *phyB-9hos1* plants were grown under 22°C or 20°C day and 24°C night. Leaves were taken for impressions of the abaxial epidermis and the number of stomata and pavement cells were counted and the percentage of stomata compared to total number of cells were counted for the stomatal index **(A)** and the number of stomata per mm^2 was counted **(B)**. Graphs were generated in GraphPad prism, box and whisker plots show the median and the whiskers represent the largest and smallest values respectively. Statistical analysis was carried out in GraphPad using a two-way ANOVA and Tukey's multiple comparisons test, n=30. Significant p-values ≤0.05 are shown and non-significant p-values > 0.05 are not.

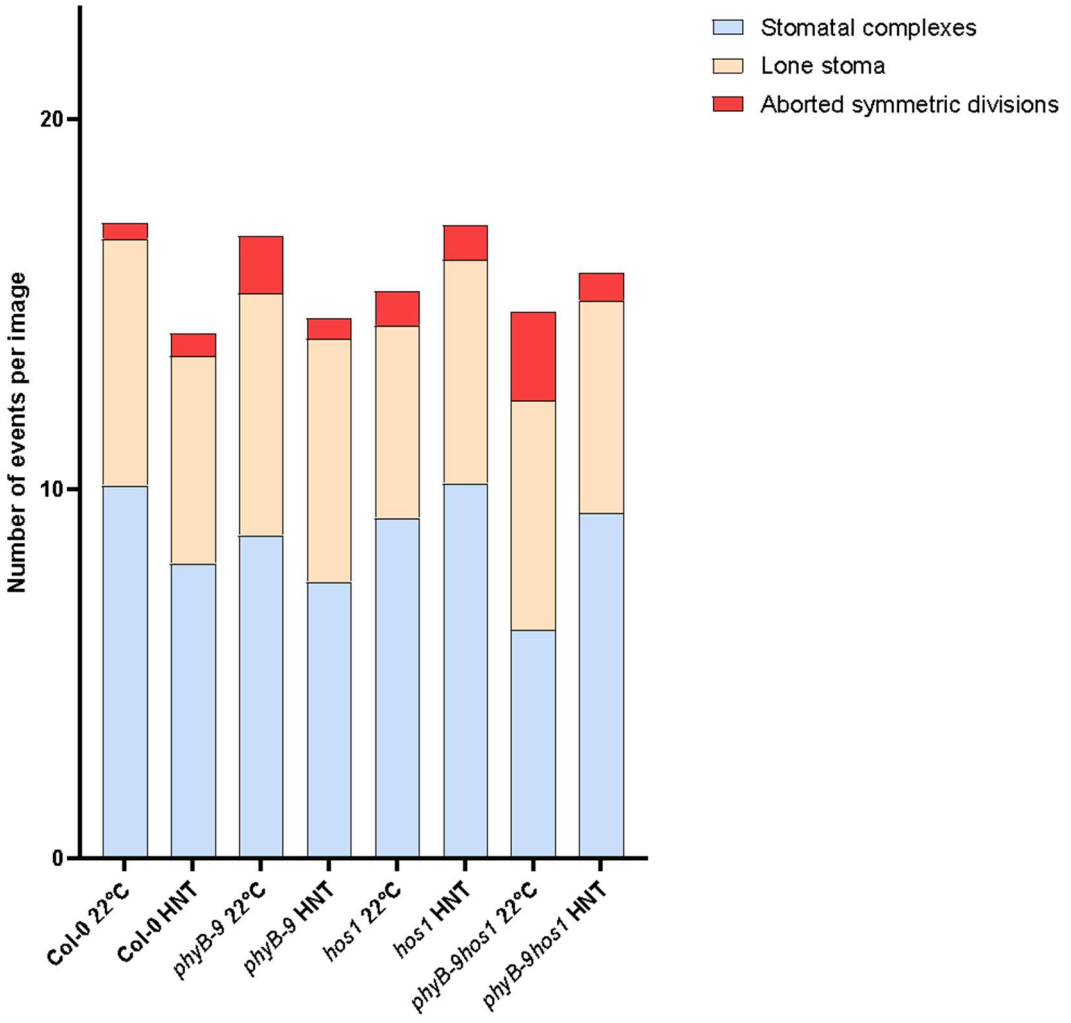

Figure 4.7. The number of certain epidermal patterning events from leaf impressions. Col-0, *phyB-9*, *hos1* and *phyB-9hos1* leaves were taken for impressions and the number of stomatal complexes, lone stoma and aborted meristemoid symmetrical divisions were counted. Each genotype was grown under 22°C and HNT and the average number of each event was recorded per genotype. Graphs were generated in GraphPad prism. Statistical analysis was carried out in GraphPad prism using a two-way ANOVA and Tukey's multiple comparisons test, p-values are shown in Table 4.2.

Stomatal complexes	Col-0 HNT	*phyB-9* 22°C	*phyB-9* HNT	*hos1* 22°C	*hos1* HNT	*hos1phyB-9* 22°C	*hos1phyB-9* HNT
Col-0 22°C	0.0160	0.3761	0.0007	0.8548	>0.9999	<0.0001	0.9349
Col-0 HNT	N/A	0.9186	0.9925	0.4824	0.0110	0.0703	0.3430
phyB-9 22°C	0.9186	N/A	0.4460	0.9951	0.3115	0.0009	0.9781
phyB-9 HNT	0.9925	0.4460	N/A	0.0939	0.0005	0.4105	0.0519
hos1 22°C	0.4824	0.9951	0.0939	N/A	0.8001	<0.0001	>0.9999
hos1 HNT	0.0110	0.3115	0.0005	0.8001	N/A	<0.0001	0.8998
phyB-9hos1 22°C	0.0703	0.0009	0.4105	<0.0001	<0.0001	N/A	<0.0001
Lone stoma	Col-0 HNT	*phyB-9* 22°C	*phyB-9* HNT	*hos1* 22°C	*hos1* HNT	*hos1phyB-9* 22°C	*hos1phyB-9* HNT
Col-0 22°C	0.6676	>0.9999	>0.9999	0.2535	0.9703	0.9951	0.8001
Col-0 HNT	N/A	0.8001	0.7695	0.9981	0.9969	0.9781	>0.9999
phyB-9 22°C	0.8001	N/A	>0.9999	0.3761	0.9925	0.9994	0.8998
phyB-9 HNT	0.7695	>0.9999	N/A	0.3430	0.9890	0.9989	0.8785
hos1 22°C	0.9981	0.3761	0.3430	N/A	0.8785	0.7371	0.9890
hos1 HNT	0.9969	0.9925	0.9890	0.8785	N/A	>0.9999	0.9997
phyB-9hos1 22°C	0.9781	0.9994	0.9989	0.7371	>0.9999	N/A	0.9951
phyB-9hos1 HNT	>0.9999	0.8998	0.8785	0.9890	0.9997	0.9951	N/A
Symmetric divisions	Col-0 HNT	*phyB-9* 22°C	*phyB-9* HNT	*hos1* 22°C	*hos1* HNT	*hos1phyB-9* 22°C	*hos1phyB-9* HNT
Col-0 22°C	>0.9999	0.5942	>0.9999	0.9925	0.9925	0.0320	0.9994
Col-0 HNT	N/A	0.8001	>0.9999	0.9997	0.9997	0.0814	>0.9999
phyB-9 22°C	0.8001	N/A	0.7371	0.9703	0.9703	0.8785	0.8998
phyB-9 HNT	>0.9999	0.7371	N/A	0.9989	0.9989	0.0605	>0.9999
hos1 22°C	0.9997	0.9703	0.9989	N/A	>0.9999	0.2535	>0.9999
hos1 HNT	0.9997	0.9703	0.9989	>0.9999	N/A	0.2535	>0.9999
phyB-9hos1 22°C	0.0814	0.8785	0.0605	0.2535	0.2535	N/A	0.1405
phyB-9hos1 HNT	>0.9999	0.8998	>0.9999	>0.9999	>0.9999	0.1405	N/A

Table 4.2. Statistical p-values from Two-way ANOVA and Tukey's multiple comparisons test from Figure 4.9. Significant p-values ≤0.05 are highlighted in green.

4.4 Cyclin mutants have similar responses to *phyB-9* under HNT

My analysis so far has shown that mutations in *phyB* alters epidermal patterning in response to changes in the distribution of the temperature load. This suggests that phyB activity is required to buffer against these changes in distribution. The analysis of the *pif4* and *hos1* mutants suggest that HOS1, more so than PIF4, may have a role in this phyB mediated change in sensitivity.

The core stomatal development genes regulate the cell cycle and hence cell division through regulation of cell cycles genes. The cyclins are key components of the cell cycle. CYCD3;1 when overexpressed, increased the numbers of G2 phase cells compared to G1 phase cells, suggesting that it has a key role in progress of cells through the G1 and S phase causing a backlog of cells in the G2 phase (Menges *et al.*, 2006). Recent work has determined that a symmetric division in the epidermal cells of leaves in Arabidopsis occur slower than asymmetric divisions, prolonging cell cycle length (Han *et al.*, 2022). This slowing down of the divisions is thought to be due to the association between a cyclin-dependant kinase inhibitor called SMR4 which is induced by MUTE during the stomatal lineage. Binding of SMR4 to CYCD3;1 slows down the asymmetric divisions by causing a lag in the G1 phase of these cells (Han *et al.*, 2022). Another key cyclin is also induced by MUTE and that is CYCD5;1 which when not associated with SMR4 prevents the occurrence of cell divisions (Han *et al.*, 2022).

These studies show that there is a possibility that the increase in symmetric divisions in a *phyB-9* mutant grown under 22°C compared to those grown under a HNT could be due to impacts on the cell cycle and in particular the association between SMR4, MUTE and CYCD3;1 and CYCD5;1. Therefore, Col-0 along with the mutants *cycd3;1* and *cycd5;1* were grown under a HNT and their stomatal index, density and epidermal patterning were studied. Both *cycd3;1* and *cycd5;1* had a significantly higher SI than the Col-0 and *cycd5;1* had a SI that was significantly higher than *cycd3;1* (Figure 4.8A). The stomatal density of *cycd3;1* was significantly decreased compared to Col-0 and *cycd5;1,* which had no significant differences between them (Figure 4.8B). This is an interesting result because the percentage of stomata was higher in *cycd3;1* compared to Col-0 and yet the density is lower suggesting very few and larger pavement cells in this line. This is reflected in the patterning, with the total number of epidermal events

being fewer in the *cycd3;1* mutants compared to the Col-0 and *cycd5;1* (Figure 4.8C). The number of stomatal complexes and lone stomata were similar between the Col-0 and *cycd5;1* lines. However, the number of symmetrical divisions was decreased in both mutant cyclin lines compared to the wild-type, which was a similar phenotype seen when *phyB-9* was grown under HNT.

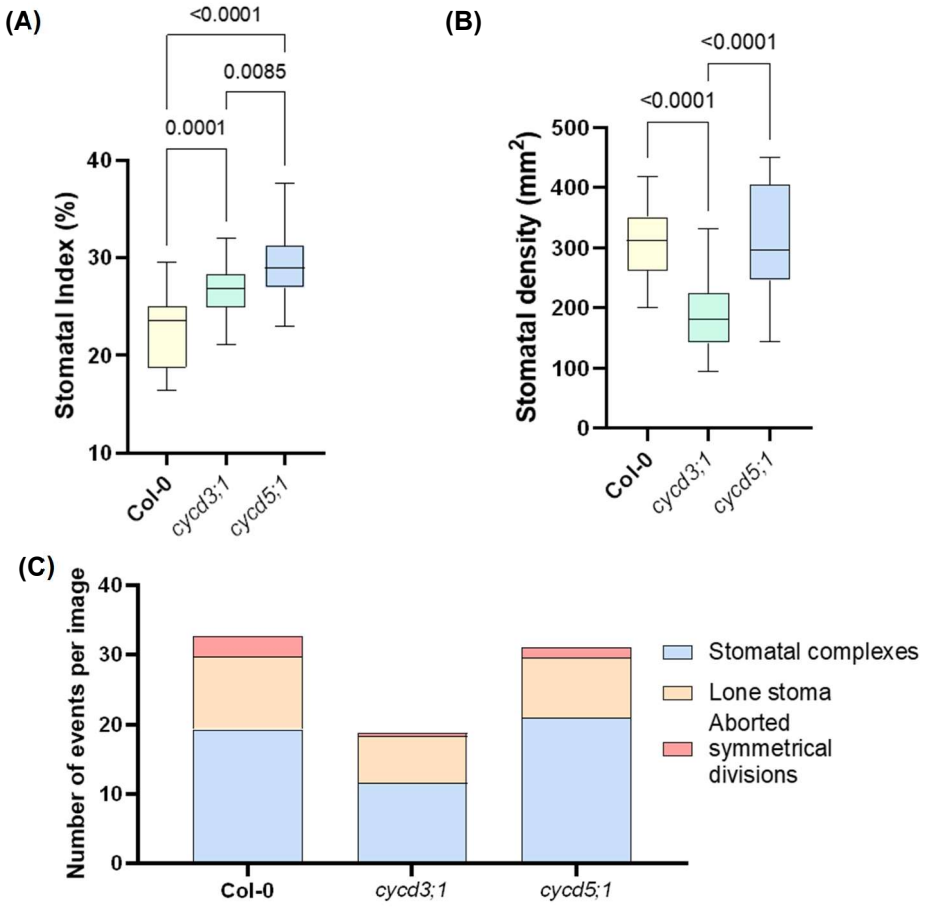

Figure 4.8. Cyclin mutants compared to *phyB-9* when grown under HNT. Col-0, *cycd3;1* and *cycd5;1* were grown under HNT and the stomatal index **(A)** stomatal density **(B)** and the epidermal patterning were studied **(C)**. Graphs were generated in GraphPad prism, box plots have the median shown as a line with the whiskers showing the greatest and lowest value of the dataset. Statistical analysis was also carried out in GraphPad using a two-way ANOVA and Tukey's multiple comparisons test. Significant p-values ≤0.05 are shown whereas non-significant p-values > 0.05 are not. Statistical analysis of **(C)** is shown in Table 4.3.

Stomatal complexes	*cycd3*	*cycd5*
Col-0	<0.0001	0.1920
cycd3	N/A	<0.0001
Lone stoma	*cycd3*	*cycd5*
Col-0	0.0003	0.1570
cycd3	N/A	0.0940
Symmetric divisions	*cycd3*	*cycd5*
Col-0	0.0257	0.1570
cycd3	N/A	0.0940

Table 4.3. Statistical p-values generated for Figure 4.7C. Significant p-values ≤0.05 are highlighted in green.

4.5 End of day far-red light rescues symmetrical divisions phenotype suggesting it is a phytochrome response

The data in this chapter has indicated that phyB is required for buffering stomatal patterning in response to changes in the distribution of the temperature load, potentially through the cyclins, SMR4 and MUTE. To determine if the responses at HNT were indeed due to the increased night temperatures impacting upon thermal reversion of the phytochrome Pfr, Col-0 and *phyB*-9 plants were grown either at 22°C day and night temperature either with the addition of 50µmolm^{-2}s^{-1} far-red light in the last 10 minutes of the photoperiod or without this far-red addition.

Similarly to the plants grown under a HNT, an EoD FR treatment resulted in an increased in SI for both Col-0 and *phyB-9*, although this was not significant at the 5% levels for *phyB-9* (Figure 4.8A). This coupled with no increase in density suggests that the epidermis had larger/more pavement cells in these plants.

Within the genotypes there was little difference between the number of stomatal complexes and the number of lone stomata for both temperatures. Under 22°C, the number of aborted symmetric meristemoid divisions was reduced when Col-0 had far-red addition compared to when it didn't (Figure 4.8B). The same pattern was present in *phyB-9* grown under the same temperature, which was a trend that matched the increase in HNT. The same pattern can be seen in the *phyB-9* mutants with an increase in the number of symmetric divisions on the epidermis compared in the

leaves of plants grown under far-red supplemented light compared to those grown without it.

This data suggests that there is a greater impact on the epidermal patterning state of plants by temperature and not the lighting as there were fewer divisions when plants were grown under a HNT compared to those grown under far-red light. Also, that Col-0 when grown under FR acts more like *phyB-9* when grown under a HNT in terms of patterning as more stomatal complexes are generated along with fewer symmetric divisions.

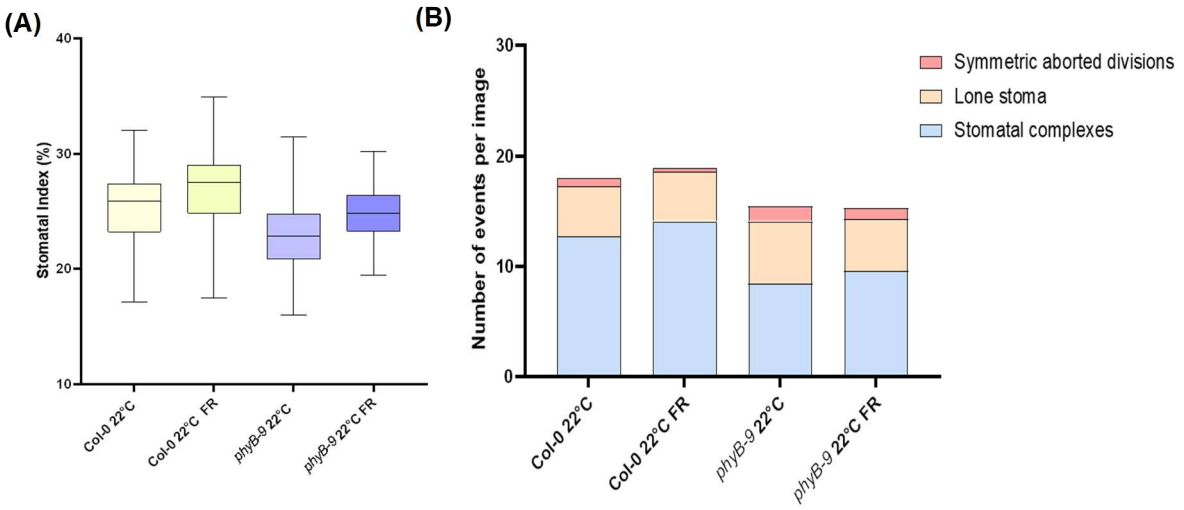

Figure 4.9. Stomatal phenotypes and epidermal patterning with and without end of day far-red. Col-0 and *phyB-9* were grown at 22°C and either supplemented with 50µmolm^{-2}s^{-1} end of day far-red light in the last 10 mins of the photoperiod or not. **(A)** Stomatal index was calculated from leaf impressions. **(B)** The number of stomatal complexes, lone stomata and aborted symmetric divisions found on the epidermis of Col-0 and *phyB-9* plants grown under a constant temperature of 22°C either supplemented with or without far-red light. Graphs were generated in GraphPad prism and statistical analysis was also carried out in GraphPad using a two-way ANOVA with a Tukey's multiple comparisons test, n=30. Significant p-values ≤0.05 for index are shown while non-significant p-values >0.05 are not.

4.6 Discussion

Patterning of the epidermis is a well-regulated developmental process to spatially distribute stomata, pavement cells and trichomes (Glover, 2000; Javelle *et al.*, 2011). Due to the role of phyB in regulating improved WUE under increased temperature loads, it is likely that these temperatures also influence epidermal patterning through

phyB. The first experiment included a *pif4* mutant and a *PHYB*OE. This is because PIF4 directly interacts with phyB and may be acting downstream to regulate these temperature dependent responses through its inhibition of SPCH at higher temperatures (Kumar *et al.*, 2012). As phyB also is a negative regulator of PIF4, levels of PIF4 accumulate in a *phyB-9* mutant and in higher temperature environments and so it was logical to study the role of PIF4 in temperature dependent patterning (Lau *et al.*, 2018). The *PHYB*OE was included to determine if the opposite response to a *phyB-9* mutant could be seen. As with the previous experiment, the *phyB-9* mutants increased in their SI with increasing night temperature and the opposite was reflected in the *PHYB*OE with no significant differences in the stomatal density for these lines (Figure 4.3A-B). The SI of *pif4* under the three temperature regimes were slightly higher than Col-0 but follow the same trend, therefore the change in SI may reflect higher levels of SPCH expression than in Col-0 but also suggest that the breakdown in the buffering mechanism seen in *phyB-9* is not likely to happen through PIF4, though further analysis of a *phyB pif4* double mutant would allow further clarification. As expected due to its role in promoting stomatal development (Casson and Hetherington, 2014), there were large reductions in the number of stomatal complexes in *phyB-9* compared to Col-0, *pif4* and *PHYBOE* in all temperature regimes. While the number of lone stomata appeared mostly consistent across the genotypes and temperatures, the number of symmetric divisions in *phyB-9* decreased with increasing night temperatures (Figure 4.5). *PHYBOE* showed an increase in the number of symmetric divisions under HNT compared to 22°C, which is the opposite trend to *phyB-9* under the same temperatures. It can be deduced from this that the increase in symmetric divisions in *phyB-9* under HNT are most likely due to the absence of phyB. Therefore, the hypothesis was put forward that functional phyB has a role in buffering the system against how changes in the timing of changes in temperature during epidermal patterning.

As PIF4 was unlikely to be involved in the symmetrical divisions that were seen at 22°C and not under an HNT, the next gene that could be acting downstream of phyB to regulate temperature dependant patterning is HOS1. HOS1 is an E3 ubiquitin ligase that targets the bHLH transcription factor ICE1/SCRM for degradation, particularly under colder temperatures (Dong *et al.*, 2006). Both a *hos1* single mutant and the *phyB-9hos1* double mutant were used in this study, the double was included to see if

there were any epistatic or additive effects. The trend of SI for *phyB-9* once again increased with increasing night temperatures. Though the *hos1* single mutant had no significant difference in SI to Col-0 plants grown at both temperatures, there was evidence for an increase at HNT similar to that shown by *phyB-9*, though this was not due to a decrease in symmetric divisions (Figure 4.6). The *phyB-9hos1* double mutant had an increase in the SI when the plants were grown under a HNT compared to those grown under 22°C, which was similar to the single *phyB* mutant (Figure 4.6A) and the patterning was similar to that of the *phyB-9* mutant with a decrease in symmetric divisions (Figure 4.7). Whilst not completely clear, this analysis presents some evidence that HOS1 and subsequently ICE1 may be involved in buffering epidermal patterning under these conditions. This is complicated by the fact the HOS1 can also target PIF4 for degradation but *pif4* was more similar to Col-0 in its response, and therefore PIF4 is likely not involved.

As previous work had shown that the cyclins were involved via their interaction with SMR4 and MUTE at driving both asymmetric and symmetric divisions, they were prime candidates to study next. Both *cycd3;1* and *cycd5*;1 were chosen because of their direct roles in generating asymmetric and symmetric divisions throughout the stomatal linage progression (Han *et al.*, 2022). Interestingly, both the cyclin mutants had a similar response to what had been seen multiple times in a *phyB-9* mutant grown under a HNT which was an increased stomatal index. However, while the *phyB-9* mutants had no change in the SD, *cycd3;1* had a decrease suggesting that it could have larger pavement cells than *phyB-9* when grown under an HNT (Figure 4.8A-B). In further studies, it would be useful to measure the size of the epidermal cells. This is difficult to confirm, however, without having the data for 22°C or the HDT as the patterning may be different under these conditions. In terms of patterning, a similar pattern also emerges, with the *cycd3;1* mutant having fewer symmetrical divisions occurring (Figure 4.8C). However, because *cycd3;1* has an overall reduction in the number of complexes and lone stoma, more evidence is required. The *cycd5;1* mutant had a reduction in the number of stomatal complexes and lone stoma when compared to Col-0 and has a similar phenotype to *phyB-9* when grown under HNT. In future experiments it would have been interesting to have grown the *cycd3;1* and *cycd5;1* mutants under all three temperature regimes to more fully assess whether the response is indeed similar to that of *phyB-9.* However, due to a small number of

homozygous mutants being identified from a mixed population and timing constraints this could not be carried out for this experiment. Inclusion of a SMR4 and MUTE mutants in future studies under the three temperature regimes could give a better insight into the role of the cyclins in the buffering response.

A good proxy for phytochrome thermal reversion due to increased HNT would be to grow plants under a supplemented far-red light at the end of the photoperiod. This enables the distinguishing between a HNT effect or a cooler day effect which HNT only cannot account for. The far-red supplementation did lead to an increase in the stomatal index in both Col-0 and *phyB-9* mutants which follows the same trend as if it was mimicking a higher night temperature response (Figure 4.9A). The number of stomatal complexes in Col-0 increased with EOD FR which does also follow the trend of HNT. The number of complexes also increased in *phyB-9* EOD FR, which, when coupled with the decrease in the number of symmetric divisions supports the hypothesis that it is the HNT effect that is causing these responses and not a cooler day (Figure 4.9B). The number of lone stomata also decreases in both Col-0 and *phyB-9* when supplemented with EOD FR, which along with the increase in complexes, suggests more M's are going on to form stomata and not SLGC under these conditions.

Although more work needs to be done to determine the likelihood of their role in patterning, the cyclins provided promising results under an HNT. It is possible that the removal of phyB under higher night temperatures may remove some inhibition on SMR4 and therefore allow more interactions with MUTE and the generation of more symmetric cell divisions. However, to date there have been no studies that have shown that phyB interacts directly with SMR4 and the cyclins. Therefore, a good start would be to test protein: protein interactions of SMR4 with phyB and its downstream components.

4.7 Key findings

1. Active phyB is likely acting to buffer cell fate decisions in the epidermis against changes in distribution of temperature load.

2. This buffering is likely independent of PIF4, however could be acting through the HOS1, cyclins and SMR4.

Chapter 5: The physiological role of phyB in rice flowering and fertiliser use.

5.1 Introduction

Over half of the world's population consume rice every day (Fukagawa and Ziska, 2019). In addition to this, rice is a major calorie contributor to the world's poorest communities (Verma *et al.*, 2021). In most cases, rice plants need to be grown in well-irrigated fields such as paddy fields and well fertilised to enable good growth and yield. Regions such as South America, Africa and Southeast Asia are major providers of rice to the global food market and these regions are very susceptible to climate change disasters such as drought. The ever-growing challenge of climate change coupled with increasing population growth means that it is vital to find a way to maintain and increase rice production.

Like in Arabidopsis, the phytochromes, namely OsphyB, are a key regulator of flowering in rice (Ishikawa *et al.*, 2009). This is seen when *phyB* mutants flower earlier in long day (LD) growth conditions (Ishikawa *et al.*, 2009). However, the day length conditions for flowering can differ as some cultivars of rice flower under short days whereas Arabidopsis flowers under long days (Figure 5.1). One way in which OsphyB regulates rice flowering time is by interactions with the evening complex, a key component of the circadian clock consisting of ELF3 and LUX (Andrade *et al.*, 2022). As in the flowering time pathway in Arabidopsis, Hd3a (an orthologue of FT) is suppressed by light, a process mediated by the post translational modification of the Hd1 (an orthologue of CO) by OsphyB (Ishikawa *et al.*, 2011). Hd1 upregulates the transcriptional expression of *Hd3a*. OsphyB may also recruit the circadian and light controlled domain (CCT) containing protein Grain number, Plant Height, and Heading date1 (Ghd7) to interact with Hd1 (an orthologue of Arabidopsis CONSTANS) and together these regulate the transcriptional repression of *Edh1* which is key to floral induction (Vicentini *et al.*, 2023). Another CCT domain containing protein, PSEUDO-RESPONSE REGULATOR37 (PRR37) is part of the circadian clock and has a role in the determination of switching Hd1 from between a flowering promoter and repressor although the exact mechanism behind this remains unclear (Zhang *et al.*, 2021).

To enable good growth, grain filling, healthy leaves and production of secondary metabolites, a source of nitrogen is needed for rice plants. Most nitrogen taken up by the plants is used in the generation of photosynthetic apparatus, with up to 75% of nitrogen in the leaf being used for this purpose. In the context of stomata, nitrogen has

been shown to influence the extent of stomatal opening. Nitrogen is the key resource for healthy rice plant growth and fertility, with nitrogen application usually leading to delayed flowering in crops (T. Ye *et al.*, 2019). The main uptake of nitrogen in flooded soils due to the inhibition of nitrification is in the form of ammonia (NH_4^+) (Wang *et al.*, 1993). There are several ammonia transporters (AMT) in the roots of rice with two (OsAMT1:3 and OsNRT2.4) being activated by Nhd1 to increase nitrogen uptake (Zhang *et al.*, 2021). Interestingly, Nhd1 itself is activated by a separate source of nitrogen, glutamine. Recent studies have shown that high or extreme low levels of nitrogen application both delay flowering (Zhang *et al.*, 2021). This suggests that intermediate levels of fertiliser could have reduced flowering time. Because of nitrogen's role in flowering by initiating Nhd1 and therefore indirectly Hd3a, phyB may also play a role in influencing the nitrogen mediated flowering time and fertility in rice (Zhang *et al.*, 2021).

Previous work in the Casson lab showed that when grown without any fertiliser addition, wild-type rice plants produced no seed yield, while *phyB* plants did produce seed (Mawodza, 2019) (Figure 5.2). This could be due to the blocking of two pathways that activate the flowering gene Hd3a. Firstly, not only is OsphyB not present but the removal of nitrogen from the system means that the *Nhd1* transcript is not expressed and therefore Hd3a cannot be activated via this route either (Mawodza, 2019). As well as this, studies have shown that *OsphyB* mutants in rice produce more panicles, but these are not filled as much, suggesting an important role for *phyB* in fertility (Shethi, 2023). However, little work has been done to study the impact of varying nitrogen application upon flowering and photosynthesis in *phyB* plants. If varying nitrogen levels along with the mutation of OsphyB could lead to more water use efficient plants and less nitrogen application, this could potentially save large amounts of water and be economically more efficient to farmers as they might be able to apply less fertiliser to the paddy fields. However, the yield production of such plants needs to be considered as a major factor.

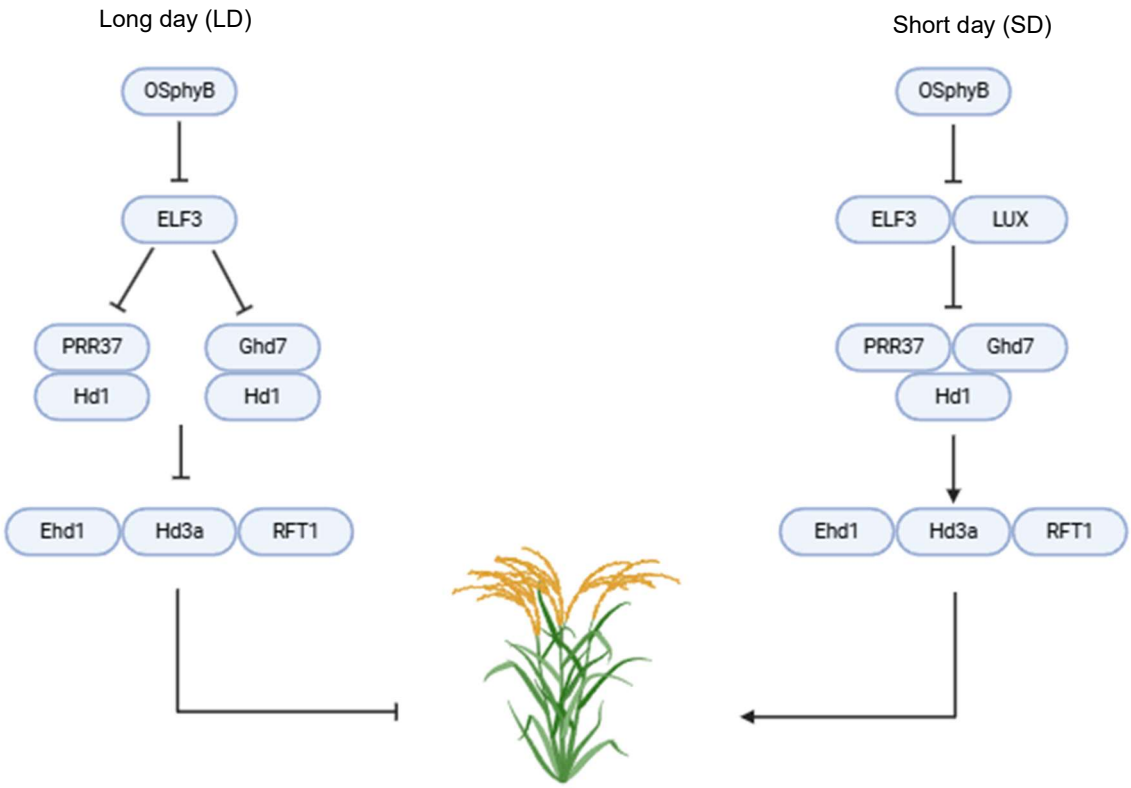

Figure 5.1. Flowering time pathways in rice. Light activation of phyB plays an important role in both long day and short day grown rice plants via two different pathways. OsphyB represses the evening complex of the circadian clock which in turn represses the action of the Hd1 interactors Ghd7 and PRR37. These proteins form a complex that either represses the activity of Hd3a (long day) or activates expression of *Hd3a* allowing flowering under short days. Adapted from (Andrade *et al.*, 2022). Image created in BioRender.com.

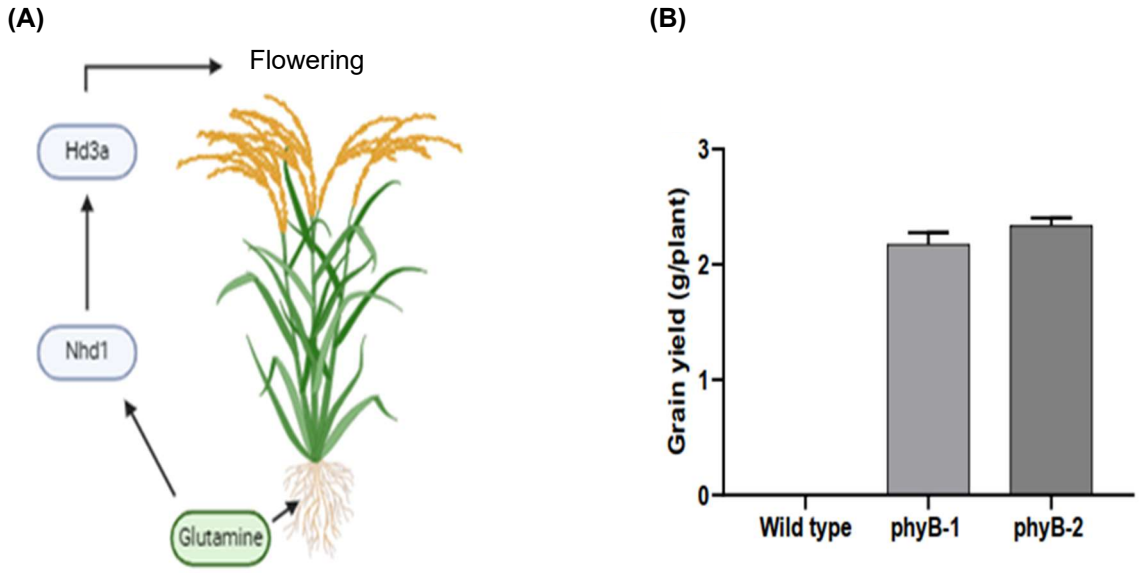

Figure 5.2 Impact of nitrogen on flowering. (A). The uptake of nitrogen in the form of glutamine activates Nhd1 which can accelerate flowering through the action of Hd3a. Image created in Biorender.com. Adapted from (Zhang *et al.*, 2021). **(B)**. Data showing that Nipponbare wild-type rice did not flower under conditions of no added fertiliser whereas *OsphyB* plants did. Taken from (Mawodza, 2019).

5.1.2 Aims and objectives

Aim: To investigate the role of OsphyB in regulating flowering time, yield and water use efficiency in rice under different fertiliser treatments.

1. To determine how different nitrogen applications can impact upon flowering time and photosynthetic activity in rice plants.

2. To study how the impact of different nitrogen fertiliser application levels coupled with phyB mutation influences water use efficiency.

5.2 *OsphyB* plants flower faster than Nipponbare wild-type and this is independent of fertiliser treatment

As with Arabidopsis, OsphyB has been demonstrated to positively regulate flowering time in rice (Andrade *et al.*, 2022). However, the role of OsphyB in regulating flowering under different fertiliser regimes has not been fully explored. To address this, *OsphyB-1* mutants, which are generated in a wild-type Nipponbare (NB) background, along with the wild-type were grown and the number of days post germination until the appearance of the first panicle was recorded. The fertiliser regimes used in this study were are as follows; full NPK (Nitrogen, Phosphorus and Potassium) fertiliser containing both the slow release osmocote, which contains nutrients to support early growth (Table 5.1) and the water based NPK fertiliser which contains nutrients supports flowering and grain filling (Table 5.2) (+/+), the two intermediate fertiliser states containing either just the osmocote (+/-) or the water based (-/+) and the plants with no fertiliser added (-/-). Under all treatments, *OsphyB-1* flowered significantly earlier than NB plants, over 10 days earlier on average (Figure 5.3). When no fertiliser (neither the soil based, slow release osmocote or the water-soluble fertiliser) was applied to NB, flowering was delayed slightly, but significantly, compared to the NB plants grown under the full fertiliser regime (both the soil based, slow release osmocote and the water-soluble fertiliser was added) (Figure 5.3A). There was minimal difference in the flowering time between the intermediate fertiliser treatments (either just the soil based, slow release osmocote or the water-soluble fertiliser are added and not the other treatment, see key) in both NB and *OsphyB-1* plants (Figure 5.3B). These results suggest that the lack of fertiliser treatment could delay flowering in NB compared to full fertiliser treatment, whereas intermediate fertiliser treatment does not influence flowering. Although not significant at the 5% level, *OsphyB* plants had accelerated flowering with no fertiliser application compared to the fully fertilised plants. The biggest impact on the acceleration of flowering time in *OsphyB-1* appears to be the absence of the osmocote (-/+) although this was not significant to the 5% level, p=0.5883. Because *OsphyB-1* flowered considerably faster than Nipponbare, the next step was to look at the impact on yield to see how these were impacted by different fertiliser regimes.

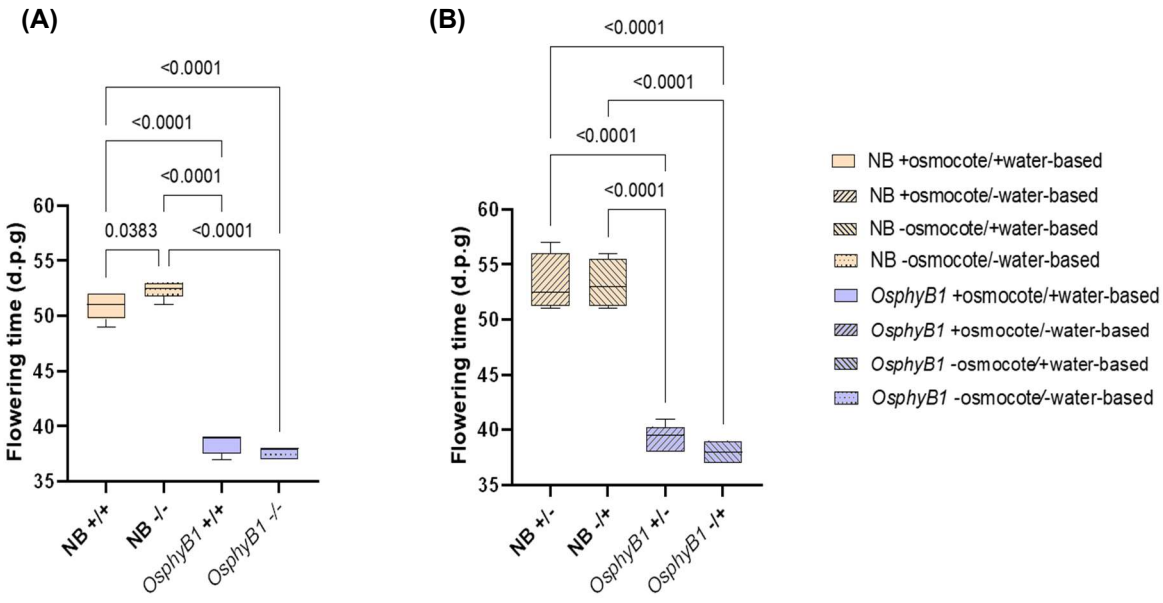

Figure 5.3. Flowering time of Nipponbare and *OsphyB1* rice plants under differing fertiliser regimes. (A). Nipponbare and *OsphyB1* plants with either a full fertiliser regime (+/+) including the slow release fertiliser, osmocote, and the water-based soluble fertiliser or without either present (-/-) (n=5-6). **(B)**. Nipponbare and *OsphyB1* with intermediate fertiliser regimes. This consisted of either only the slow release osmocote applied and no water-based fertiliser applied or vice versa (+/- and -/+) (n=4-6). Box-plots show the full range of data, and the line represents the median value, whiskers show the maximum and minimum values. Statistical analysis was carried out in GraphPad Prism using a 2-way ANOVA with a Tukey's multiple comparisons test, p-values that are significant ≤0.05 are shown and non significant p-values >0.05 are absent.

5.3 *OsphyB-1* plants have significantly reduced yield under all fertiliser applications

As previously shown fertiliser regimes impact upon yield in rice (Mawodza, 2019). To investigate this further and to see if the osmocote or water-based fertiliser are more important for yield, Nipponbare and *OsphyB-1* had their yield analysed. Once the last panicles had been produced and filled, the watering of the plants was stopped, and they were allowed to dry down before the panicles were collected from each individual plant. The number of panicles were counted from each plant, and this included the number of filled and unfilled panicles (Figure 5.5).

Once counted, the panicles were weighed and recorded. The fully fertilised NB had on average a higher number of panicles than the wild-type non-fertilised plants

(Figure 5.4A). Comparing NB and *OsphyB-1* within a fertiliser treatment, *OsphyB-1* mutants produced significantly more panicles than NB. Indeed, in the absence of fertiliser, *OsphyB-1* mutants produced a comparable number of panicles to NB plants grown with the full fertiliser treatment. For the intermediate fertiliser plants NB with only osmocote present had on average more panicles compared to when only the water-based fertiliser was used, however these differences were not significant to the 5% level ($p=0.5848$) (Figure 5.4B). There was also no significant difference between the intermediately fertilised phyB plants, although the plants that had only the water-based fertiliser did produce slightly more panicles.

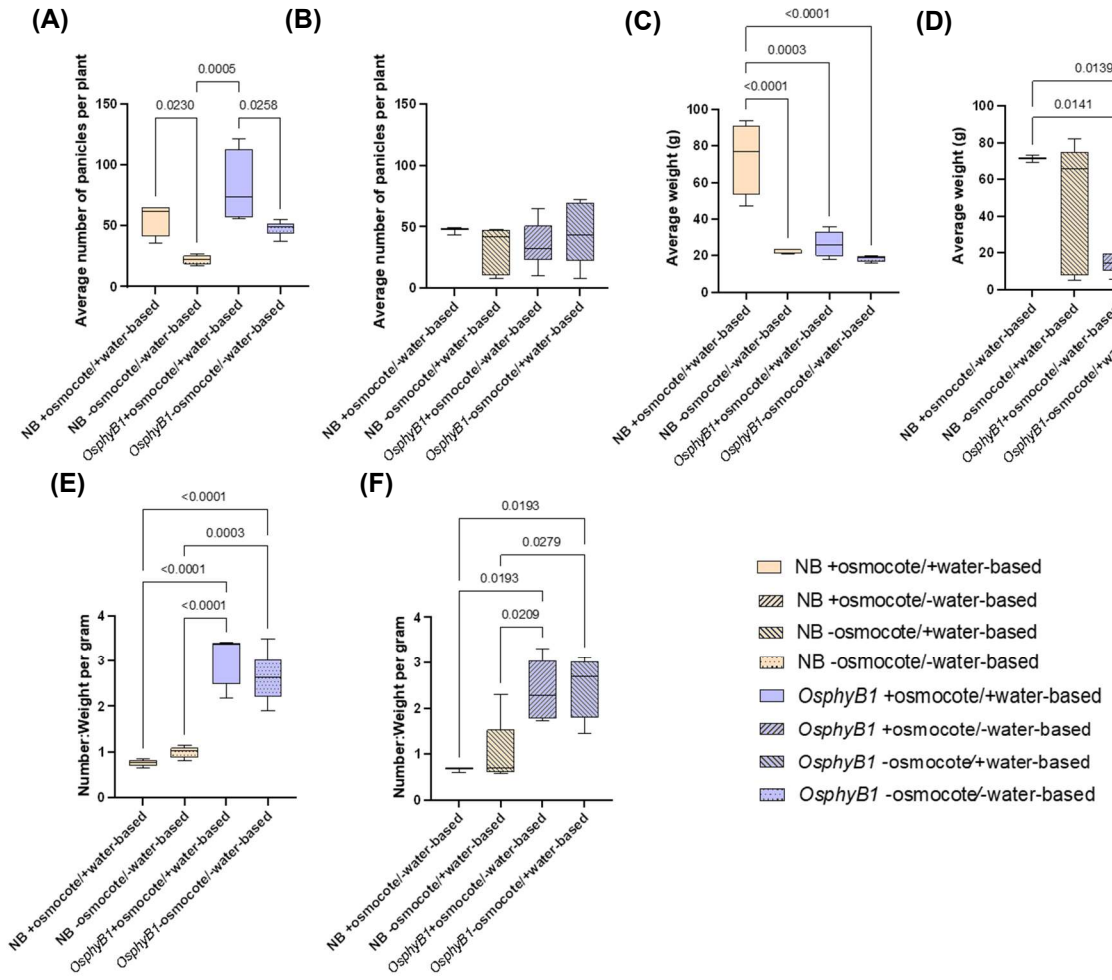

Figure 5.4 Yield data of Nipponbare and phyB grown under different fertiliser applications. **(A)**. The average number of panicles per plant for Nipponbare and phyB plants grown under full (+/+) or non-fertilised (-/-) plants, n=4-6. **(B)**. Average number of panicles per plant for Nipponbare and phyB grown under intermediate fertiliser applications, either with the addition of osmocote and not with the water-based fertiliser (+/-) or vice versa (-/+), n=3-6. **(C)**. The average total weight of the panicles from the Nipponbare and phyB plants grown under full or no fertiliser. **(D)**. Average weight of Nipponbare and phyB plants grown under intermediate fertiliser conditions. **(E)**. Ratio of the number of panicles per gram of weight for Nipponbare and phyB plants grown under full or no fertiliser application. **(F)**. Ratio of the number of panicles per gram of weight for Nipponbare and phyB plants grown under intermediate fertiliser application. Box plots are shown with the line being the median and the whiskers showing the highest and lowest values of the dataset. Statistical analysis was carried out in GraphPad prism using a two-way ANOVA. A Tukey's multiple comparisons test was carried out to compare the means. Significant p-values (values (≤0.05) are shown, whereas non-significant values (>0.05) are not.

When the average weight of panicles per plant was recorded, the fully fertilised wild-type plants had a much greater weight on average compared to the non-fertilised NB and either of the fully fertilised phyB or non-fertilised phyB averages (Figure 5.4C). The mean weight of the intermediate fertiliser applied NB plants were similar to each

other, however, there was a large variation in the NB plants grown with the water-based fertiliser and without the osmocote (Figure 5.4D). The *OsphyB-1* plants grown with intermediate fertiliser application had low average panicle weights per plant compared to the NB plants grown under any fertiliser regime and there was no significant difference between the two different intermediate treatments.

To assess the impact of soil added and water-based fertiliser added 4 weeks after planting and genotype on yield, the ratio of the number of panicles per gram of seed was calculated. This provides a proxy for how well the panicles are filling the seed and the weight of that seed in the absence of measuring seed traits themselves, which could not be measured due to time constraints. Both the fully and no fertilised NB plants had a significantly lower ratio of panicles per gram than the *OsphyB*-1 plants under the same conditions (Figure 5.4E). This suggests that the panicles of these plants were more filled and that *OsphyB-1* had fewer fully filled panicles. The same trend was seen between the NB plants grown under intermediate fertiliser regime and the *OsphyB*-1 under the same conditions (Figure 5.4F). Therefore, NB plants grown with full fertiliser produce a better yield than without and significantly better than the corresponding *OsphyB*-1 plants, even when these are grown with full fertiliser present. Nipponbare plants also outperform *OsphyB*-1 plants under either intermediate fertiliser growth conditions.

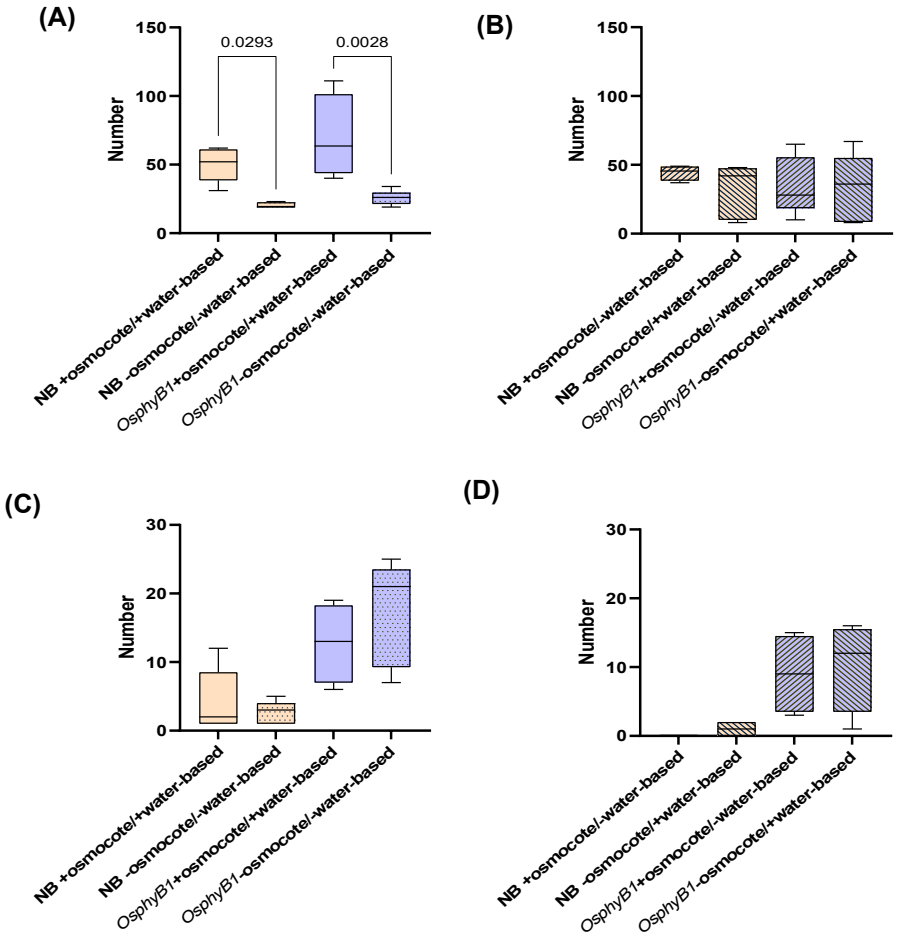

Figure 5.5. Number of filled and unfilled panicles for NB and *OsphyB-1*. (A) The average number of filled panicles for Nipponbare and phyB plants grown under full (+/+) or non-fertilised (-/-) plants, n=4-6. **(B)**. Average number of filled panicles per plant for Nipponbare and phyB grown under intermediate fertiliser applications, either with only the osmocote added (+/-) or only the water-based fertiliser added (-/+), n=3-6. **(C)** Average number of unfilled panicles for NB and *OsphyB-1* grown under full or no fertiliser regimes. **(D)** Average number of unfilled panicles for NB and *OsphyB-1* grown under intermediate fertiliser regimes. Box plots are shown with the line being the median and the whiskers showing the highest and lowest values of the dataset. Statistical analysis was carried out in GraphPad prism using a two-way ANOVA. A Tukey's multiple comparisons test was carried out to compare the means. Significant p-values (values (≤0.05) are shown, whereas non-significant values (>0.05) are not.

Unsurprisingly, there were significantly more filled panicles in both NB and *OsphyB-1* when they were grown under full fertiliser regime compared to the plants of the same genotype without any fertiliser addition (Figure 5.5A). This contrasts with those grown under an intermediate fertiliser regime which had no significant differences between the number of filled panicles (Figure 5.5B). Overall, the number of filled panicles between NB and *OsphyB-1* were similar. When the number of unfilled panicles were

measured, *OsphyB-1* had significantly more when under a no fertiliser regime than NB grown under either a full fertiliser regime or without any (Figure 5.5C). There was also a significant increase in the number of unfilled panicles when *OsphyB-1* was grown with only the water-based fertiliser addition compared to NB with only osmocote added (Figure 5.5D). Therefore, functional OsphyB is required for limiting panicle production but also ensuring that panicles are filled with seed and full fertiliser application is also required for optimum filling numbers. However, there is little impact of fertiliser application on the number of unfilled panicles.

5.4 Fertiliser treatment and OsphyB interact to influence assimilation rates.

To determine if the reduced yield of *OsphyB-1* can be attributed to assimilation changes, the photosynthetic and stomatal traits of flag leaves were analysed by IRGA. Assimilation was measured at both cabinet light levels (600 $\mu molm^{-2}s^{-1}$) and saturating light (2000 $\mu molm^{-2}s^{-1}$). Under cabinet light conditions, Nipponbare flag leaves had a significantly reduced average assimilation (A) when grown without no fertiliser (-/-) compared to those grown under full fertiliser regimes. Interestingly, under both full and no fertiliser applications, *OsphyB-1* had significantly increased assimilation compared to wild type. However, fertiliser treatment did not impact on assimilation within the *OsphyB-1* genotype with no significant differences between the two treatments (Figure 5.6A). When only the water-based fertiliser was present, there was a significant increase in A in both NB and *OsphyB-1* (Figure 5.6B). When only the osmocote was present, there was little difference between NB and *OsphyB-1*.

When assimilation rates were measured under saturating light (2000 $\mu molm^{-2}s^{-1}$), Nipponbare flag leaves had significantly reduced assimilation when grown with no fertiliser application compared to those grown with full fertiliser application. Overall, *OsphyB-1* plants had reduced assimilation levels compared to NB, and intriguingly, *OsphyB-1* plants grown with no fertiliser addition had improved assimilation compared to the fully fertilised NB plants (Figure 5.6C). The plants grown under intermediate fertiliser regimes and saturating light had the same trend as under cabinet light, however, with overall greater values (Figure 5.6D).

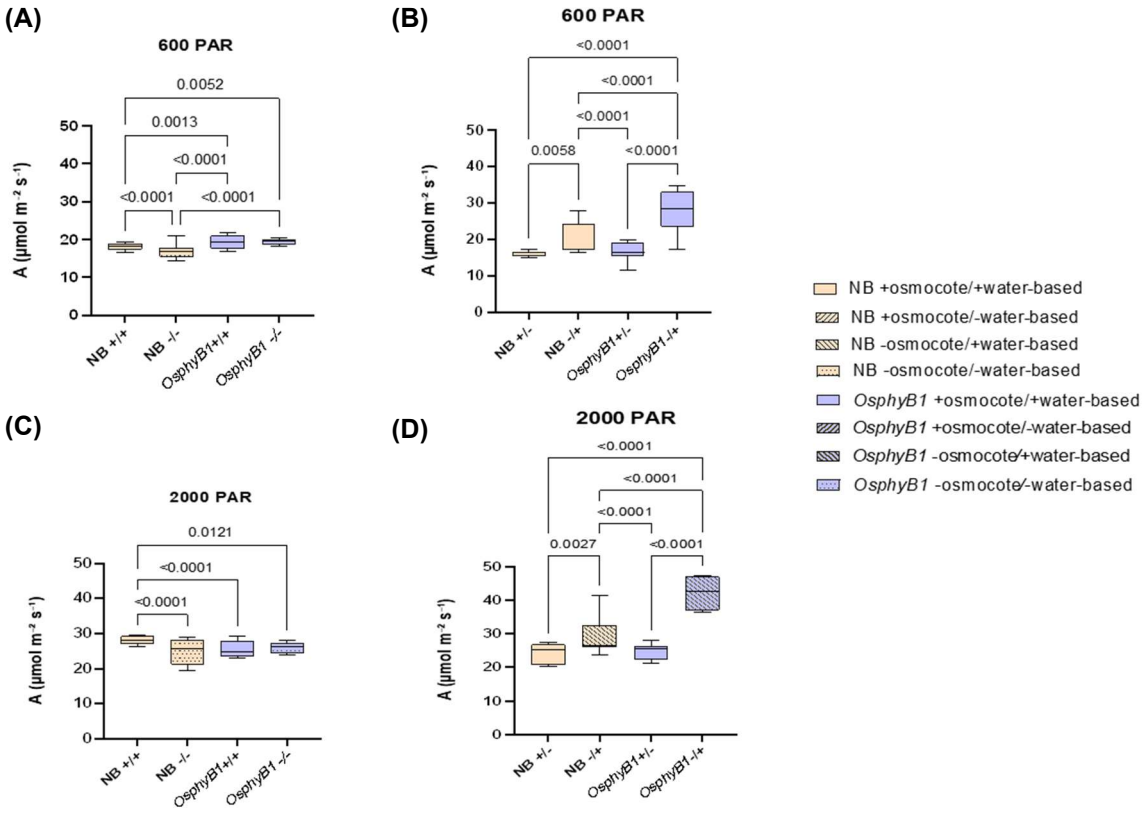

Figure 5.6. **Assimilation rates (A) of flag leaves of Nipponbare and *OsphyB-1* plants grown under different fertiliser regimes and light levels. (A)**. Flag leaf carbon assimilation rates for both NB and *OsphyB-1* were measured under (+/+) and (-/-) fertiliser conditions and cabinet light (600µmolm^{-2}s^{-1}) (n=5-6). Nipponbare and *OsphyB-1* flag leaves measured for assimilation grown with either a full fertiliser regime (+/+) with the addition of a slow release osmocote fertiliser to the soil and the addition of a water-based fertiliser at cabinet light conditions (600 µmolm^{-2}s^{-1}) (n=5-6). **(B)**. Flag leaf assimilation rates for both NB and *OsphyB-1* were measured under (+/-) and (-/+) fertiliser conditions and cabinet light (600µmolm^{-2}s^{-1}) (n=4-6). **(C)**. Flag leaf assimilation rates for both NB and *OsphyB-1* were measured under (+/+) and (-/-) fertiliser conditions and cabinet light (2000µmolm^{-2}s^{-1}) (n=5-6). **(D)**. Flag leaf assimilation rates for both NB and *OsphyB-1* were measured under (+/-) and (-/+) fertiliser conditions and cabinet light (2000µmolm^{-2}s^{-1}) (n=4-6). Box-plots have the line representing the median showing and whiskers indicate maximum and minimum values. Statistical analysis was carried out in GraphPad prism using a two-way ANOVA test and Tukey's multiple comparisons test. Significant p-values ≤0.05 are shown and non-significant p-values >0.05 are not.

This data suggests that OsphyB could be restricting photosynthesis compared to NB which is unlike the case in Arabidopsis (Boccalandro *et al.*, 2009) and this in turn is influenced by fertiliser levels and interestingly different applications of fertiliser, with

the absence of osmocote fertiliser seemingly having a greater impact in *OsphyB-1* under intermediate fertiliser conditions. To see if this increased assimilation is coupled with a lower stomatal conductance to make more water use efficient plants, the IRGA was used to measure the stomatal conductance and compared to the assimilation.

5.5 OsphyB has a greater impact on flag leaf stomatal conductance than fertiliser.

To investigate the effect of fertiliser treatments upon the wild-type and *OsphyB-1* plants, the stomatal conductance (gsw) was also measured in the Licor LI-6800 at both steady state cabinet light (600 PAR) and saturating light (2000 PAR). When measured under cabinet light conditions (Figure 5.5A), NB plants had significantly increased gsw with no fertiliser addition compared to that of the full fertiliser addition. In fact, the NB with no fertiliser addition had significantly higher conductance compared to the *OsphyB-1* plants aswell. Under intermediate fertiliser conditions (Figure 5.5B), NB plants had increased gsw when only the osmocote was added compared to when only the water-based fertiliser was present although this was not significant to the 5% level, p=0.5625. All other comparisons were significantly different. When only osmocote added to *OsphyB-1,* these plants had significantly the lowest stomatal conductance whereas the water fertiliser added to *OsphyB-1* with no osmocote had significantly the highest conductance.

As would be expected, saturating light resulted in higher gsw compared to growth light levels (Figure 5.5A-D). NB plants had similar levels of conductance in the full and no fertilised states, while *OsphyB-1* had significantly lower conductance levels than NB when no fertiliser was present (Figure 5.5C). Although a higher gsw, the intermediate fertilised plants had a smaller increase in conductance in saturating light compared to the fully and no fertilised plants. This is surprising as higher light levels should lead to more stomatal opening and hence transpiration. However, there is large variation within the plants grown with only the water-based fertiliser so this may account for some of the differences seen (Figure 5.6D). Nipponbare plants had no difference in conductance between the intermediate conditions. The *OsphyB-1* which had only osmocote present had the lowest amount of stomatal conductance overall.

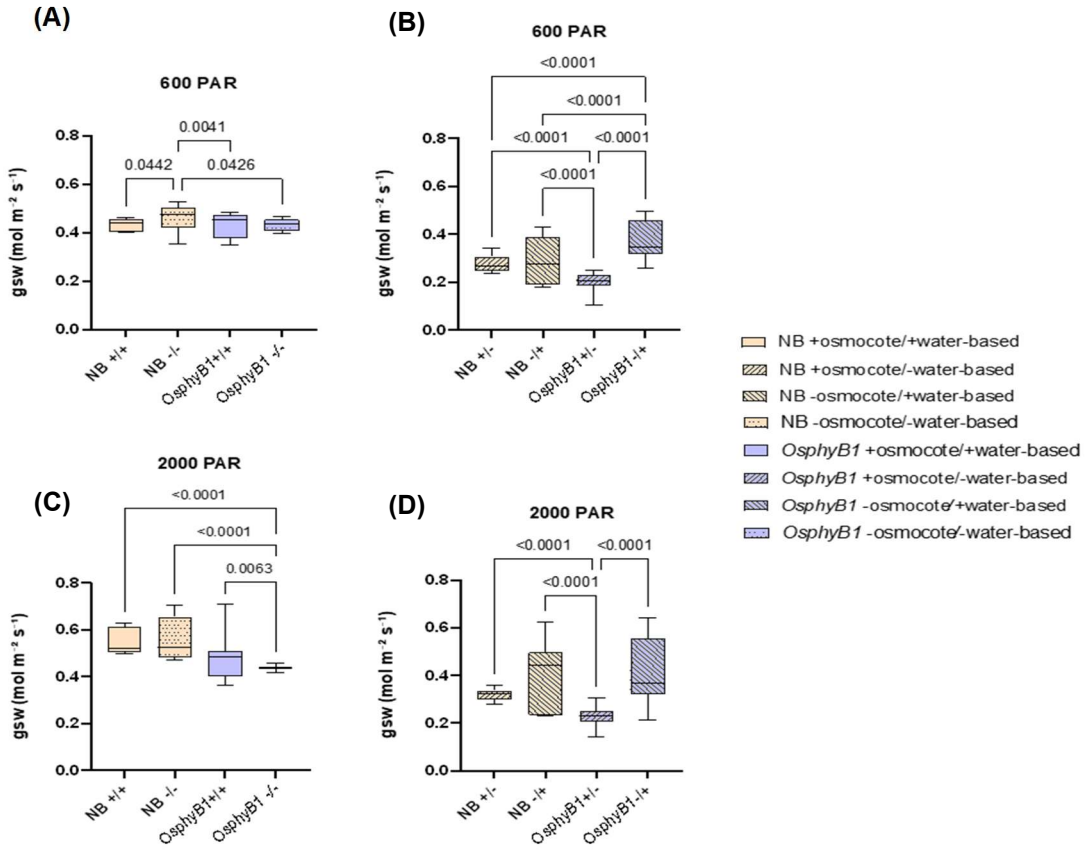

Figure 5.6. Stomatal conductance of Nipponbare and *OsphyB-1* flag leaves grown under different fertiliser regimes and light levels. A. Stomatal conductance (gsw) of flag leaves of Nipponbare and *OsphyB-1* flag leaves grown either with a full fertiliser regime (+/+) with the addition of a slow release osmocote fertiliser to the soil and the addition of a water-based fertiliser, or without either (-/-) at cabinet light conditions (600µmolm²s-1) (n=5-6) B. Nipponbare and OsphyB1 flag leaves measured gsw with intermediate fertiliser regimes. This consisted of either only the slow release osmocote applied and no water-based fertiliser applied or vice versa (+/- and -/+) grown at cabinet light conditions (600µmolm²s-1). C. Flag leaves from Nipponbare and OsphyB-1 grown with full (+/+) or no fertiliser (-/-) addition under saturating light (2000µmolm²s-1) measured for gsw in a Licor LI-6800 (n=4-6) or D. Flag leaves from Nipponbare and OsphyB-1 grown with intermediate fertiliser addition (+/-) or (-/+) under saturating light (2000µmolm²s-1) measured for gsw in a Licor LI-6800. Box-plots have the line representing the median showing and whiskers indicate maxiumum and minimum values. Statistical analysis was carried out in GraphPad prism using a two-way ANOVA test and Tukey's multiple comparisons test. Significant p-values ≤0.05 are shown and non-significant p-values >0.05 are not.

To see if the stomatal conductance data is represented by the stomatal density of the flag leaves from the same plants, impressions of the abaxial surface of the flag leaves were taken and the stomatal density calculated (Figure 5.7). The stomatal density for NB plants grown under a full fertiliser application was decreased compared to NB with no fertiliser addition, however this was not significant to the 5% level (p=0.8650). As expected, in line with published data for phyB mutants in Arabidopsis there was a significant decrease in the density for both fully and no fertilised *OsphyB-1* and little difference within the genotype between treatments (Casson *et al.*, 2009) (Figure 5.7A-B). In the case of NB grown with only osmocote and no water fertiliser, there was a reduced density when compared to the other intermediate fertiliser treatment. The number of stomata in intermediate fertilised phyB is similar whether the osmocote is absent or the water-based fertiliser is. The overall level of the stomatal density was more under intermediate fertiliser conditions compared to all other conditions and matched the density of the NB plants grown with osmocote but without the water-based fertiliser. This data suggests that stomatal conductance is not majorly impacted under cabinet light conditions with the presence of a full fertiliser regime or the absence of any fertiliser, but differences can start to be pulled apart at higher light levels. Similarly, fertiliser levels do not seem to be impacting upon gsw when intermediate amounts are used except in the case of no osmocote and only the water-based fertiliser in phyB mutants, however there is a large amount of variation in this data. Correlations between SD and gsw were generated for this data. NB under a full fertiliser regime had a strong positive correlation between gsw and SD (r = 0.9997) and this was significant. When grown without any fertiliser application, the correlation was reduced slightly (r = 0.7806), although this was not significant (p = 0.4298), meanwhile *OsphyB-1* had the opposite trend with a weaker positive correlation when fully fertiliser that got stronger in the non-fertilised plants (r = 0.2217 and 0.9073 respectively) (Figure 5.7C). For the intermediately fertilised plants, NB with only osmocote had a strong positive correlation much like the fully fertilised plants (r = 0.9785). However, the NB plants with only the water-based fertiliser added had a strong negative correlation (r = -0.7032). This change in different intermediate fertiliser regimes impacting the correlations persisted in *OsphyB-1,* with plants that only had the osmocote having a weak negative correlation (r = -0.3716), meanwhile those with only the water-based fertiliser had a strong positive correlation (r= 0.9043) (Figure 5.7D). Therefore, different fertilisers may be impacting the relationships between

stomatal conductance and stomatal density, possibly by changing the size of the stomata. The next step was to look at how the levels of assimilation and stomatal conductance impacted instantaneous water use efficiency of the flag leaves under the different fertiliser conditions and light levels.

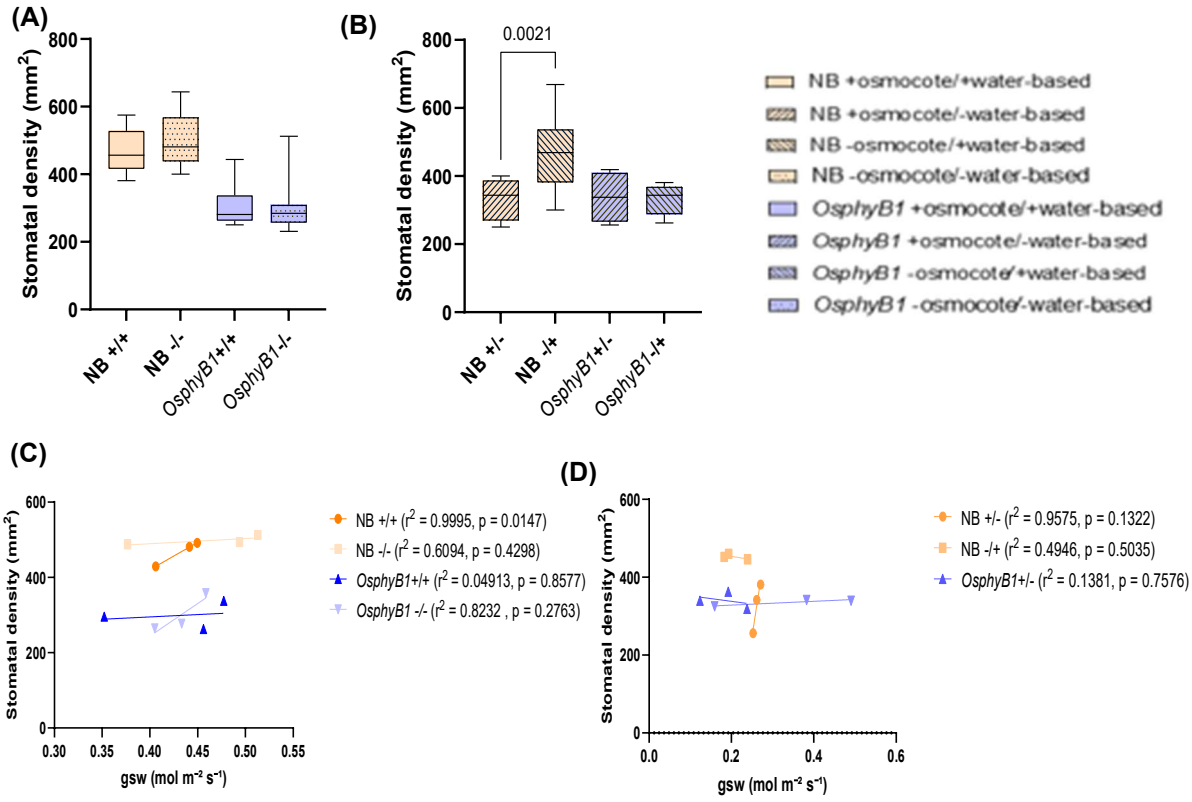

Figure 5.7. Stomatal density of Nipponbare and OsphyB-1 grown under different fertiliser regimes. Impressions of the abaxial surface of flag leaves were taken from individual plants and the stomatal density measured. (**A**). Plants were grown under either full fertiliser regime (+/+) or with no fertiliser addition (-/-). **(B)**. Plants were grown with intermediate fertiliser treatment, either with only the soil based osmocote fertiliser (+/-) or only the water-based fertiliser present (-/+) (n=3-6). Box plots are shown with the line representing the median and the whiskers the highest and lowest values of each dataset. Statistical analysis was carried out in GraphPad Prism using the two-way ANOVA and Tukey's multiple comparisons test. Significant p-values ≤0.05 are shown and non-significant p-values >0.05 are not. **(C).** Correlations for gsw against stomatal density for either fully fertilised (+/+) or no fertilised (-/-) NB and *OsphyB-1*. **(D).** Correlations for gsw against stomatal density for either the addition of only osmocote (+/-) or only a water-based fertiliser (-/+) NB and *OsphyB-1*. Graphs were generated in GraphPad prism using a simple linear regression. Lines represent lines of best fit for the individual datasets, r-values and p-values for each condition are shown in the key.

5.6 *OsphyB-1* plants have improved water use efficiency and this is unaffected by fertiliser applications

To test if the water use efficiency of *OsphyB-1* plants is unchanged compared to the wild type and if fertiliser impacts this, the instantaneous water use efficiency (iWUE) was calculated from the assimilation and gsw data under the different measurement conditions. The assimilation and conductance values were already obtained from IRGA (Figures 5.5 and 5.6 respectively).

Under full fertiliser conditions and at cabinet light, NB had a significantly higher water use efficiency than the plants grown with no fertiliser addition. Compared to *OsphyB-1,* the NB plants were significantly less water use efficient under both full and no fertiliser application (Figure 5.8A). This supports the literature which shows that Arabidopsis *phyB-5* mutants are more water use efficient than wild-type (Boccalandro *et al.*, 2009). When grown under the intermediate fertiliser conditions, there was a significant increase in water use efficiency in the NB plants grown with only the water-based fertiliser compared to when only the osmocote was present. This increase is comparable with the iWUE of *OsphyB-1* when grown with only the water-based fertiliser present. The *OsphyB-1* grown with only the osmocote had the highest iWUE, significantly higher than the other intermediate conditions due to the significantly lower gsw in these plants (Figure 5.8B).

Under saturating light, the fully and non-fertilised plants had a similar trend to those plants under cabinet light levels with *OsphyB-1* being more WUE, although to a higher level than those grown at cabinet light (Figure 5.8C). Under intermediate conditions, there was no significant difference between the NB plants with only osmocote or the water-based fertiliser. There was a significant increase in the WUE of *OsphyB-1* plants regardless of the fertiliser addition (Figure 5.8D). Therefore, *OsphyB-1* is more WUE than NB and it is unlikely that the fertiliser regimes impact this, although they may be able to improve the iWUE in NB with significant increases when only the water-based fertiliser is present.

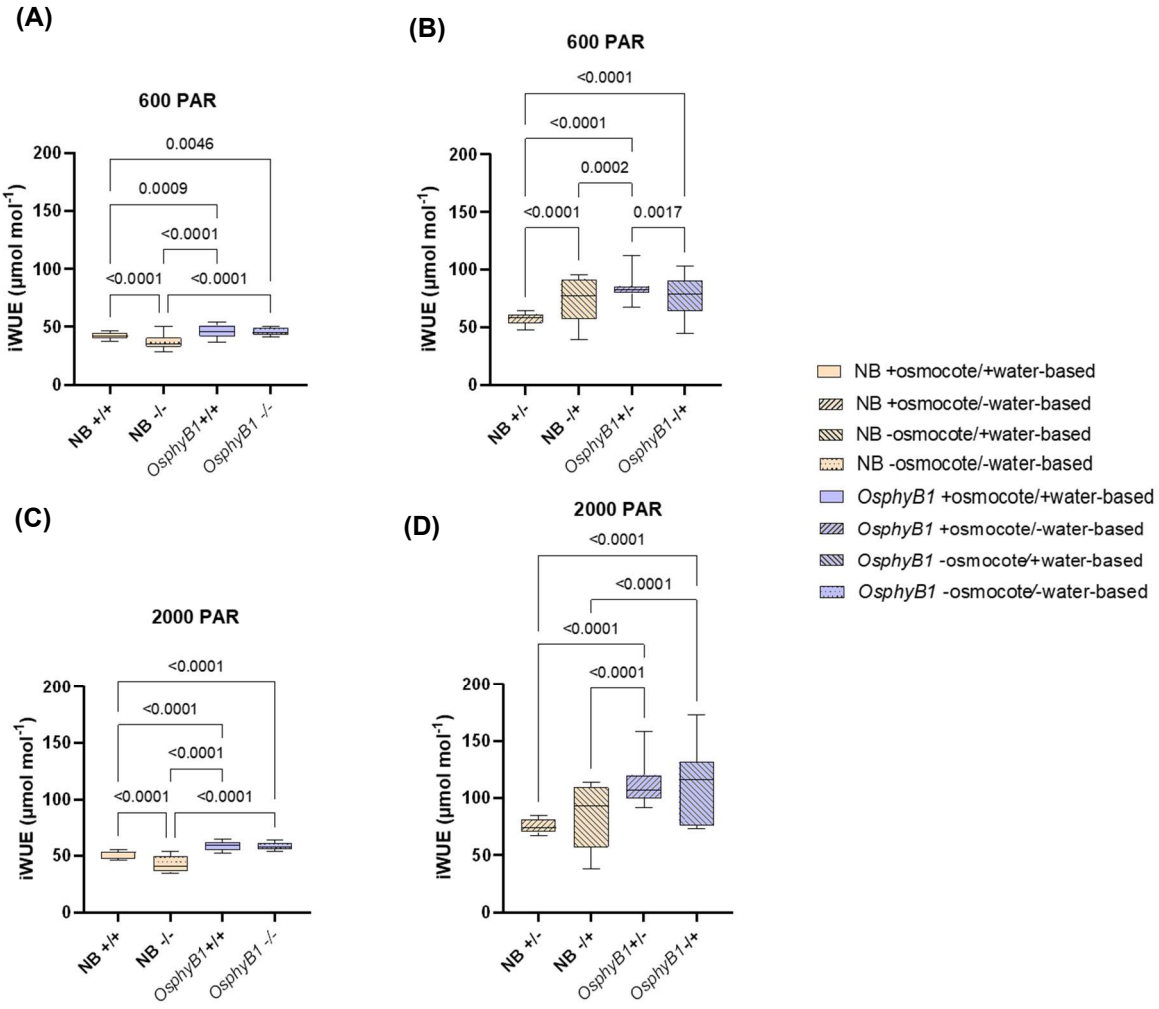

Figure 5.8. Instantaneous water use efficiency calculated from the assimilation and stomatal conductance from the Licor LI-6800. A. iWUE results for Nipponbare and *OsphyB-1* mutants grown under full (+/+) or no (-/-) fertiliser conditions and grown under 600µmolm^{-2}s^{-1} steady state lighting. B. iWUE results for Nipponbare and *OsphyB-1* plants grown under intermediate fertiliser conditions with only osmocote (+/-) or only the water based fertiliser (-/+) and grown under 600µmolm^{-2}s^{-1} steady state light. C. iWUE for Nipponbare and *OsphyB-1* plants grown with full and no fertiliser applications and saturating light (2000µmolm^{-2}s^{-1}). D. iWUE of Nipponbare and *OsphyB-1* plants grown under intermediate fertiliser conditions and saturating light conditions (2000µmolm^{-2}s^{-1}). Box plots are shown with the median line within each box and the whiskers showing the highest and lowest values. Statistical analysis was carried out in GraphPad prism using a two-way ANOVA and multiple comparisons were carried out using Tukey's multiple comparisons test. Significant p-values (≤0.05) are shown, whereas non-significant values (>0.05) are not.

5.7 Discussion

It has been known for a considerable time that a mutation of phyB in Arabidopsis and rice accelerates flowering time compared to a wild-type plant (Reed *et al.*, 1993;

Takano *et al.*, 2005). However, previous work has also shown that nitrogen levels in the form of fertiliser may influence flowering time or even the ability of a plant to flower at all (Mawodza, 2019). Therefore, the flowering time of wild-type rice Nipponbare and mutated phyB, *OsphyB-1* was studied under differing fertiliser conditions. As expected, the Nipponbare rice had an extended flowering time compared to the phyB plants regardless of fertiliser treatment (Figure 5.3). NB plants flowered under all fertiliser regimes; however, the absence of fertiliser application did significantly delay flowering, consistent with the observation that low and high nitrogen application delay flowering (Zhang *et al.*, 2021). Both fertilisers contain multiple elements including important factors that help to support the growth and flowering of rice such as phosphorus and a range of metal ions (Tables 5.1 and 5.2). Therefore, it should be considered that the absence of these other nutrients will be likely impacting upon flowering time and indeed, phosphorus and potassium have both been shown to cause earlier flowering (Ye *et al.*, 2019). Therefore, it could be possible that the absence of these two key nutrients rather than the absence of nitrogen is having a greater impact on flowering time. There is little additive effect of only osmocote and water-based fertiliser present with plants under both regimes flowering at similar times regardless of genotype (Figure 5.3B). Earlier flowering of *OsphyB-1* could be beneficial to farmers if the yield was not impacted, and so the yield of these plants was studied next.

While the average number of panicles per plant was significantly increased in a *OsphyB-1* mutant compared to NB, the weight of these panicles was significantly lower (Figure 5.4). Therefore, while OsphyB is required to produce fewer panicles, it is the combination of active OsphyB and full fertiliser application that is most important in determining the weight of panicles and therefore likely the quality of the seed too, as weight can indicate seed quality (Zhang *et al.*, 2012). This can be further seen in the ratio of panicle number per gram with NB under all fertiliser conditions having significantly reduced number of panicles per gram, indicating they have more higher quality/weight of seed. Although the NB plants with no fertiliser application did flower, the number of panicles were reduced, and the weight was similar to *OsphyB-1* (Figure 5.4). To study the impact of *OsphyB-1* and fertiliser combinations on the impact of panicle filling, the number of filled and unfilled panicles were recorded (Figure 5.5). Fertiliser regimes did impact the number of filled panicles with both NB and *OsphyB-1* having fewer when no fertiliser was applied compared to the fully fertilised plants

(Figure 5.5A), while the intermediate fertilised plants all had similar numbers of filled panicles (Figure 5.5B). The mutation in OsphyB seemed to impact the number of unfilled panicles more than fertiliser regime, with unfilled panicle production being consistently high in these plants, although fertiliser did have an impact because the plants with the highest number of unfilled panicles were the *OsphyB-1* with no fertiliser addition (Figure 5.5C-D).

It has been shown that both fertiliser application and functional OsphyB are important for determining high yields and increased filled and decreased unfilled panicle production. However, this does not answer the question of whether *OsphyB-1* and fertiliser regimes impact upon WUE, therefore IRGA was conducted on these plants. For these studies, the flag leaf was chosen to be studied in the Licor gas exchange system because it is the main photosynthetic output of a rice plant and is also important for yield (Sicher, 1993; Adachi *et al.*, 2017). Although the non-fertilised NB plants had a reduction in assimilation when fertiliser application was reduced, the *OsphyB-1* mutants had improved assimilation suggesting that OsphyB in rice could be impacting upon the photosynthetic pathways as is the case in Arabidopsis (Figure 5.6) (Boccalandro *et al.*, 2009). Under the fertiliser regime of having only the water-based fertiliser available to the *OsphyB-1* plants, there was a significant increase in the assimilation, suggesting that the osmocote fertiliser in combination with active OsphyB may be reducing assimilation. The light level increase to 2000$\mu molm^{-2}s^{-1}$ increases the level of assimilation as expected, although the trends between the genotypes stayed the same (Figure 5.6). Although in NB plants there is a significant reduction in A between the fully and non-fertilised plants, this cannot account for the significant differences in yield and so other factors could be influencing these yield changes.

Along with the assimilation, the stomatal conductance was measured to determine the amount of gas exchange occurring and enabling the calculation of iWUE. Interestingly, NB plants grown under 600$\mu molm^{-2}s^{-1}$ showed a significantly higher gsw for the plants that had no fertiliser treatment compared to the plants that had full fertiliser regimes (Figure 5.7). The possibility of rice plants under nitrogen stress enhancing stomatal conductance has been suggested previously (Li *et al.*, 2023). This is possibly due to a reduction in the amount of chlorophyll being generated when grown under nitrogen deficiency and an increased stomatal conductance may be a way to try to increase photosynthesis under these conditions, although assimilation never reaches the extent

of the fully fertilised plants. The *OsphyB-1* plants with either full or no fertiliser treatment had little difference between the treatments and little difference compared to the NB plants grown under the same conditions. Once again, the *OsphyB-1* plants grown under intermediate fertiliser with only the water-based fertiliser had increased stomatal conductance compared to NB which, considering that there are fewer stomata, is surprising and suggesting that perhaps the water-based fertiliser application could be increasing the size of stomata or the efficiency of them to absorb carbon from the atmosphere (Figure 5.7). Further studies could be undertaken in the future to measure the size of the stomata involved to see if there is a change in the size under the different applications. The stomatal density of the plants was also measured before a correlation was generated to observe the relationship between the SD and gsw (Figure 5.8). Under both full and no fertiliser application, NB plants had significantly more stomata than *OsphyB-1,* which from previous studies in Arabidopsis was to be expected. However, under intermediate fertiliser levels, only the NB that has only the water-based fertiliser added has significantly increased SD. The increased number of stomata in NB under the full and no fertilsier states correlates positively with the gsw and the SD of *OsphyB-1* under these conditions also correlates positively. However, only the NB plants with only osmocote and *OsphyB-1* with only the water-based fertiliser positively has a SD that positively correlated to the gsw. Therefore, the gsw of plants under these conditions may be being influenced by stomatal size with larger stomata potentially explaining how fewer stomata in NB with only the water based fertiliser and *OsphyB-1* with only the osmocote have increased gsw.

The mutation of OsphyB leads to a more water use efficient rice plant and fertiliser levels and type of fertiliser addition do not seem to have an impact on this within this genotype (Figure 5.8). Interestingly however, within the wild type, there is an increase in iWUE at both steady state and saturating light when only the water-based fertiliser is added. This suggests that there is the possibility of removing osmocote to improve water use, due to a small improvement on assimilation and reduction in stomatal conductance. Under both full and no fertiliser application, NB plants had significantly more stomata than *OsphyB-1*

While there could be an improvement on water use and photosynthesis in the case of NB and *OsphyB-1* when osmocote is not present and the water fertiliser is compared to other fertiliser conditions in either genotype, there is a large reduction in the yield,

which is not beneficial to farmers (Figure 5.3). Although *OsphyB-1* plants grown with full fertiliser have many panicles compared to NB, most of these are unfilled and there is a clear fertility impact by mutating OsphyB. Further studies into the molecular pathway to see how proteins downstream of OsphyB influence fertility is required. As OsphyB is required to produce fewer panicles, there could be several proteins in this pathway that is negatively regulated by OsphyB and hence upon its mutation, is able to produce more panicles. If these proteins could be upregulated in a NB plant, there is the possibility of a gain in the number of panicles without the loss of filling.

Unfortunately, due to timing constraints and cabinet space a repeat of the experiment was not able to be undertaken which would have enabled the collection of soil samples and the amount of nitrogen in these to be quantified. However, future experiments would have included this analysis to determine whether the osmocote or water-based fertiliser have a greater impact upon root nitrogen uptake. This in turn with looking at the expression of nitrogen transporters to see if their expression is changed in a phyB mutant and under the different nitrogen applications. Equally, the timing of nitrogen application on the growth stages of rice could be explored as this could lead to insights into whether fertiliser could be added later in the life cycle of wild-type plants so that the amount of fertiliser could be reduced without compromising yield and water use. Further to this, if the experiment were to be expanded upon, the inclusion of a high nitrogen fertiliser application to go along with the normal and low/no nitrogen applications would give a greater insight into the role of nitrogen and phytochrome B in rice flowering, photosynthetic performance and water use.

Slow release osmocote contains several different nutrients that plants require such as nitrogen, phosphorus, potassium, magnesium, sulphur, calcium and trace metals (see Table 5.1). Therefore, it is possible that the reason there is a greater impact on photosynthesis, stomatal conductance consequently water use is due to the absence of other nutrients in combination with the nitrogen. Compared to the water-based fertiliser, it may be easier for the plants to obtain the osmocote, which is already present in the soil compared to the water-based fertiliser, which is added at a later stage and has to be removed from the water via the roots and taken up into the plant to be distributed.

Ingredients	Percentage content
Nitrogen	15% (6.6% Nitrate and 8.4% Ammonium)
Phosphorus Pentoxide	9%
Potassium oxide	11%
Magnesium oxide	2%
Boron	0.03%
Copper	0.05%
Iron	0.45%
Manganese	0.06%
Molybdenum	0.02%
Zinc	0.015%

Table 5.1. Ingredients and their percentage abundance in the slow-release Osmocote extract fertiliser (from Osmocote, Ipswich, UK).

Ingredients	Percentage content
Nitrogen	25% (4% Nitrate, 2.5% Ammonium and 18.5% Urea)
Phosphorus Pentoxide	15%
Potassium oxide	15%
Magnesium oxide	2%
Boron	0.020%
Copper	0.010%
Iron	0.200%
Manganese	0.020%
Molybdenum	0.002%
Zinc	0.050%

Table 5.2 Ingredients and their percentage abundance in the water-based fertiliser (ChemPak High Nitrogen Feed Number 2, Thompson and Morgan, Ipswich, UK).

5.8 Key findings

1. Nipponbare wild-type rice can flower in the absence of fertiliser treatment, although this flowering is delayed compared to fully fertilised plants.

2. OsphyB is required to limit the panicle production in rice and this is worsened by removal of fertiliser.

3. *OsphyB-1* improves iWUE and this is unaffected by fertiliser treatments.

Chapter 6: General discussion

6.1 Introduction

The ability of plants to use water efficiently for survival under higher temperature climates is becoming increasingly vital. With expected temperatures to increase further unless mitigations are made. These include increased night temperatures, which are increasing at a faster rate than the corresponding day temperatures (Peng *et al.*, 2004). Important factors in a plant's ability to use water efficiently are the stomata, through which water is lost via evapotranspiration. Water is required for many metabolic processes such as photosynthesis and seed production (Johnson, 2016; Jimenez-Lopez, 2017). Phytochromes are key regulators of many plant developmental processes such as stomatal development, flowering and growth and because of the impact of increased temperatures upon their activity through thermal reversion, they are important candidates to study for enhancing the WUE and yield of plants under higher night temperatures (Devlin *et al.*, 1996; Takano *et al.*, 2005; Casson and Hetherington, 2014; Legris *et al.*, 2016). In addition to this, many of the downstream interactions that the phytochromes influence are important for epidermal patterning and healthy growth and yield of crops. This study focused on the ability of the phytochromes, specifically phyB, the major regulator of many developmental and physiological responses, to regulate WUE and epidermal patterning under different temperature regimes. Along with this, the ability of phyB to regulate flowering, photosynthesis and WUE in rice under varying fertiliser regimes.

6.2 Functional phyB is required for improved WUE under high night temperatures.

It has been noted that a mutation in phyB causes a reduction in the stomatal density and as such a reduction in stomatal conductance (Casson *et al.*, 2009; Boccalandro *et al*., 2009; Brown, 2018). However, with increasing global temperatures due to climate change, including increased frequency of warmer nights, few studies have been carried out to investigate the ability of phyB to improve WUE under increased temperatures. Higher temperatures impact upon phytochrome activity by reducing the pool of the active form of phytochromes, Pfr, through thermal reversion (Legris *et al.*, 2016). Decreases in stomatal development, often correlate with improvements in WUE. Therefore, a hypothesis was put forward that higher temperatures will improve WUE up to an optimum point, beyond which the WUE decreases due to trade offs in

traits influencing WUE (Figure 3.2). Unlike previous studies, functional phyB was found to be required for improved WUE under virtually all treatments within this study, with *phyB* mutants being consistently less WUE than Col-0 as determined by carbon isotope discrimination. This is despite the fact that *phyB* mutants consistently had lower SD than Col-0, suggesting that under these study conditions, other factors mitigated these impact of these lower SD (section 3.2). In addition to this the timing of a higher temperature during the day influences WUE with active phyB being required to negate impacts of HDT. However, EoD FR did improve WUE of both Col-0 and *phyB* mutants suggest that faster thermal reversion and hence depletion of the Pfr pool at night can drive improvements in WUE. Again, this was independent of impacts on SD (section 3.3). Supporting this disconnect between SD and carbon isotope discrimination data, thermal imaging showed the impacts on WUE were likely not due to evapotranspiration during the growth of the plants as Col-0 was significantly cooler than *phyB-9* under different temperature regimes (Figure 3.7C). For further analysis of the impact of transpiration, IRGA was performed on Col-0 and *phyB-9* at 22°C/16°C and the outcome was similar to the thermal imaging, with Col-0 having more transpiration and at this temperature *phyB-9* was significantly more WUE (Figure 3.8).

The impact of thermal reversion on the phytochromes and the impact on photosynthesis were considered. To study these, under mimicked increased temperature conditions, a ‘phytochrome gradient’ was generated. This consisted of a range of single and higher order phy mutants as well as *ft*, which has been previously shown to have a potential role in carbon assimilation (Andrés *et al.*, 2020). The higher order mutants genetically represented the outcome of an increase in temperature on total phy activity (Pfr:Pf), without the need for extra growing conditions. Unfortunately, due to timings, no triple phy mutants were able to be generated for this study, however a *phyabcde (phyQ)* mutant in a Ler background was used. This was used as an example of all of the Pfr being converted back to their Pr form due to the highest temperatures. Due to the removal of all Pfr, *phyQ* had a significantly reduced number of stomata. However, the CID was increased, indicating a less water use efficient plant (Figures 3.9B-C). Therefore, *phyQ* could demonstrate the extreme part of the bell-shaped curve hypothesis of Pfr activity under increasing temperatures (Figure 3.2). It would have been interesting to see the CID of *phyQ* had it been grown under a cooler temperature than used in this study to see if the WUE would have decreased as a

result. While the CID did not match up with the IRGA from section 3.3, *phyB-9* did behave more like a Col-0 plant in terms of WUE (Figure 3.9A). The major differences in the phenotypes between the phy mutants were in SD (Figure 3.10), with *phyAC, phyBD* and the *PHYBOE* all having significantly fewer stomata than the WT. However, without the higher order mutants, it is difficult to make statements about the relationship between the phy mutants in the gradient and WUE. The data also did not suggest a major role for FT in combination with phyB regulating WUE. Thermal imagery of these phy mutants suggests that phyD/E when associated with phyB are important for regulating leaf temperature, due to the significant increase in the double mutants for these lines.

Although FT through phyB does not appear to be regulating plant WUE, there were potential additive affects in flowering time when *phyB-9 ft* was studied (Figure 3.12). *phyBD* had a strong positive correlation between CID and flowering time, which suggests that increases in CID coincide with delayed flowering, the opposite of which is expected. This could mean that not only do phyB and phyD combine to regulate leaf temperature but also WUE in relation to flowering in an additive fashion. It has been shown recently that phyD is able to impact the expression of gene targets in the absence of phyB and that phyD and phyC can interact to mitigate against phyB absence in changes in the environment (Péter *et al.*, 2024). It has also been shown that phyB and phyD do form heterodimers with each other (Sharrock and Clack, 2004) and so have the potential to co-regulate responses. Development of a *phyBDE* triple mutant in a Columbia background would be interesting to see the impact of removal of these phytochromes that are most similar in structure to each other and bind together. Although there is a *phyBDE* mutant in a Landsberg-*erecta* background, the aim was to carry out experiments in Columbia background as different ecotypes would have different responses to temperature stimuli (Franklin *et al.*, 2003; Adams *et al.*, 2016).

There were large reductions in biomass in *phyBE* and the *PHYB*OE and this was also reflected in the biomass growth curve (Figure 3.13). Again, suggesting that it is the interaction between phyB and phyE that is most important for the regulation of growth size with the phyBE mutant looking more closer to a phyQ (Supplementary Figure 1). *phyBE* was also most impaired in photosynthetic function, although there were few changes across all other mutants (Figure 3.14). Previous studies have shown that

phyB is important in shade avoidance responses and phyD and phyE also have redundant functions in this response. The biomass of a *phyBD* mutant was less impacted in its growth. Therefore, it is possible that the ability of phyE without phyB and phyD to regulate shade avoidance responses is not sufficient, whereas phyD in the absence of phyB and phyE can still regulate the shade avoidance response (Franklin, 2009; Casal, 2013).

6.3 phyB buffers epidermal cell development under changes in the distribution of temperature loads

The leaf epidermis is the interface between the external and internal environments. Therefore, it needs to be carefully regulated to be best equipped for the environment the plant is growing in. phyB has a key role in regulating the leaf epidermis, due to its role in stomatal development and regulating WUE under different temperature regimes (Casson and Hetherington, 2014, chapter 3, present study). In the absence of phyB, there were increases in SI with increasing night temperatures, that did not correspond with increases in the SD (Figure 4.3A-B). Due to these changes in SI, the epidermis of phyB and related mutants was studied (Figure 4.4). Ordinarily, early divisions within the stomatal lineage are asymmetric however, it was determined that symmetric divisions were present, suggestive of exit from the stomatal lineage. The number of symmetric divisions in *phyB-9* when plants were grown at 22°C compared to HNT was reduced. As this was not the case in Col-0, a hypothesis could be generated that functional phyB is required to buffer against aborted symmetric divisions occurring under different temperature regimes. PIF4 acts downstream of phyB and regulates stomatal development through the inhibition of *SPCH* transcription under warmer temperatures (Kim *et al.*, 2020). However, because PIF4 matched the trend of Col-0 for both SI and had a similar trend in the patterning, it is unlikely that the inhibition of *SPCH* transcription by PIF4 is contributing to this buffering by phyB (section 4.2).

Another factor that phyB interacts with is HOS1 which targets ICE1 for degradation under colder temperatures and so influences stomatal development in a temperature dependent manner (Dong *et al.*, 2006). In an ideal study, an ICE1 mutant would be have used additionally, however, this line was not available in this study (Chinnusamy *et al.*, 2003). The SI of the double mutant *phyB-9hos1* was decreased compared to

the parental lines under both 22°C and 22°C/16°C which could suggest an additive impact of phyB and HOS1 on SI (Figure 4.8A). The number of symmetric divisions of *phyB-9hos1* both at 22°C and 22°C/16°C had a similar pattern to that of *phyB-9,* but not to *hos1*¸which is suggestive of an epistatic interaction (Figure 4.9). Therefore, it is difficult to determine the genetic relationship between phyB and HOS1 in regulating this response. Further research into the role of HOS1/ICE1 in epidermal patterning under different temperature regimes is required as a result. An ICE1proICE1:GFP line was available for study but time limitations meant that it was not possible to analyse this in any detail.

The study of epidermal patterning under different temperature regimes requires the inclusion of cell cycle genes. Both CYCD3;1 and CYCD5;1 have been shown to influence epidermal patterning via interactions with SMR4 and the bHLH MUTE (Han *et al.*, 2022; Zuch *et al.*, 2023). The two cyclin mutants had reduced numbers of symmetric divisions compared to Col-0, much like *phyB-9* under an HNT. However, due to timing constraints, unfortunately two mutants and Col-0 were only able to be grown under a HNT rather than a full range of temperature regimes (section 4.4). Therefore, it cannot be discussed with confidence that the cyclins could be acting downstream of phyB to regulate the buffering against symmetric divisions at HNT until studies have been undertaken at 22°C as well. If the pattern at 22°C was similar to *phyB-9* under the same temperature conditions, it could be inferred that they are involved with greater confidence. These results could generate a new hypothesis that under increased temperatures, phyB Pfr removal could be releasing inhibition of SMR4 which is able to inhibit the transcription of CYCD3;1 but upregulate transcription of CYCD5;1 and therefore generate more symmetric divisions. The inhibition of CYCD7;1 means that the symmetric divisions cannot progress to form stomata (Figure 4.1) (Han *et al.*, 2022).

To determine if the response was indeed due to the increase in night temperature and not decrease in day temperatures in *phyB-9* at HNT, EOD FR was used as a proxy for increased night temperatures (section 4.5). Under these conditions, it can be assumed that Col-0 would behave more like a phytochrome mutant and in terms of both the SI and patterning, Col-0 does follow the same trend as *phyB-9* when exposed to EOD FR (Figure 4.8). phyB is required to buffer against symmetric

divisions under EOD FR and so it is likely that the buffering response is due to an increased night temperature and not a cooler day temperature.

Further analysis into the downstream components of phyB and their impacts on epidermal patterning are required. To this effect, generation of a dominant HOS1 mutant would be useful to be studied in a *phyB-9hos1* double mutant and further study of the role of the cyclins, SMR4 and MUTE under different temperature regimes would also be useful in determining if they have an involvement in the phyB dependant buffering against symmetric divisions at HNT.

6.4 *OsphyB-1* improves WUE and accelerates flowering at the expense of yield.

Previous work had shown that NB plants did not flower when grown without the addition of fertiliser but that *OsphyB-1* mutants did (Mawodza, 2019). This coupled with OsphyB's ability to regulate flowering time and WUE led to investigating the impact of different fertiliser treatments on NB and *OsphyB-1* (Reed *et al.*, 1993; Boccalandro *et al.*, 2009; Kenney *et al.*, 2014). Mutation of OsphyB in rice impacted flowering and yield significantly. Similar to Arabidopsis, *OsphyB-1* flowered significantly earlier than the wild-type NB (Reed *et al.*, 1993, current study) (section 5.2). Fertiliser levels did not influence the flowering time of *OsphyB-1*; however, unlike previous studies, no fertiliser delayed but did not inhibit flowering in NB (Figure 5.3A). To determine how the fertiliser treatments impacted yield, a range of yield measurements were recorded. While in *OsphyB-1* there was a significant increase in the number of panicles, compared to NB, these panicles were less filled and there was a significant increase in the number of unfilled panicles (section 5.3) (Figure 5.5). Previous work had shown that *OsphyB-1* has defects in panicle filling (Takano *et al.*, 2005; Shethi, 2023) however, further molecular work is required to determine downstream factors. IRGA was used to determine the A in NB and *OsphyB-1* and under most fertiliser conditions at 600µmolm^{-2}s^{-1} cabinet light, *OsphyB-1* had a higher assimilation rate. This changed at 2000µmolm^{-2}s^{-1} saturating light, with NB increasing in proportion to *OsphyB-1,* this could be due to more stomata being open at saturating light for NB, whereas *OsphyB-1*, due to its lower SD had a smaller proportion to open. Fertiliser levels did impact A, in particular the increase in A for *OsphyB-1* grown with

only the water-based fertiliser (section 5.4). While fertiliser regime was shown to impact upon A, this was less of the case for full and no fertiliser addition of NB and *OsphyB-1* at both cabinet and saturating light, in this case it was the absence of OsphyB that influenced the gsw. Similarly, the plants grown under intermediate fertiliser regimes had a similar trend, except the *OsphyB-1* with only the water-based fertiliser, which like the A had a significant increase (section 5.5). The overall impact of these factors meant that *OsphyB-1* was more WUE than NB under all fertiliser regimes. No fertiliser addition meant that NB was less WUE than fully fertilised NB and *OsphyB-1* was unaffected by fertiliser treatment under these conditions. The result of this study was that while *OsphyB-1* can improve the WUE and number of panicles produced by rice, there is a large yield deficit as a consequence and fertilisers do not influence the WUE of these plants. Although, OsphyB-1 is required for improved yield, the levels of fertiliser used to grow rice could potentially be reduced as growing NB with intermediate fertiliser did not impact upon WUE, flowering or yield. This could save farmers in the cost of fertilisers which are increasingly becoming more expensive (Eardley, 2022).

6.5 Conclusions and future directions

phyB was found to be required for improving WUE under increased temperature loads. The mode of action for this requirement is likely not through transpiration of the stomata and instead may be acting through photosynthetic or canopy architecture means. Increased thermal reversion of the phytochromes, represented by double mutants determined that phyB and phyD/E may be required for delayed flowering, stomatal development and biomass accumulation. This could be through their interactions which form phytochrome heterodimers (Sharrock and Clack, 2004). Generation of phy triple mutants, particularly *phyBDE*, is important determine the impact of higher amounts of thermal reversion on WUE. Also, growth of mutants at cooler temperature loads may provide further insights. phyB was also found to be required for the buffering against the formation of aborted symmetrical meristemoid divisions in the stomatal lineage. This could be through a possible direct or indirect interaction with MUTE, which upregulates SMR4 or SMR4 directly, a key cell cycle regulator that in turn will inhibit asymmetric divisions through the inhibition of CYCD3;1 transcripts and promote symmetric divisions through its upregulation of CYCD5;1 transcripts. (Han *et al.*, 2022). Further analysis of the cyclins and SMR4 is needed at

22°C and HDT to have more clarity around their impact. Although it cannot be fully ruled out, the impact of cooler days on this buffering is likely to be less impactful than higher night temperatures. In rice, OsphyB was found to be required for delayed flowering time under all fertiliser regimes, and improvements in WUE, although at the expense of yield. The generation of more unfilled panicles in *OsphyB-1,* however, does suggest that OsphyB impacts fertility and if these impacts could be reversed in a OsphyB mutant through a molecular method, the yield could be boosted while retaining the accelerated flowering which would be useful to farmers. The finding that intermediate fertiliser treatments have similar impacts to full fertiliser regimes suggest the possibility that farmers can reduce their fertiliser usage which would save money. However, more studies have to be undertaken to determine if this is viable.

References

Adachi, S. *et al.* (2017) ‘Fine Mapping of Carbon Assimilation Rate 8, a Quantitative Trait Locus for Flag Leaf Nitrogen Content, Stomatal Conductance and Photosynthesis in Rice’, *Frontiers in Plant Science*, 8. Available at: https://doi.org/10.3389/fpls.2017.00060.

Adams, W.W. *et al.* (2016) ‘Habitat Temperature and Precipitation of Arabidopsis thaliana Ecotypes Determine the Response of Foliar Vasculature, Photosynthesis, and Transpiration to Growth Temperature’, *Frontiers in Plant Science*, 7, p. 1026. Available at: https://doi.org/10.3389/fpls.2016.01026.

Andrade, L. *et al.* (2022) ‘The evening complex integrates photoperiod signals to control flowering in rice’, *Proceedings of the National Academy of Sciences of the United States of America*, 119(26), p. e2122582119. Available at: https://doi.org/10.1073/pnas.2122582119.

Andrés, F. *et al.* (2020) ‘The sugar transporter SWEET10 acts downstream of FLOWERING LOCUS T during floral transition of Arabidopsis thaliana’, *BMC Plant Biology*, 20(1), p. 53. Available at: https://doi.org/10.1186/s12870-020-2266-0.

‘AR6 Synthesis Report: Climate Change 2023 — IPCC’ (no date). Available at: https://www.ipcc.ch/report/sixth-assessment-report-cycle/ (Accessed: 14 June 2024).

Atkin, O.K. *et al.* (2006) ‘Phenotypic plasticity and growth temperature: understanding interspecific variability’, *Journal of Experimental Botany*, 57(2), pp. 267–281. Available at: https://doi.org/10.1093/jxb/erj029.

Bae, G. and Choi, G. (2008) ‘Decoding of light signals by plant phytochromes and their interacting proteins’, *Annual Review of Plant Biology*, 59, pp. 281–311. Available at: https://doi.org/10.1146/annurev.arplant.59.032607.092859.

Balasubramanian, S. and Weigel, D. (2006) ‘Temperature Induced Flowering in Arabidopsis thaliana’, *Plant Signaling & Behavior*, 1(5), pp. 227–228.

Beerling, D.J. and Chaloner, W.G. (1993) ‘The Impact of Atmospheric CO2 and Temperature Changes on Stomatal Density: Observation from *Quercus robur* Lammas Leaves’, *Annals of Botany*, 71(3), pp. 231–235. Available at: https://doi.org/10.1006/anbo.1993.1029.

Berg, C.S., Brown, J.L. and Weber, J.J. (2019) ‘An examination of climate-driven flowering-time shifts at large spatial scales over 153 years in a common weedy annual’, *American Journal of Botany*, 106(11), pp. 1435–1443. Available at: https://doi.org/10.1002/ajb2.1381.

Bergmann, D.C., Lukowitz, W. and Somerville, C.R. (2004) ‘Stomatal development and pattern controlled by a MAPKK kinase’, *Science (New York, N.Y.)*, 304(5676), pp. 1494–1497. Available at: https://doi.org/10.1126/science.1096014.

Blatt, M.R. (2000) ‘Cellular signaling and volume control in stomatal movements in plants’, *Annual Review of Cell and Developmental Biology*, 16, pp. 221–241. Available at: https://doi.org/10.1146/annurev.cellbio.16.1.221.

Boccalandro, H.E. *et al.* (2009) ‘Phytochrome B Enhances Photosynthesis at the Expense of Water-Use Efficiency in Arabidopsis’, *Plant Physiology*, 150(2), pp. 1083–1092. Available at: https://doi.org/10.1104/pp.109.135509.

Bouman, B.A.M. and Tuong, T.P. (2001) ‘Field water management to save water and increase its productivity in irrigated lowland rice’, *Agricultural Water Management*, 49(1), pp. 11–30. Available at: https://doi.org/10.1016/S0378-3774(00)00128-1.

Bridge, L.J., Franklin, K.A. and Homer, M.E. (2013) ‘Impact of plant shoot architecture on leaf cooling: a coupled heat and mass transfer model’, *Journal of The Royal Society Interface*, 10(85), p. 20130326. Available at: https://doi.org/10.1098/rsif.2013.0326.

Brown, J. (2018) *Photoreceptor regulation of plant responses to light and carbon dioxide*, *Google Docs*. Available at: https://docs.google.com/document/d/1eXoJZrtGiA4gMw35ryLp9uTpuxyZcN7nDumpWG6tAhM/edit?usp=drive_web&ouid=109942104056936810921&usp=embed_facebook (Accessed: 5 September 2024).

Cabral, D. *et al.* (2024) ‘Exploring Rice Consumption Habits and Determinants of Choice, Aiming for the Development and Promotion of Rice Products with a Low Glycaemic Index’, *Foods*, 13(2), p. 301. Available at: https://doi.org/10.3390/foods13020301.

Casal, J.J. (2013) ‘Photoreceptor Signaling Networks in Plant Responses to Shade’, *Annual Review of Plant Biology*, 64(Volume 64, 2013), pp. 403–427. Available at: https://doi.org/10.1146/annurev-arplant-050312-120221.

Casson, S.A. *et al.* (2009) ‘phytochrome B and *PIF4* Regulate Stomatal Development in Response to Light Quantity’, *Current Biology*, 19(3), pp. 229–234. Available at: https://doi.org/10.1016/j.cub.2008.12.046.

Casson, S.A. and Hetherington, A.M. (2010) ‘Environmental regulation of stomatal development’, *Current Opinion in Plant Biology*, 13(1), pp. 90–95. Available at: https://doi.org/10.1016/j.pbi.2009.08.005.

Casson, S.A. and Hetherington, A.M. (2014) ‘phytochrome B Is required for light-mediated systemic control of stomatal development’, *Current biology: CB*, 24(11), pp. 1216–1221. Available at: https://doi.org/10.1016/j.cub.2014.03.074.

Cerdán, P.D. and Chory, J. (2003) ‘Regulation of flowering time by light quality’, *Nature*, 423(6942), pp. 881–885. Available at: https://doi.org/10.1038/nature01636.

Chen, D. *et al.* (2022) ‘Integration of light and temperature sensing by liquid-liquid phase separation of phytochrome B’, *Molecular Cell*, 82(16), pp. 3015-3029.e6. Available at: https://doi.org/10.1016/j.molcel.2022.05.026.

Chen, M. *et al.* (2005) ‘Regulation of phytochrome B nuclear localization through light-dependent unmasking of nuclear-localization signals’, *Current biology: CB*, 15(7), pp. 637–642. Available at: https://doi.org/10.1016/j.cub.2005.02.028.

Chinnusamy, V. *et al.* (2003) ‘ICE1: a regulator of cold-induced transcriptome and freezing tolerance in Arabidopsis’, *Genes & Development*, 17(8), pp. 1043–1054. Available at: https://doi.org/10.1101/gad.1077503.

Chiu, R.S. *et al.* (2016) ‘ABA-dependent inhibition of the ubiquitin proteasome system during germination at high temperature in Arabidopsis’, *The Plant Journal: For Cell and Molecular Biology*, 88(5), pp. 749–761. Available at: https://doi.org/10.1111/tpj.13293.

Cho, K.H. *et al.* (2007) ‘Developmental processes of leaf morphogenesis inarabidopsis’, *Journal of Plant Biology*, 50(3), pp. 282–290. Available at: https://doi.org/10.1007/BF03030656.

Chung, B.Y.W. *et al.* (2020) ‘An RNA thermoswitch regulates daytime growth in Arabidopsis’, *Nature Plants*, 6(5), pp. 522–532. Available at: https://doi.org/10.1038/s41477-020-0633-3.

Clack, T. *et al.* (2009) ‘Obligate Heterodimerization of Arabidopsis Phytochromes C and E and Interaction with the PIF3 Basic Helix-Loop-Helix Transcription Factor’, *The Plant Cell*, 21(3), pp. 786–799. Available at: https://doi.org/10.1105/tpc.108.065227.

Clack, T., Mathews, S. and Sharrock, R.A. (1994) ‘The phytochrome apoprotein family in Arabidopsis is encoded by five genes: the sequences and expression of PHYD and PHYE’, *Plant Molecular Biology*, 25(3), pp. 413–427. Available at: https://doi.org/10.1007/BF00043870.

Condon, A.G. *et al.* (2004) ‘Breeding for high water-use efficiency’, *Journal of Experimental Botany*, 55(407), pp. 2447–2460. Available at: https://doi.org/10.1093/jxb/erh277.

Corbesier, L. *et al.* (2007) ‘FT protein movement contributes to long-distance signaling in floral induction of Arabidopsis’, *Science (New York, N.Y.)*, 316(5827), pp. 1030–1033. Available at: https://doi.org/10.1126/science.1141752.

Crawford, A.J. *et al.* (2012) ‘High temperature exposure increases plant cooling capacity’, *Current biology: CB*, 22(10), pp. R396-397. Available at: https://doi.org/10.1016/j.cub.2012.03.044.

Crawford, N.M. and Forde, B.G. (2002) ‘Molecular and developmental biology of inorganic nitrogen nutrition’, *The Arabidopsis Book*, 1, p. e0011. Available at: https://doi.org/10.1199/tab.0011.

Devlin, P.F. *et al.* (1996) ‘The rosette habit of Arabidopsis thaliana is dependent upon phytochrome action: novel phytochromes control internode elongation and

flowering time', *The Plant Journal*, 10(6), pp. 1127–1134. Available at: https://doi.org/10.1046/j.1365-313X.1996.10061127.x.

Devlin, P.F., Patel, S.R. and Whitelam, G.C. (1998) 'Phytochrome E influences internode elongation and flowering time in Arabidopsis', *The Plant Cell*, 10(9), pp. 1479–1487. Available at: https://doi.org/10.1105/tpc.10.9.1479.

Dong, C.-H. *et al.* (2006) 'The negative regulator of plant cold responses, HOS1, is a RING E3 ligase that mediates the ubiquitination and degradation of ICE1', *Proceedings of the National Academy of Sciences of the United States of America*, 103(21), pp. 8281–8286. Available at: https://doi.org/10.1073/pnas.0602874103.

Dong, J. *et al.* (2017) 'Light-Dependent Degradation of PIF3 by SCFEBF1/2 Promotes a Photomorphogenic Response in Arabidopsis', *Current biology: CB*, 27(16), pp. 2420-2430.e6. Available at: https://doi.org/10.1016/j.cub.2017.06.062.

Dow, G.J., Bergmann, D.C. and Berry, J.A. (2014) 'An integrated model of stomatal development and leaf physiology', *New Phytologist*, 201(4), pp. 1218–1226. Available at: https://doi.org/10.1111/nph.12608.

Dubois, M. *et al.* (2023) 'SIAMESE-RELATED1 imposes differentiation of stomatal lineage ground cells into pavement cells', *Nature Plants*, 9(7), pp. 1143–1153. Available at: https://doi.org/10.1038/s41477-023-01452-7.

Dusenge, M.E., Duarte, A.G. and Way, D.A. (2019) 'Plant carbon metabolism and climate change: elevated CO2 and temperature impacts on photosynthesis, photorespiration and respiration', *New Phytologist*, 221(1), pp. 32–49. Available at: https://doi.org/10.1111/nph.15283.

Eardley, F. (2022) 'Rising cost of agricultural fertiliser and feed: Causes, impacts and government policy'. Available at: https://lordslibrary.parliament.uk/rising-cost-of-agricultural-fertiliser-and-feed-causes-impacts-and-government-policy/ (Accessed: 7 August 2024).

Enderle, B. *et al.* (2017) 'PCH1 and PCHL promote photomorphogenesis in plants by controlling phytochrome B dark reversion', *Nature Communications*, 8(1), p. 2221. Available at: https://doi.org/10.1038/s41467-017-02311-8.

Endo, M. *et al.* (2013) 'PHYTOCHROME-DEPENDENT LATE-FLOWERING accelerates flowering through physical interactions with phytochrome B and CONSTANS', *Proceedings of the National Academy of Sciences of the United States of America*, 110(44), pp. 18017–18022. Available at: https://doi.org/10.1073/pnas.1310631110.

Endo, M. *et al.* (2014) 'Light-dependent destabilization of PHL in Arabidopsis', *Plant Signaling & Behavior*, 9, p. e28118. Available at: https://doi.org/10.4161/psb.28118.

Endo, M. and Nagatani, A. (2008) 'Flowering regulation by tissue specific functions of photoreceptors', *Plant Signaling & Behavior*, 3(1), pp. 47–48.

Engineer, C.B. *et al.* (2014) 'Carbonic anhydrases, EPF2 and a novel protease mediate CO2 control of stomatal development', *Nature*, 513(7517), pp. 246–250. Available at: https://doi.org/10.1038/nature13452.

Fang-Fang, W. *et al.* (2010) 'Phytochrome B Is Involved in Mediating Red Light-Induced Stomatal Opening in *Arabidopsis thaliana*', *Molecular Plant*, 3(1), pp. 246–259. Available at: https://doi.org/10.1093/mp/ssp097.

Farquhar, G.D. and Ehleringer, I.J.R. (1989) 'CARBON ISOTOPE DISCRIMINATION AND PHOTOSYNTHESIS'.

Ferguson, J.N. *et al.* (2019) 'Accelerated flowering time reduces lifetime water use without penalizing reproductive performance in Arabidopsis', *Plant, Cell & Environment*, 42(6), pp. 1847–1867. Available at: https://doi.org/10.1111/pce.13527.

Franklin, K.A. *et al.* (2003) 'Phytochromes B, D, and E Act Redundantly to Control Multiple Physiological Responses in Arabidopsis', *Plant Physiology*, 131(3), pp. 1340–1346. Available at: https://doi.org/10.1104/pp.102.015487.

Franklin, K.A. (2009) 'Light and temperature signal crosstalk in plant development', *Current Opinion in Plant Biology*, 12(1), pp. 63–68. Available at: https://doi.org/10.1016/j.pbi.2008.09.007.

Franklin, K.A. *et al.* (2011) 'Phytochrome-interacting factor 4 (PIF4) regulates auxin biosynthesis at high temperature', *Proceedings of the National Academy of Sciences*

of the United States of America, 108(50), pp. 20231–20235. Available at: https://doi.org/10.1073/pnas.1110682108.

Franks, P.J. and Beerling, D.J. (2009) 'CO(2)-forced evolution of plant gas exchange capacity and water-use efficiency over the Phanerozoic', *Geobiology*, 7(2), pp. 227–236. Available at: https://doi.org/10.1111/j.1472-4669.2009.00193.x.

Franks, P.J., Drake, P.L. and Beerling, D.J. (2009) 'Plasticity in maximum stomatal conductance constrained by negative correlation between stomatal size and density: an analysis using Eucalyptus globulus', *Plant, Cell & Environment*, 32(12), pp. 1737–1748. Available at: https://doi.org/10.1111/j.1365-3040.2009.002031.x.

Frink, C.R., Waggoner, P.E. and Ausubel, J.H. (1999) 'Nitrogen fertilizer: retrospect and prospect', *Proceedings of the National Academy of Sciences of the United States of America*, 96(4), pp. 1175–1180. Available at: https://doi.org/10.1073/pnas.96.4.1175.

Fu, G. *et al.* (2012) 'Thermal Resistance of Common Rice Maintainer and Restorer Lines to High Temperature During Flowering and Early Grain Filling Stages', *Rice Science*, 19(4), pp. 309–314. Available at: https://doi.org/10.1016/S1672-6308(12)60055-9.

Fukagawa, N.K. and Ziska, L.H. (2019) 'Rice: Importance for Global Nutrition', *Journal of Nutritional Science and Vitaminology*, 65(Supplement), pp. S2–S3. Available at: https://doi.org/10.3177/jnsv.65.S2.

Galvão, V.C. and Fankhauser, C. (2015) 'Sensing the light environment in plants: photoreceptors and early signaling steps', *Current Opinion in Neurobiology*, 34, pp. 46–53. Available at: https://doi.org/10.1016/j.conb.2015.01.013.

Geisler, M., Nadeau, J. and Sack, F.D. (2000) 'Oriented asymmetric divisions that generate the stomatal spacing pattern in arabidopsis are disrupted by the too many mouths mutation', *The Plant Cell*, 12(11), pp. 2075–2086. Available at: https://doi.org/10.1105/tpc.12.11.2075.

Genoud, T. *et al.* (2008) 'FHY1 mediates nuclear import of the light-activated phytochrome A photoreceptor', *PLoS genetics*, 4(8), p. e1000143. Available at: https://doi.org/10.1371/journal.pgen.1000143.

Glover, B.J. (2000) 'Differentiation in plant epidermal cells', *Journal of Experimental Botany*, 51(344), pp. 497–505. Available at: https://doi.org/10.1093/jexbot/51.344.497.

Gray, W.M. *et al.* (1998) 'High temperature promotes auxin-mediated hypocotyl elongation in Arabidopsis', *Proceedings of the National Academy of Sciences of the United States of America*, 95(12), pp. 7197–7202. Available at: https://doi.org/10.1073/pnas.95.12.7197.

Gu, J. and Yang, J. (2022) 'Nitrogen (N) transformation in paddy rice field: Its effect on N uptake and relation to improved N management', *Crop and Environment*, 1(1), pp. 7–14. Available at: https://doi.org/10.1016/j.crope.2022.03.003.

Gudesblat, G.E. *et al.* (2012) 'SPEECHLESS integrates brassinosteroid and stomata signalling pathways', *Nature Cell Biology*, 14(5), pp. 548–554. Available at: https://doi.org/10.1038/ncb2471.

Guo, M., Xu, Y. and Gruebele, M. (2012) 'Temperature dependence of protein folding kinetics in living cells', *Proceedings of the National Academy of Sciences of the United States of America*, 109(44), pp. 17863–17867. Available at: https://doi.org/10.1073/pnas.1201797109.

Halliday, K.J. *et al.* (2003) 'Phytochrome control of flowering is temperature sensitive and correlates with expression of the floral integrator FT', *The Plant Journal*, 33(5), pp. 875–885. Available at: https://doi.org/10.1046/j.1365-313X.2003.01674.x.

Han, S.-K. *et al.* (2018) 'MUTE Directly Orchestrates Cell-State Switch and the Single Symmetric Division to Create Stomata', *Developmental Cell*, 45(3), pp. 303-315.e5. Available at: https://doi.org/10.1016/j.devcel.2018.04.010.

Han, S.-K. *et al.* (2022) 'Deceleration of the cell cycle underpins a switch from proliferative to terminal divisions in plant stomatal lineage', *Developmental Cell*, 57(5), pp. 569-582.e6. Available at: https://doi.org/10.1016/j.devcel.2022.01.014.

Hara, K. *et al.* (2007) 'The secretory peptide gene EPF1 enforces the stomatal one-cell-spacing rule', *Genes & Development*, 21(14), pp. 1720–1725. Available at: https://doi.org/10.1101/gad.1550707.

Hara, K. *et al.* (2009) 'Epidermal cell density is autoregulated via a secretory peptide, EPIDERMAL PATTERNING FACTOR 2 in Arabidopsis leaves', *Plant & Cell Physiology*, 50(6), pp. 1019–1031. Available at: https://doi.org/10.1093/pcp/pcp068.

Harashima, H., Dissmeyer, N. and Schnittger, A. (2013) 'Cell cycle control across the eukaryotic kingdom', *Trends in Cell Biology*, 23(7), pp. 345–356. Available at: https://doi.org/10.1016/j.tcb.2013.03.002.

He, K., Xu, S. and Li, J. (2013) 'BAK1 directly regulates brassinosteroid perception and BRI1 activation', *Journal of Integrative Plant Biology*, 55(12), pp. 1264–1270. Available at: https://doi.org/10.1111/jipb.12122.

Hetherington, A.M. and Woodward, F.I. (2003) 'The role of stomata in sensing and driving environmental change', *Nature*, 424(6951), pp. 901–908. Available at: https://doi.org/10.1038/nature01843.

Hu, C. *et al.* (2022) 'Heat shock proteins: Biological functions, pathological roles, and therapeutic opportunities', *MedComm*, 3(3), p. e161. Available at: https://doi.org/10.1002/mco2.161.

Hu, W. *et al.* (2013) 'Unanticipated regulatory roles for Arabidopsis phytochromes revealed by null mutant analysis', *Proceedings of the National Academy of Sciences*, 110(4), pp. 1542–1547. Available at: https://doi.org/10.1073/pnas.1221738110.

Huang, H. *et al.* (2016) 'PCH1 integrates circadian and light-signaling pathways to control photoperiod-responsive growth in Arabidopsis', *eLife*, 5, p. e13292. Available at: https://doi.org/10.7554/eLife.13292.

Huché-Thélier, L. *et al.* (2016) 'Light signaling and plant responses to blue and UV radiations—Perspectives for applications in horticulture', *Environmental and Experimental Botany*, 121, pp. 22–38. Available at: https://doi.org/10.1016/j.envexpbot.2015.06.009.

Hunt, L. and Gray, J.E. (2009) 'The Signaling Peptide EPF2 Controls Asymmetric Cell Divisions during Stomatal Development', *Current Biology*, 19(10), pp. 864–869. Available at: https://doi.org/10.1016/j.cub.2009.03.069.

Inagaki, N. *et al.* (2015) 'Phytochrome B Mediates the Regulation of Chlorophyll Biosynthesis through Transcriptional Regulation of ChlH and GUN4 in Rice Seedlings', *PLoS ONE*, 10(8), p. e0135408. Available at: https://doi.org/10.1371/journal.pone.0135408.

Ishikawa, R. *et al.* (2009) 'Phytochrome dependent quantitative control of Hd3a transcription is the basis of the night break effect in rice flowering', *Genes & Genetic Systems*, 84(2), pp. 179–184. Available at: https://doi.org/10.1266/ggs.84.179.

Ishikawa, R. *et al.* (2011) 'Phytochrome B regulates Heading date 1 (Hd1)-mediated expression of rice florigen Hd3a and critical day length in rice', *Molecular Genetics and Genomics*, 285(6), pp. 461–470. Available at: https://doi.org/10.1007/s00438-011-0621-4.

Ishitani, M. *et al.* (1998) 'HOS1, a genetic locus involved in cold-responsive gene expression in arabidopsis', *The Plant Cell*, 10(7), pp. 1151–1161. Available at: https://doi.org/10.1105/tpc.10.7.1151.

Izawa, T. *et al.* (2002) 'Phytochrome mediates the external light signal to repress FT orthologs in photoperiodic flowering of rice', *Genes & Development*, 16(15), pp. 2006–2020. Available at: https://doi.org/10.1101/gad.999202.

Jacqmard, A., Gadisseur, I. and Bernier, G. (2003) 'Cell division and morphological changes in the shoot apex of Arabidopsis thaliana during floral transition', *Annals of Botany*, 91(5), pp. 571–576. Available at: https://doi.org/10.1093/aob/mcg053.

Jaeger, K.E. and Wigge, P.A. (2007) 'FT protein acts as a long-range signal in Arabidopsis', *Current biology: CB*, 17(12), pp. 1050–1054. Available at: https://doi.org/10.1016/j.cub.2007.05.008.

Jagadish, S.V.K. *et al.* (2016) 'Implications of High Temperature and Elevated CO2 on Flowering Time in Plants', *Frontiers in Plant Science*, 7, p. 913. Available at: https://doi.org/10.3389/fpls.2016.00913.

Jang, S. *et al.* (2008) ‘Arabidopsis COP1 shapes the temporal pattern of CO accumulation conferring a photoperiodic flowering response’, *The EMBO journal*, 27(8), pp. 1277–1288. Available at: https://doi.org/10.1038/emboj.2008.68.

Janni, M. *et al.* (2024) ‘Plant responses to climate change, how global warming may impact on food security: a critical review’, *Frontiers in Plant Science*, 14, p. 1297569. Available at: https://doi.org/10.3389/fpls.2023.1297569.

Javelle, M. *et al.* (2011) ‘Epidermis: the formation and functions of a fundamental plant tissue’, *The New Phytologist*, 189(1), pp. 17–39. Available at: https://doi.org/10.1111/j.1469-8137.2010.03514.x.

Jimenez-Lopez, J.C. (2017) *Advances inSeed Biology*. BoD – Books on Demand.

Johanson, U. *et al.* (2000) ‘Molecular analysis of FRIGIDA, a major determinant of natural variation in Arabidopsis flowering time’, *Science (New York, N.Y.)*, 290(5490), pp. 344–347. Available at: https://doi.org/10.1126/science.290.5490.344.

John, S., Olas, J.J. and Mueller-Roeber, B. (2021) ‘Regulation of alternative splicing in response to temperature variation in plants’, *Journal of Experimental Botany*, 72(18), pp. 6150–6163. Available at: https://doi.org/10.1093/jxb/erab232.

Johnson, M.P. (2016) ‘Photosynthesis’, *Essays in Biochemistry*, 60(3), pp. 255–273. Available at: https://doi.org/10.1042/EBC20160016.

Joshi, P.N., Biswal, B. and Biswal, U.C. (1991) ‘Effect of u.v.-A on aging of wheat leaves and role of phytochrome’, *Environmental and Experimental Botany*, 31(3), pp. 267–276. Available at: https://doi.org/10.1016/0098-8472(91)90050-X.

Jung, J.-H. *et al.* (2016) ‘Phytochromes function as thermosensors in Arabidopsis’, *Science (New York, N.Y.)*, 354(6314), pp. 886–889. Available at: https://doi.org/10.1126/science.aaf6005.

Jung, J.-H. *et al.* (2020) ‘A prion-like domain in ELF3 functions as a thermosensor in Arabidopsis’, *Nature*, 585(7824), pp. 256–260. Available at: https://doi.org/10.1038/s41586-020-2644-7.

Kanaoka, M.M. *et al.* (2008) 'SCREAM/ICE1 and SCREAM2 Specify Three Cell-State Transitional Steps Leading to Arabidopsis Stomatal Differentiation', *The Plant Cell*, 20(7), pp. 1775–1785. Available at: https://doi.org/10.1105/tpc.108.060848.

Kazan, K. and Lyons, R. (2016) 'The link between flowering time and stress tolerance', *Journal of Experimental Botany*, 67(1), pp. 47–60. Available at: https://doi.org/10.1093/jxb/erv441.

Kenney, A.M. *et al.* (2014) 'Direct and indirect selection on flowering time, water-use efficiency (WUE, δ 13C), and WUE plasticity to drought in Arabidopsis thaliana', *Ecology and Evolution*, 4(23), pp. 4505–4521. Available at: https://doi.org/10.1002/ece3.1270.

Kim, C. *et al.* (2023) 'Phytochrome B photobodies are comprised of phytochrome B and its primary and secondary interacting proteins', *Nature Communications*, 14(1), p. 1708. Available at: https://doi.org/10.1038/s41467-023-37421-z.

Kim, E.-J. *et al.* (2023) 'Cell type-specific attenuation of brassinosteroid signaling precedes stomatal asymmetric cell division', *Proceedings of the National Academy of Sciences of the United States of America*, 120(36), p. e2303758120. Available at: https://doi.org/10.1073/pnas.2303758120.

Kim, J.-H. *et al.* (2017) 'HOS1 Facilitates the Phytochrome B-Mediated Inhibition of PIF4 Function during Hypocotyl Growth in *Arabidopsis*', *Molecular Plant*, 10(2), pp. 274–284. Available at: https://doi.org/10.1016/j.molp.2016.11.009.

Kim, Sara *et al.* (2020) 'The epidermis coordinates thermoresponsive growth through the phyB-PIF4-auxin pathway', *Nature Communications*, 11(1), p. 1053. Available at: https://doi.org/10.1038/s41467-020-14905-w.

Kinoshita, A. *et al.* (2020) 'Regulation of shoot meristem shape by photoperiodic signaling and phytohormones during floral induction of Arabidopsis', *eLife*, 9, p. e60661. Available at: https://doi.org/10.7554/eLife.60661.

Kinoshita, T. *et al.* (2005) 'Binding of brassinosteroids to the extracellular domain of plant receptor kinase BRI1', *Nature*, 433(7022), pp. 167–171. Available at: https://doi.org/10.1038/nature03227.

Klose, C., Nagy, F. and Schäfer, E. (2020) ‘Thermal Reversion of Plant Phytochromes’, *Molecular Plant*, 13(3), pp. 386–397. Available at: https://doi.org/10.1016/j.molp.2019.12.004.

Koini, M.A. *et al.* (2009) ‘High temperature-mediated adaptations in plant architecture require the bHLH transcription factor PIF4’, *Current biology: CB*, 19(5), pp. 408–413. Available at: https://doi.org/10.1016/j.cub.2009.01.046.

Kojima, S. *et al.* (2002) ‘Hd3a, a rice ortholog of the Arabidopsis FT gene, promotes transition to flowering downstream of Hd1 under short-day conditions’, *Plant & Cell Physiology*, 43(10), pp. 1096–1105. Available at: https://doi.org/10.1093/pcp/pcf156.

Kostaki, K.-I. *et al.* (2020) ‘Guard Cells Integrate Light and Temperature Signals to Control Stomatal Aperture1 [OPEN]’, *Plant Physiology*, 182(3), pp. 1404–1419. Available at: https://doi.org/10.1104/pp.19.01528.

Kreslavski, V.D. *et al.* (2018) ‘The impact of the phytochromes on photosynthetic processes’, *Biochimica et Biophysica Acta (BBA) - Bioenergetics*, 1859(5), pp. 400–408. Available at: https://doi.org/10.1016/j.bbabio.2018.03.003.

Kumar, S.V. *et al.* (2012) ‘PHYTOCHROME INTERACTING FACTOR4 controls the thermosensory activation of flowering’, *Nature*, 484(7393), pp. 242–245. Available at: https://doi.org/10.1038/nature10928.

Kumar, S.V. and Wigge, P.A. (2010) ‘H2A.Z-Containing Nucleosomes Mediate the Thermosensory Response in Arabidopsis’, *Cell*, 140(1), pp. 136–147. Available at: https://doi.org/10.1016/j.cell.2009.11.006.

Lai, L.B. *et al.* (2005) ‘The Arabidopsis R2R3 MYB Proteins FOUR LIPS and MYB88 Restrict Divisions Late in the Stomatal Cell Lineage’, *The Plant Cell*, 17(10), pp. 2754–2767. Available at: https://doi.org/10.1105/tpc.105.034116.

Lampard, G.R., Macalister, C.A. and Bergmann, D.C. (2008) ‘Arabidopsis stomatal initiation is controlled by MAPK-mediated regulation of the bHLH SPEECHLESS’, *Science (New York, N.Y.)*, 322(5904), pp. 1113–1116. Available at: https://doi.org/10.1126/science.1162263.

Lang, A. and Nitsch, J. P. (1965) ‘Blüten- und Fruchtbildung. — Flower and fruit formation’, in A. Allsopp et al. (eds) *Differentiation and Development / Differenzierung und Entwicklung: Part 1 / Teil 1*. Berlin, Heidelberg: Springer, pp. 1380–1647. Available at: https://doi.org/10.1007/978-3-662-36273-0_32.

Lau, O.S. *et al.* (2014) ‘Direct roles of SPEECHLESS in the specification of stomatal self-renewing cells’, *Science (New York, N.Y.)*, 345(6204), pp. 1605–1609. Available at: https://doi.org/10.1126/science.1256888.

Lau, O.S. *et al.* (2018) ‘Direct Control of SPEECHLESS by PIF4 in the High-Temperature Response of Stomatal Development’, *Current biology : CB*, 28(8), pp. 1273-1280.e3. Available at: https://doi.org/10.1016/j.cub.2018.02.054.

Lawson, T. and Matthews, J. (2020) ‘Guard Cell Metabolism and Stomatal Function’, *Annual Review of Plant Biology*, 71, pp. 273–302. Available at: https://doi.org/10.1146/annurev-arplant-050718-100251.

Lazaro, A. *et al.* (2012) ‘The Arabidopsis E3 ubiquitin ligase HOS1 negatively regulates CONSTANS abundance in the photoperiodic control of flowering’, *The Plant Cell*, 24(3), pp. 982–999. Available at: https://doi.org/10.1105/tpc.110.081885.

Lee, J.-H., Jung, J.-H. and Park, C.-M. (2017) ‘Light Inhibits COP1-Mediated Degradation of ICE Transcription Factors to Induce Stomatal Development in Arabidopsis’, *The Plant Cell*, 29(11), pp. 2817–2830. Available at: https://doi.org/10.1105/tpc.17.00371.

Lee, J.S. *et al.* (2012) ‘Direct interaction of ligand–receptor pairs specifying stomatal patterning’, *Genes & Development*, 26(2), pp. 126–136. Available at: https://doi.org/10.1101/gad.179895.111.

Lee, J.S. *et al.* (2015) ‘Competitive binding of antagonistic peptides fine-tunes stomatal patterning’, *Nature*, 522(7557), pp. 439–443. Available at: https://doi.org/10.1038/nature14561.

Lee, J.S. and Bowling, D.J.F. (1995) ‘Influence of the Mesophyll on Stomatal Opening’, *Functional Plant Biology*, 22(3), pp. 357–363. Available at: https://doi.org/10.1071/pp9950357.

Lefebvre, S. *et al.* (2005) ‘Increased sedoheptulose-1,7-bisphosphatase activity in transgenic tobacco plants stimulates photosynthesis and growth from an early stage in development’, *Plant Physiology*, 138(1), pp. 451–460. Available at: https://doi.org/10.1104/pp.104.055046.

Legris, M. *et al.* (2016) ‘Phytochrome B integrates light and temperature signals in Arabidopsis’, *Science (New York, N.Y.)*, 354(6314), pp. 897–900. Available at: https://doi.org/10.1126/science.aaf5656.

Legris, M., Ince, Y.Ç. and Fankhauser, C. (2019) ‘Molecular mechanisms underlying phytochrome-controlled morphogenesis in plants’, *Nature Communications*, 10(1), p. 5219. Available at: https://doi.org/10.1038/s41467-019-13045-0.

Leinonen, I. *et al.* (2006) ‘Estimating stomatal conductance with thermal imagery’, *Plant, Cell & Environment*, 29(8), pp. 1508–1518. Available at: https://doi.org/10.1111/j.1365-3040.2006.01528.x.

Leivar, P. and Quail, P.H. (2011) ‘PIFs: pivotal components in a cellular signaling hub’, *Trends in Plant Science*, 16(1), pp. 19–28. Available at: https://doi.org/10.1016/j.tplants.2010.08.003.

Li, F.-W. *et al.* (2015) ‘Phytochrome diversity in green plants and the origin of canonical plant phytochromes’, *Nature Communications*, 6, p. 7852. Available at: https://doi.org/10.1038/ncomms8852.

Li, H. *et al.* (2024) ‘A warm temperature-released negative feedback loop fine-tunes PIF4-mediated thermomorphogenesis in Arabidopsis’, *Plant Communications*, 5(5). Available at: https://doi.org/10.1016/j.xplc.2024.100833.

Li, Y. *et al.* (2016) ‘Water Conservation and Nitrogen Loading Reduction Effects with Controlled and Mid-Gathering Irrigation in a Paddy Field’, *Polish Journal of Environmental Studies*, 25(3), pp. 1085–1091. Available at: https://doi.org/10.15244/pjoes/61835.

Li, Y. *et al.* (2023) ‘Rice *dep1* variety maintains larger stomatal conductance to enhance photosynthesis under low nitrogen conditions’, *Crop Design*, 2(1), p. 100025. Available at: https://doi.org/10.1016/j.cropd.2023.100025.

Liu, H. *et al.* (2011) ‘The action mechanisms of plant cryptochromes’, *Trends in Plant Science*, 16(12), pp. 684–691. Available at: https://doi.org/10.1016/j.tplants.2011.09.002.

Liu, X. *et al.* (2013) ‘PHYTOCHROME INTERACTING FACTOR3 Associates with the Histone Deacetylase HDA15 in Repression of Chlorophyll Biosynthesis and Photosynthesis in Etiolated Arabidopsis Seedlings[W][OA]’, *The Plant Cell*, 25(4), pp. 1258–1273. Available at: https://doi.org/10.1105/tpc.113.109710.

Luo, L. *et al.* (2012) ‘The development of stomata and other epidermal cells on the rice leaves’, *Biologia Plantarum*, 56(3), pp. 521–527. Available at: https://doi.org/10.1007/s10535-012-0045-y.

MacAlister, C.A., Ohashi-Ito, K. and Bergmann, D.C. (2007) ‘Transcription factor control of asymmetric cell divisions that establish the stomatal lineage’, *Nature*, 445(7127), pp. 537–540. Available at: https://doi.org/10.1038/nature05491.

MacAlpine, D.M. (2021) ‘Stochastic initiation of DNA replication across the human genome’, *Molecular Cell*, 81(14), pp. 2873–2874. Available at: https://doi.org/10.1016/j.molcel.2021.06.022.

Makino, A. (2011) ‘Photosynthesis, Grain Yield, and Nitrogen Utilization in Rice and Wheat’, 155.

Masle, J., Gilmore, S.R. and Farquhar, G.D. (2005) ‘The ERECTA gene regulates plant transpiration efficiency in Arabidopsis’, *Nature*, 436(7052), pp. 866–870. Available at: https://doi.org/10.1038/nature03835.

Mathieu, J. *et al.* (2007) ‘Export of FT protein from phloem companion cells is sufficient for floral induction in Arabidopsis’, *Current biology: CB*, 17(12), pp. 1055–1060. Available at: https://doi.org/10.1016/j.cub.2007.05.009.

Mawodza, T. (2019) *Plant-soil interactions: the impact of plant water use efficiency on root architecture and soil structure*. phd. University of Sheffield. Available at: https://etheses.whiterose.ac.uk/25992/ (Accessed: 31 May 2024).

Meng, X. *et al.* (2015) ‘Differential Function of Arabidopsis SERK Family Receptor-like Kinases in Stomatal Patterning’, *Current biology: CB*, 25(18), pp. 2361–2372. Available at: https://doi.org/10.1016/j.cub.2015.07.068.

Menges, M. *et al.* (2006) ‘The D-Type Cyclin CYCD3;1 Is Limiting for the G1-to-S-Phase Transition in Arabidopsis’, *The Plant Cell*, 18(4), pp. 893–906. Available at: https://doi.org/10.1105/tpc.105.039636.

Michaels, S.D. *et al.* (2003) ‘Attenuation of FLOWERING LOCUS C activity as a mechanism for the evolution of summer-annual flowering behavior in Arabidopsis’, *Proceedings of the National Academy of Sciences of the United States of America*, 100(17), pp. 10102–10107. Available at: https://doi.org/10.1073/pnas.1531467100.

Michaels, S.D. and Amasino, R.M. (1999) ‘FLOWERING LOCUS C encodes a novel MADS domain protein that acts as a repressor of flowering’, *The Plant Cell*, 11(5), pp. 949–956. Available at: https://doi.org/10.1105/tpc.11.5.949.

Mockler, T. *et al.* (2003) ‘Regulation of photoperiodic flowering by Arabidopsis photoreceptors’, *Proceedings of the National Academy of Sciences of the United States of America*, 100(4), pp. 2140–2145. Available at: https://doi.org/10.1073/pnas.0437826100.

Monte, E. *et al.* (2003) ‘Isolation and Characterization of phyC Mutants in Arabidopsis Reveals Complex Crosstalk between Phytochrome Signaling Pathways’, *The Plant Cell*, 15(9), pp. 1962–1980. Available at: https://doi.org/10.1105/tpc.012971.

Murata, Y., Mori, I.C. and Munemasa, S. (2015) ‘Diverse stomatal signaling and the signal integration mechanism’, *Annual Review of Plant Biology*, 66, pp. 369–392. Available at: https://doi.org/10.1146/annurev-arplant-043014-114707.

Murcia, G. *et al.* (2021) ‘Phytochrome B and PCH1 protein dynamics store night temperature information’, *The Plant Journal: For Cell and Molecular Biology*, 105(1), pp. 22–33. Available at: https://doi.org/10.1111/tpj.15034.

Nadeau, J.A. and Sack, F.D. (2002) ‘Stomatal Development in Arabidopsis’, *The Arabidopsis Book / American Society of Plant Biologists*, 1, p. e0066. Available at: https://doi.org/10.1199/tab.0066.

Naikwade, P. (2017) ‘Impact of climate change on agricultural production in India: effect on rice productivity’, *Bioscience Discovery*, 8, pp. 897–914.

Nations, U. (no date) *Population*, *United Nations*. United Nations. Available at: https://www.un.org/en/global-issues/population (Accessed: 16 June 2024).

Nieto, C. *et al.* (2015) ‘ELF3-PIF4 interaction regulates plant growth independently of the Evening Complex’, *Current biology: CB*, 25(2), pp. 187–193. Available at: https://doi.org/10.1016/j.cub.2014.10.070.

Noir, S. *et al.* (2013) ‘Jasmonate Controls Leaf Growth by Repressing Cell Proliferation and the Onset of Endoreduplication while Maintaining a Potential Stand-By Mode’, *Plant Physiology*, 161(4), pp. 1930–1951. Available at: https://doi.org/10.1104/pp.113.214908.

Ohashi-Ito, K. and Bergmann, D.C. (2006) ‘Arabidopsis FAMA Controls the Final Proliferation/Differentiation Switch during Stomatal Development’, *The Plant Cell*, 18(10), pp. 2493–2505. Available at: https://doi.org/10.1105/tpc.106.046136.

Osterlund, M.T., Ang, L.-H. and Deng, X.W. (1999) ‘The role of COP1 in repression of *Arabidopsis* photomorphogenic development’, *Trends in Cell Biology*, 9(3), pp. 113–118. Available at: https://doi.org/10.1016/S0962-8924(99)01499-3.

Osugi, A. *et al.* (2011) ‘Molecular Dissection of the Roles of Phytochrome in Photoperiodic Flowering in Rice’, *Plant Physiology*, 157(3), p. 1128. Available at: https://doi.org/10.1104/pp.111.181792.

Outlaw, Jr., William H. (2003) ‘Integration of Cellular and Physiological Functions of Guard Cells’, *Critical Reviews in Plant Sciences*, 22(6), pp. 503–529. Available at: https://doi.org/10.1080/713608316.

Paik, I. and Huq, E. (2019) ‘Plant photoreceptors: Multi-functional sensory proteins and their signaling networks’, *Seminars in cell & developmental biology*, 92, pp. 114–121. Available at: https://doi.org/10.1016/j.semcdb.2019.03.007.

Pechan, T. *et al.* (2002) ‘Insect feeding mobilizes a unique plant defense protease that disrupts the peritrophic matrix of caterpillars’, *Proceedings of the National Academy of Sciences of the United States of America*, 99(20), pp. 13319–13323. Available at: https://doi.org/10.1073/pnas.202224899.

Pei, Z.-M. *et al.* (1998) ‘Role of Farnesyltransferase in ABA Regulation of Guard Cell Anion Channels and Plant Water Loss’, *Science*, 282(5387), pp. 287–290. Available at: https://doi.org/10.1126/science.282.5387.287.

Peng, S. *et al.* (2004) ‘Rice yields decline with higher night temperature from global warming’, *Proceedings of the National Academy of Sciences of the United States of America*, 101(27), p. 9971. Available at: https://doi.org/10.1073/pnas.0403720101.

Péter, C. *et al.* (2024) ‘Phytochrome C and Low Temperature Promote the Protein Accumulation and Red-Light Signaling of Phytochrome D’, *Plant and Cell Physiology*, p. pcae089. Available at: https://doi.org/10.1093/pcp/pcae089.

Peterson, K.M. *et al.* (2013) ‘Arabidopsis homeodomain-leucine zipper IV proteins promote stomatal development and ectopically induce stomata beyond the epidermis’, *Development (Cambridge, England)*, 140(9), pp. 1924–1935. Available at: https://doi.org/10.1242/dev.090209.

Pillitteri, L.J. *et al.* (2007) ‘Termination of asymmetric cell division and differentiation of stomata’, *Nature*, 445(7127), pp. 501–505. Available at: https://doi.org/10.1038/nature05467.

Putterill, J. *et al.* (1995) ‘The CONSTANS gene of Arabidopsis promotes flowering and encodes a protein showing similarities to zinc finger transcription factors’, *Cell*, 80(6), pp. 847–857. Available at: https://doi.org/10.1016/0092-8674(95)90288-0.

Qi, X. *et al.* (2017) ‘Autocrine regulation of stomatal differentiation potential by EPF1 and ERECTA-LIKE1 ligand-receptor signaling’, *eLife*, 6. Available at: https://doi.org/10.7554/eLife.24102.

Qiu, D. *et al.* (2023) ‘Editorial: Stress-induced flowering in plants’, *Frontiers in Plant Science*, 14, p. 1338150. Available at: https://doi.org/10.3389/fpls.2023.1338150.

Quail, P.H. (1997) ‘An emerging molecular map of the phytochromes’, *Plant, Cell & Environment*, 20(6), pp. 657–665. Available at: https://doi.org/10.1046/j.1365-3040.1997.d01-108.x.

Reed, J.W. *et al.* (1993) ‘Mutations in the gene for the red/far-red light receptor phytochrome B alter cell elongation and physiological responses throughout Arabidopsis development.’, *The Plant Cell*, 5(2), pp. 147–157.

Rizzini, L. *et al.* (2011) ‘Perception of UV-B by the Arabidopsis UVR8 protein’, *Science (New York, N.Y.)*, 332(6025), pp. 103–106. Available at: https://doi.org/10.1126/science.1200660.

Rockwell, N.C., Su, Y.-S. and Lagarias, J.C. (2006) ‘Phytochrome structure and signaling mechanisms’, *Annual Review of Plant Biology*, 57, pp. 837–858. Available at: https://doi.org/10.1146/annurev.arplant.56.032604.144208.

Roelfsema, M.R.G. and Hedrich, R. (2005) ‘In the light of stomatal opening: new insights into “the Watergate”’, *The New Phytologist*, 167(3), pp. 665–691. Available at: https://doi.org/10.1111/j.1469-8137.2005.01460.x.

Sachs, T. (1991) *Pattern Formation in Plant Tissues*. Cambridge: Cambridge University Press (Developmental and Cell Biology Series). Available at: https://doi.org/10.1017/CBO9780511574535.

Sack, L. *et al.* (2003) ‘The “hydrology” of leaves: co-ordination of structure and function in temperate woody species’, *Plant, Cell & Environment*, 26(8), pp. 1343–1356. Available at: https://doi.org/10.1046/j.0016-8025.2003.01058.x.

Saini, K., Dwivedi, A. and Ranjan, A. (2022) ‘High temperature restricts cell division and leaf size by coordination of PIF4 and TCP4 transcription factors’, *Plant Physiology*, 190(4), pp. 2380–2397. Available at: https://doi.org/10.1093/plphys/kiac345.

Samset, B.H. *et al.* (2023) ‘Steady global surface warming from 1973 to 2022 but increased warming rate after 1990’, *Communications Earth & Environment*, 4(1), pp. 1–6. Available at: https://doi.org/10.1038/s43247-023-01061-4.

Satake, T. and Yoshida, S. (1978) ‘High Temperature-Induced Sterility in Indica Rices at Flowering’, *Japanese Journal of Crop Science*, 47(1), pp. 6–17. Available at: https://doi.org/10.1626/jcs.47.6.

Sawa, M. *et al.* (2007) ‘FKF1 and GIGANTEA complex formation is required for day-length measurement in Arabidopsis’, *Science (New York, N.Y.)*, 318(5848), pp. 261–265. Available at: https://doi.org/10.1126/science.1146994.

Schoch, P., Zinsou, C. and Sibi, M. (1980) ‘Dependence of the Stomatal Index on Environmental-Factors During Stomatal Differentiation in Leaves of Vigna-Sinensis L .1. Effect of Light-Intensity’, *JOURNAL OF EXPERIMENTAL BOTANY*, 31(124), pp. 1211–1216. Available at: https://doi.org/10.1093/jxb/31.5.1211.

Schulze, E.D. *et al.* (1972) ‘Stomatal responses to changes in humidity in plants growing in the desert’, *Planta*, 108(3), pp. 259–270. Available at: https://doi.org/10.1007/BF00384113.

Searle, I. *et al.* (2006) ‘The transcription factor FLC confers a flowering response to vernalization by repressing meristem competence and systemic signaling in Arabidopsis’, *Genes & Development*, 20(7), pp. 898–912. Available at: https://doi.org/10.1101/gad.373506.

Seibt, U. *et al.* (2008) ‘Carbon isotopes and water use efficiency: sense and sensitivity’, *Oecologia*, 155(3), pp. 441–454. Available at: https://doi.org/10.1007/s00442-007-0932-7.

Seo, P.J. and Mas, P. (2015) ‘STRESSing the role of the plant circadian clock’, *Trends in Plant Science*, 20(4), pp. 230–237. Available at: https://doi.org/10.1016/j.tplants.2015.01.001.

Sharkey, T.D. (2023) ‘The discovery of rubisco’, *Journal of Experimental Botany*, 74(2), pp. 510–519. Available at: https://doi.org/10.1093/jxb/erac254.

Sharrock, R.A. and Clack, T. (2004) ‘Heterodimerization of type II phytochromes in Arabidopsis’, *Proceedings of the National Academy of Sciences of the United States of America*, 101(31), pp. 11500–11505. Available at: https://doi.org/10.1073/pnas.0404286101.

Sheerin, D.J. *et al.* (2015) ‘Light-Activated Phytochrome A and B Interact with Members of the SPA Family to Promote Photomorphogenesis in Arabidopsis by Reorganizing the COP1/SPA Complex’, *The Plant Cell*, 27(1), pp. 189–201. Available at: https://doi.org/10.1105/tpc.114.134775.

Shethi, K. (2023) *The role of phytohormones and light signalling in the guard cell CO2 response*. phd. University of Sheffield. Available at: https://etheses.whiterose.ac.uk/33876/ (Accessed: 31 May 2024).

Shindo, C. *et al.* (2005) ‘Role of FRIGIDA and FLOWERING LOCUS C in Determining Variation in Flowering Time of Arabidopsis’, *Plant Physiology*, 138(2), pp. 1163–1173. Available at: https://doi.org/10.1104/pp.105.061309.

Sicher, R.C. (1993) ‘Assimilate Partitioning within Leaves of Small Grain Cereals’, in Y.P. Abrol, P. Mohanty, and Govindjee (eds) *Photosynthesis: Photoreactions to Plant Productivity*. Dordrecht: Springer Netherlands, pp. 351–360. Available at: https://doi.org/10.1007/978-94-011-2708-0_14.

Simon, N.M.L. *et al.* (2020) ‘The Circadian Clock Influences the Long-Term Water Use Efficiency of Arabidopsis1[OPEN]’, *Plant Physiology*, 183(1), pp. 317–330. Available at: https://doi.org/10.1104/pp.20.00030.

Smith, R.W. *et al.* (2017) ‘Interactions Between phyB and PIF Proteins Alter Thermal Reversion Reactions in vitro’, *Photochemistry and Photobiology*, 93(6), pp. 1525–1531. Available at: https://doi.org/10.1111/php.12793.

Stavang, J.A. *et al.* (2009) ‘Hormonal regulation of temperature-induced growth in Arabidopsis’, *The Plant Journal*, 60(4), pp. 589–601. Available at: https://doi.org/10.1111/j.1365-313X.2009.03983.x.

Stephenson, P.G., Fankhauser, C. and Terry, M.J. (2009) 'PIF3 is a repressor of chloroplast development', *Proceedings of the National Academy of Sciences*, 106(18), pp. 7654–7659. Available at: https://doi.org/10.1073/pnas.0811684106.

Su, Z. *et al.* (2013) 'Flower Development under Drought Stress: Morphological and Transcriptomic Analyses Reveal Acute Responses and Long-Term Acclimation in Arabidopsis[C][W]', *The Plant Cell*, 25(10), pp. 3785–3807. Available at: https://doi.org/10.1105/tpc.113.115428.

Sugano, S.S. *et al.* (2010) 'Stomagen positively regulates stomatal density in Arabidopsis', *Nature*, 463(7278), pp. 241–244. Available at: https://doi.org/10.1038/nature08682.

Takano, M. *et al.* (2005) 'Distinct and Cooperative Functions of Phytochromes A, B, and C in the Control of Deetiolation and Flowering in Rice', *The Plant Cell*, 17(12), pp. 3311–3325. Available at: https://doi.org/10.1105/tpc.105.035899.

Tamaki, S. *et al.* (2007) 'Hd3a protein is a mobile flowering signal in rice', *Science (New York, N.Y.)*, 316(5827), pp. 1033–1036. Available at: https://doi.org/10.1126/science.1141753.

Tanaka, Y. *et al.* (2013) 'ABA inhibits entry into stomatal-lineage development in Arabidopsis leaves', *The Plant Journal*, 74(3), pp. 448–457. Available at: https://doi.org/10.1111/tpj.12136.

Tasset, C. *et al.* (2018) 'POWERDRESS-mediated histone deacetylation is essential for thermomorphogenesis in Arabidopsis thaliana', *PLOS Genetics*, 14(3), p. e1007280. Available at: https://doi.org/10.1371/journal.pgen.1007280.

Tcherkez, G. and Farquhar, G.D. (2005) 'Carbon isotope effect predictions for enzymes involved in the primary carbon metabolism of plant leaves', *Functional Plant Biology*, 32(4), pp. 277–291. Available at: https://doi.org/10.1071/FP04211.

Thomashow, M.F. (2001) 'So what's new in the field of plant cold acclimation? Lots!', *Plant Physiology*, 125(1), pp. 89–93. Available at: https://doi.org/10.1104/pp.125.1.89.

Toledo-Ortiz, G. *et al.* (2014) ‘The HY5-PIF regulatory module coordinates light and temperature control of photosynthetic gene transcription’, *PLoS genetics*, 10(6), p. e1004416. Available at: https://doi.org/10.1371/journal.pgen.1004416.

Urban, J. *et al.* (2017) ‘Increase in leaf temperature opens stomata and decouples net photosynthesis from stomatal conductance in Pinus taeda and Populus deltoides x nigra’, *Journal of Experimental Botany*, 68(7), pp. 1757–1767. Available at: https://doi.org/10.1093/jxb/erx052.

US Department of Commerce, N. (no date) *Global Monitoring Laboratory - Carbon Cycle Greenhouse Gases*. Available at: https://gml.noaa.gov/ccgg/trends/ (Accessed: 14 June 2024).

Verma, V. *et al.* (2021) ‘Systems-based rice improvement approaches for sustainable food and nutritional security’, *Plant Cell Reports*, 40(11), pp. 2021–2036. Available at: https://doi.org/10.1007/s00299-021-02790-6.

Vicentini, G. *et al.* (2023) ‘Environmental control of rice flowering time’, *Plant Communications*, 4(5), p. 100610. Available at: https://doi.org/10.1016/j.xplc.2023.100610.

Wang, F. *et al.* (2020) ‘Contributions of cryptochromes and phototropins to stomatal opening through the day’, *Functional plant biology: FPB*, 47(3), pp. 226–238. Available at: https://doi.org/10.1071/FP19053.

Wang, F.-F. *et al.* (2010) ‘Phytochrome B Is Involved in Mediating Red Light-Induced Stomatal Opening in *Arabidopsis thaliana*’, *Molecular Plant*, 3(1), pp. 246–259. Available at: https://doi.org/10.1093/mp/ssp097.

Wang, H. *et al.* (1998) ‘ICK1, a cyclin-dependent protein kinase inhibitor from Arabidopsis thaliana interacts with both Cdc2a and CycD3, and its expression is induced by abscisic acid’, *The Plant Journal: For Cell and Molecular Biology*, 15(4), pp. 501–510. Available at: https://doi.org/10.1046/j.1365-313x.1998.00231.x.

Wang, H. *et al.* (2007) ‘Stomatal Development and Patterning Are Regulated by Environmentally Responsive Mitogen-Activated Protein Kinases in Arabidopsis’, *The Plant Cell*, 19(1), pp. 63–73. Available at: https://doi.org/10.1105/tpc.106.048298.

Wang, X. *et al.* (2020) ‘Emergent constraint on crop yield response to warmer temperature from field experiments’, *Nature Sustainability*, 3(11), pp. 908–916. Available at: https://doi.org/10.1038/s41893-020-0569-7.

Wei, H. *et al.* (2020) ‘Light Regulation of Stomatal Development and Patterning: Shifting the Paradigm from *Arabidopsis* to Grasses’, *Plant Communications*, 1(2), p. 100030. Available at: https://doi.org/10.1016/j.xplc.2020.100030.

Wu, M. *et al.* (2018) ‘SPATULA regulates floral transition and photomorphogenesis in a PHYTOCHROME B-dependent manner in Arabidopsis’, *Biochemical and Biophysical Research Communications*, 503(4), pp. 2380–2385. Available at: https://doi.org/10.1016/j.bbrc.2018.06.165.

Xia, J. *et al.* (2009) ‘Role of cytokinin and salicylic acid in plant growth at low temperatures’, *Plant Growth Regulation*, 57(3), pp. 211–221. Available at: https://doi.org/10.1007/s10725-008-9338-8.

Yan, L. *et al.* (2014) ‘New phenotypic characteristics of three tmm alleles in Arabidopsis thaliana’, *Plant Cell Reports*, 33(5), pp. 719–731. Available at: https://doi.org/10.1007/s00299-014-1571-1.

Yang, S.W. *et al.* (2009) ‘FAR-RED ELONGATED HYPOCOTYL1 and FHY1-LIKE Associate with the Arabidopsis Transcription Factors LAF1 and HFR1 to Transmit Phytochrome A Signals for Inhibition of Hypocotyl Elongation’, *The Plant Cell*, 21(5), pp. 1341–1359. Available at: https://doi.org/10.1105/tpc.109.067215.

Yano, M. *et al.* (2000) ‘Hd1, a major photoperiod sensitivity quantitative trait locus in rice, is closely related to the Arabidopsis flowering time gene CONSTANS’, *The Plant Cell*, 12(12), pp. 2473–2484. Available at: https://doi.org/10.1105/tpc.12.12.2473.

Yanovsky, M.J. and Kay, S.A. (2002) ‘Molecular basis of seasonal time measurement in Arabidopsis’, *Nature*, 419(6904), pp. 308–312. Available at: https://doi.org/10.1038/nature00996.

Ye, K. *et al.* (2019) ‘BRASSINOSTEROID-INSENSITIVE2 Negatively Regulates the Stability of Transcription Factor ICE1 in Response to Cold Stress in Arabidopsis’,

The Plant Cell, 31(11), pp. 2682–2696. Available at: https://doi.org/10.1105/tpc.19.00058.

Ye, T. *et al.* (2019) 'Nitrogen, phosphorus, and potassium fertilization affects the flowering time of rice (*Oryza sativa* L.)', *Global Ecology and Conservation*, 20, p. e00753. Available at: https://doi.org/10.1016/j.gecco.2019.e00753.

Yoshida, Y. *et al.* (2018) 'The Arabidopsis phyB-9 Mutant Has a Second-Site Mutation in the VENOSA4 Gene That Alters Chloroplast Size, Photosynthetic Traits, and Leaf Growth1', *Plant Physiology*, 178(1), pp. 3–6. Available at: https://doi.org/10.1104/pp.18.00764.

van Zanten, M. *et al.* (2009) 'Hormone- and light-mediated regulation of heat-induced differential petiole growth in Arabidopsis', *Plant Physiology*, 151(3), pp. 1446–1458. Available at: https://doi.org/10.1104/pp.109.144386.

Zhang, S. *et al.* (2021) 'Nitrogen Mediates Flowering Time and Nitrogen Use Efficiency via Floral Regulators in Rice', *Current Biology*, 31(4), pp. 671-683.e5. Available at: https://doi.org/10.1016/j.cub.2020.10.095.

Zhang, X. *et al.* (2012) 'Rare allele of OsPPKL1 associated with grain length causes extra-large grain and a significant yield increase in rice', *Proceedings of the National Academy of Sciences*, 109(52), pp. 21534–21539. Available at: https://doi.org/10.1073/pnas.1219776110.

Zhu, J.-K. (2016) 'Abiotic stress signaling and responses in plants', *Cell*, 167(2), pp. 313–324. Available at: https://doi.org/10.1016/j.cell.2016.08.029.

Zhu, X.-G., de Sturler, E. and Long, S.P. (2007) 'Optimizing the Distribution of Resources between Enzymes of Carbon Metabolism Can Dramatically Increase Photosynthetic Rate: A Numerical Simulation Using an Evolutionary Algorithm', *Plant Physiology*, 145(2), pp. 513–526. Available at: https://doi.org/10.1104/pp.107.103713.

Zoulias, N. *et al.* (2018) 'Molecular control of stomatal development', *Biochemical Journal*, 475(2), pp. 441–454. Available at: https://doi.org/10.1042/BCJ20170413.

Zoulias, N. *et al.* (2021) ‘Inhibition of Arabidopsis stomatal development by plastoquinone oxidation’, *Current Biology*, 31(24), pp. 5622-5632.e7. Available at: https://doi.org/10.1016/j.cub.2021.10.018.

Zuch, D.T. *et al.* (2023) ‘Cell Cycle Dynamics during Stomatal Development: Window of MUTE Action and Ramification of Its Loss-of-Function on an Uncommitted Precursor’, *Plant and Cell Physiology*, 64(3), pp. 325–335. Available at: https://doi.org/10.1093/pcp/pcad002.

Appendix

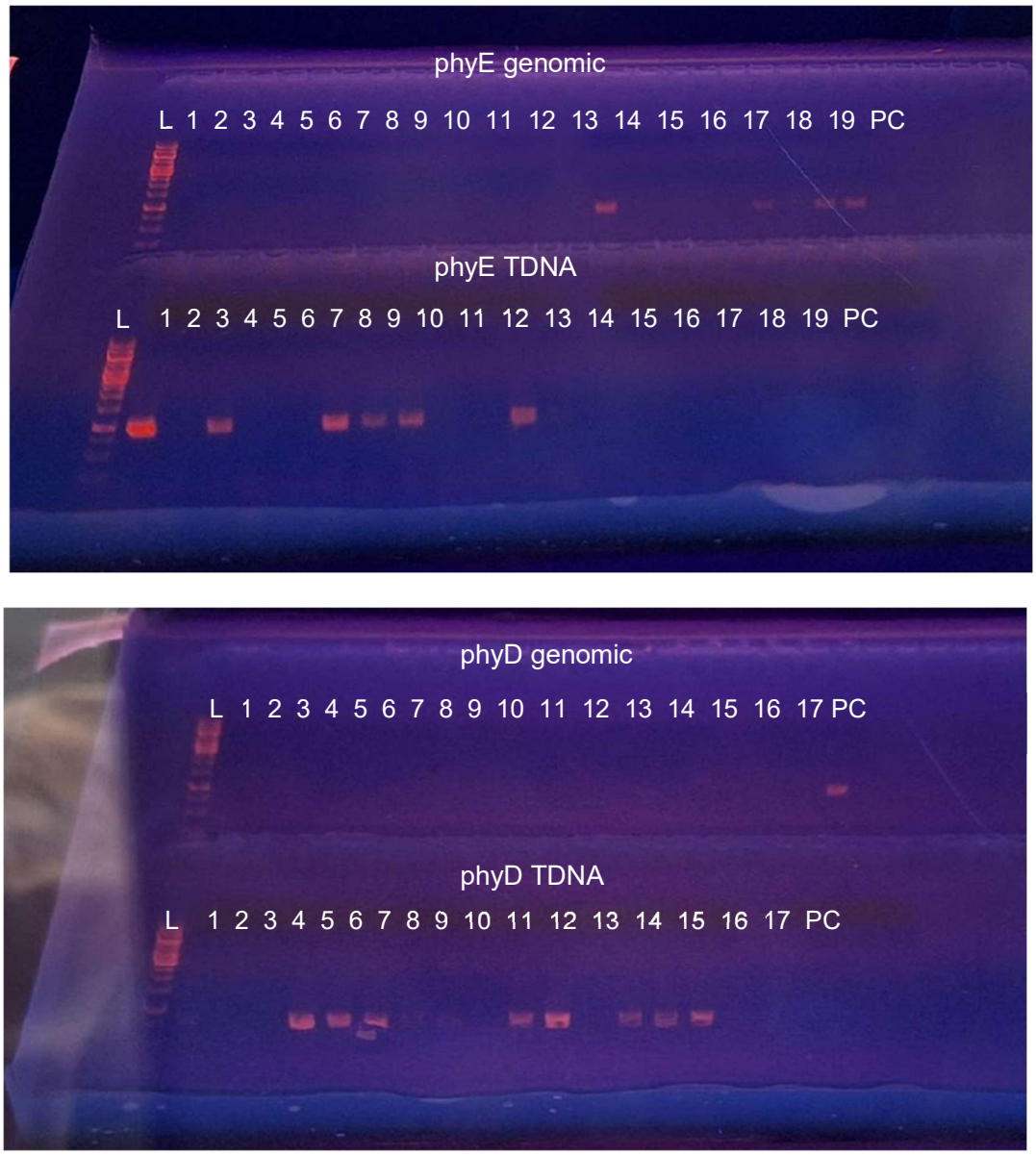

Supplementary Figure 2.1. 1% agarose gel to show confirmation of phyE and phyD homozygous mutants in *phyBE and phyBD* plants. The top half of each gel represents the genomic DNA of 19 samples for phyE and 17 for phyD while the bottom half represents the TDNA insertion. PC = Positive control for genomic (Col-0).

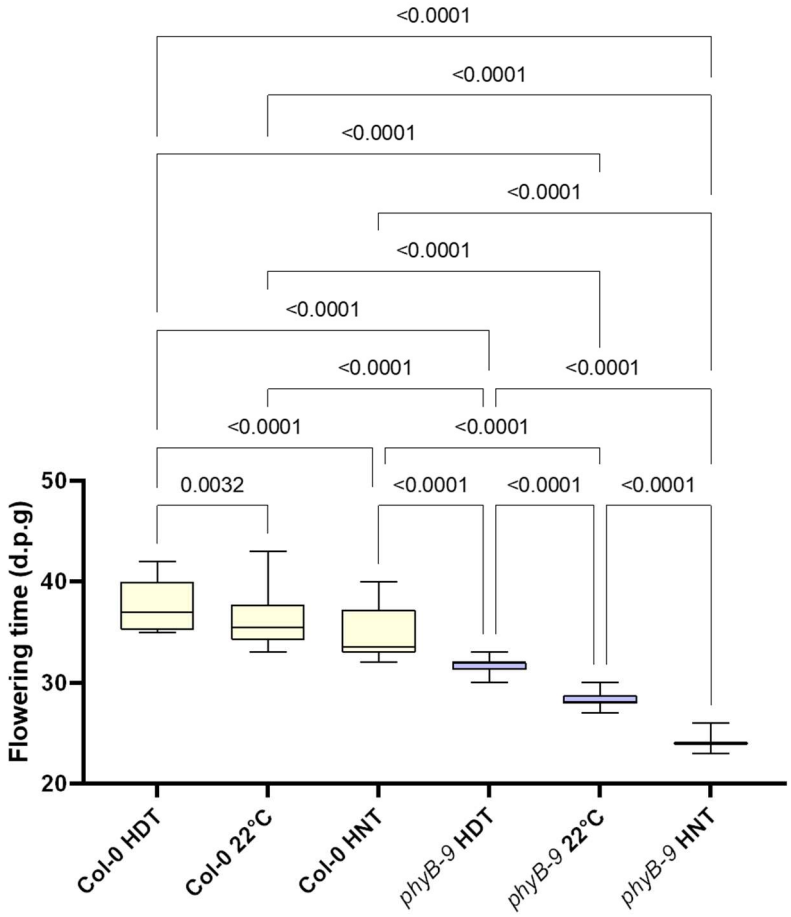

Supplementary Figure 3.1. Higher night temperatures accelerate flowering. The flowering time of Col-0 and *phyB-9* plants were measured under three temperature regimes: HDT, 22°C and HNT. Box and whisker plot was generated in GraphPad prism, where the box represents 25%-75% percentile of the data and the line represents the median. The whiskers show the largest and smallest values of the dataset respectively, n=20. Statistical analysis was carried out in GraphPad using a Two-way ANOVA with Tukey's multiple comparisons test. Significant p-values ≤0.05 are shown whereas non-significant p-values >0.05 are not.

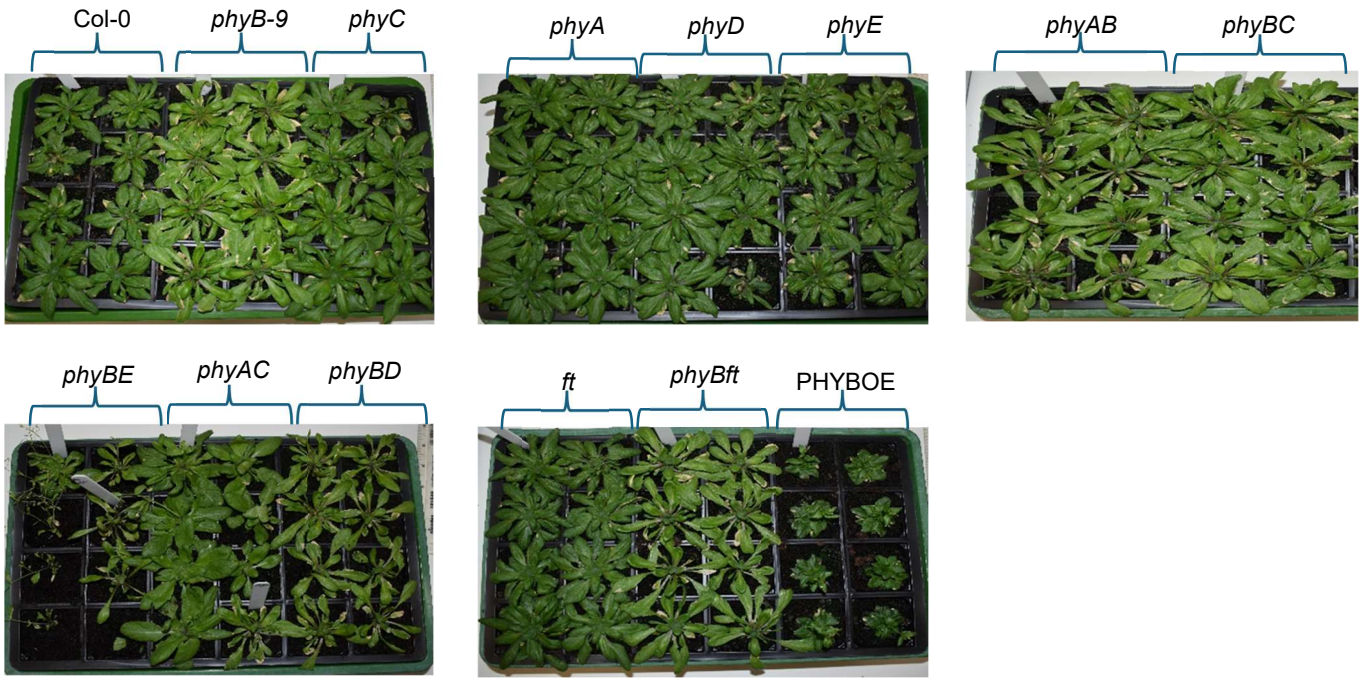

Supplementary figure 3.2 Photos of Col-0 and the mutants in the phytochrome gradient taken at 40 days post germination, to show potential canopy impacts on WUE. The phytochrome single mutants had larger rosettes and this could be impacting upon the ability of these plants to lose water.